

The Economic Optimization of Wind Turbine Design

A Thesis
Presented to
The Academic Faculty

by

Michael Schmidt

In Partial Fulfillment
of the Requirements for the Degree
Master of Science in the
School of Mechanical Engineering

Georgia Institute of Technology
December 2007

The Economic Optimization of Wind Turbine Design

Approved by:

Dr. Sam V. Shelton, Advisor
Strategic Energy Institute
Georgia Institute of Technology

Dr. Berdinus A. Bras
School of Mechanical Engineering
Georgia Institute of Technology

Dr. Sheldon M. Jeter
School of Mechanical Engineering
Georgia Institute of Technology

Date Approved: 11/9/07

Acknowledgements

I would like to thank the people who have made this work possible. First, I would like to give special thanks to my advisor, Dr. Sam V. Shelton. Dr. Shelton gave me the opportunity to begin working at the Strategic Energy Institute as an undergraduate student more than two years ago. Through his guidance, I have gained invaluable experience and insight related to the field of energy. I could not have had a better advisor.

I would also like to thank everyone at the Strategic Energy Institute for their help and support. The atmosphere has made working at the Strategic Energy Institute a delightful experience. Specifically, I would like to thank Dr. Susan Stewart and Kirk Martin, whose work laid the foundation for this thesis study.

Finally, I would like to thank my family and friends. They have always encouraged me throughout all my endeavors. Their support and advice has given me the motivation to achieve my goals.

Table of Contents

| | |
|---|------------|
| ACKNOWLEDGEMENTS | III |
| LIST OF TABLES | VI |
| LIST OF FIGURES | VII |
| NOMENCLATURE..... | X |
| SUMMARY... .. | XII |
| CHAPTER 1:INTRODUCTION..... | 1 |
| 1.1 LITERATURE REVIEW | 2 |
| 1.1.1 Site-Specific Design Optimization of 1.5 – 2.0 MW Wind Turbines [1] | 2 |
| 1.1.2 Wind Turbine Generator Trends for Site-specific Tailoring [2]..... | 2 |
| 1.1.3 WindPACT Turbine Rotor Design, Specific Rating Study [3]..... | 3 |
| 1.1.4 Site Specific Optimization of Rotor / Generator Sizing of Wind Turbines [4]..... | 4 |
| 1.2 WIND ENERGY INDUSTRY BACKGROUND | 4 |
| 1.2.1 Factors Affecting Continued Growth of the U.S. Wind Industry | 7 |
| 1.2.2 Offshore Wind Farms | 10 |
| 1.3 WIND TURBINE TECHNOLOGY | 12 |
| 1.3.1 History | 12 |
| 1.3.2 Modern Wind Turbine | 13 |
| 1.3.3 U.S. Wind Turbine Market | 15 |
| 1.3.4 Wind Turbine Size..... | 16 |
| 1.4 WIND ENERGY FUNDAMENTALS | 18 |
| 1.4.1 Weibull Distribution | 18 |
| 1.4.2 Atmospheric Boundary Layer and Wind Shear | 20 |
| 1.4.3 Wind Power Classes | 21 |
| 1.5 INTRODUCTION TO EXTRACTING ENERGY FROM THE WIND..... | 22 |
| 1.5.1 Kinetic Energy of Wind..... | 22 |
| 1.5.2 Extractable Energy of Wind | 24 |
| CHAPTER 2:RESEARCH METHODOLOGY | 27 |
| 2.1 MODEL ARCHITECTURE | 27 |
| 2.2 ROTOR DIAMETER OPTIMIZATION | 28 |
| 2.3 IMPROVEMENTS OVER PREVIOUS MODEL | 30 |
| CHAPTER 3:ECONOMIC EVALUATION MODEL AND COST MODELS..... | 33 |
| 3.1 ECONOMIC EVALUATION MODEL | 33 |
| 3.1.1 Levelized Cost of Energy | 33 |
| 3.1.2 Simple Payback | 35 |
| 3.1.3 Net Present Value | 36 |
| 3.1.4 Internal Rate of Return | 38 |
| 3.1.5 NPV vs. SPB and IRR..... | 39 |
| 3.2 COST MODELS | 40 |
| 3.2.1 Land Based Cost Models..... | 40 |
| 3.2.2 Additional Offshore Cost Models..... | 60 |
| 3.2.3 Summary of Cost Models | 67 |
| 3.3 BASE CASE COST ANALYSIS | 71 |
| CHAPTER 4:ELECTRIC POWER MODEL | 80 |
| 4.1 BLADE ELEMENT MOMENTUM THEORY..... | 80 |

| | | |
|--|---|------------|
| 4.1.1 | Thrust and Torque from Lift and Drag | 85 |
| 4.1.2 | Thrust and Torque from Momentum | 86 |
| 4.1.3 | Solving Torque and Thrust Equations | 88 |
| 4.1.4 | Pitch and Rotor RPM Optimization..... | 88 |
| 4.2 | DRIVE TRAIN EFFICIENCY MODEL | 89 |
| 4.3 | MODEL VALIDATION | 91 |
| CHAPTER 5:ECONOMIC DATA ANALYSIS | | 93 |
| 5.1 | WIND DATA | 93 |
| 5.2 | RATE DATA..... | 94 |
| 5.3 | ELECTRICAL RATE AND WIND DATA ANALYSIS | 95 |
| CHAPTER 6:RESULTS, DISCUSSION, AND CONCLUSIONS..... | | 100 |
| 6.1 | RESULTS AND DISCUSSION..... | 100 |
| 6.1.1 | Sensitivity Analysis of Specific Rotor Rating and COE | 100 |
| 6.1.2 | Minimizing COE and SPB for a Coastal Georgia Site | 107 |
| 6.2 | CONCLUSIONS..... | 109 |
| APPENDIX A: ROTOR DATA..... | | 112 |
| REFERENCES..... | | 114 |

List of Tables

| | |
|--|-----|
| Table 1.1: Potential U.S. Offshore Wind Projects [7] | 11 |
| Table 1.2: Size Distribution of Wind Turbines [7] | 17 |
| Table 1.3: Classes of Wind Power at 10 m and 50 m Above Surface [17] | 22 |
| Table 3.1: Summary of Initial Capital Cost Components for Land Based Turbine | 69 |
| Table 3.2: Summary of Initial Capital Cost Components for Offshore Turbine | 70 |
| Table 3.3: Component Cost of Base Case Design with Minimum COE | 72 |
| Table 3.4: ICC of an Optimal 1500 kW Turbine with Base Case Wind Resource..... | 77 |
| Table 3.5: ICC of an Optimal 4500 kW Turbine with Base Case Wind Resource..... | 78 |
| Table 6.1: Results of Minimizing COE and SPB for a Coastal Georgia Site..... | 109 |
| Table A.1: Published C_L and C_D Values for the S809 Aerofoil [21]..... | 112 |
| Table A.2: Blade Element Specifications [21] | 113 |

List of Figures

| | |
|---|----|
| Figure 1.1: Global Ranking of Total Installed Capacity and Added Capacity [6] | 5 |
| Figure 1.2: Wind Energy Production as % of Electricity Consumption [7] | 6 |
| Figure 1.3: Map of U.S. Wind Farm Locations [7] | 7 |
| Figure 1.4: Annual Added and Cumulative Wind Capacity in U.S. [7] | 8 |
| Figure 1.5: Wind Map of the U.S. from 3 Tier [8] | 9 |
| Figure 1.6: Map of States with Renewable Portfolio Standards [9] | 10 |
| Figure 1.7: Rotor Efficiency versus Tip-Speed Ratio for Various Rotor Types | 13 |
| Figure 1.8: Wind Turbine Layout [12] | 14 |
| Figure 1.9: Nacelle Layout [13]..... | 15 |
| Figure 1.10: U.S. Market Share of Wind Turbine Manufacturers by MW in 2006 [7].... | 16 |
| Figure 1.11: Evolution of Wind Technology [7] | 17 |
| Figure 1.12: Wind speed data histogram and Weibull model at R2 tower in 2000 | 19 |
| Figure 1.13: Weibull Distributions with Various Shape Parameters..... | 20 |
| Figure 1.14: Control Volume around Wind Turbine Rotor | 24 |
| Figure 1.15: Coefficient of Performance as a Function of V_2/V_1 | 26 |
| Figure 2.1: Flowchart of Wind Turbine Model | 27 |
| Figure 2.2: Single Minimum Value of COE..... | 29 |
| Figure 2.3: Single Minimum Value of SPB..... | 29 |
| Figure 3.1: Blade Cost as a Function of Rotor Diameter..... | 41 |
| Figure 3.2: Hub Cost as a Function of Rotor Diameter | 42 |
| Figure 3.3: Pitch System Cost as a Function of Rotor Diameter | 43 |
| Figure 3.4: Nose Cone Cost as a Function of Rotor Diameter | 44 |

| | |
|---|----|
| Figure 3.5: Low-Speed Shaft Cost as a Function of Rotor Diameter | 45 |
| Figure 3.6: Main Bearing Cost as a Function of Rotor Diameter | 46 |
| Figure 3.7: Yaw System Cost as a Function of Rotor Diameter | 49 |
| Figure 3.8: Mainframe Cost as a Function of Rotor Diameter | 51 |
| Figure 3.9: Platforms and Railings Cost as a Function of Rotor Diameter | 52 |
| Figure 3.10: Tower Cost as a Function of Rotor Diameter for Different Hub Heights | 55 |
| Figure 3.11: Foundation Cost as a Function of Rotor Diameter | 56 |
| Figure 3.12: Assembly and Installation Cost as a Function of Rotor Diameter | 58 |
| Figure 3.13: Breakdown of Base Case Capital Costs | 73 |
| Figure 3.14: Breakdown of Rotor Component Costs for Base Case | 74 |
| Figure 3.15: Breakdown of Nacelle Component Costs for Base Case | 75 |
| Figure 3.16: Breakdown of Tower and Foundation Costs for Base Case | 75 |
| Figure 3.17: Breakdown of Balance of Station Costs for Base Case | 76 |
| Figure 3.18: Initial Capital Cost of Turbines with Optimal Specific Ratings | 79 |
| Figure 4.1: Annulus Created by Blade Element as the Rotor Rotates | 81 |
| Figure 4.2: Lift and drag forces on an airfoil section | 82 |
| Figure 4.3: Lift and drag coefficients versus angle of attack for S809 airfoil [21] | 83 |
| Figure 4.4: Cross section of wind turbine airfoil showing velocity relationships | 84 |
| Figure 4.5: Energy Transfer from Wind to Electrical Grid | 90 |
| Figure 4.6: Drive Train Efficiency | 91 |
| Figure 4.7: Model Validation Using GE 3.6 MW Turbine Power Curve | 92 |
| Figure 5.1: R2 Navy Tower off the Coast of Georgia | 94 |
| Figure 5.2: 2000 Wind Speed Cubed Frequency Distribution | 95 |

| | |
|---|-----|
| Figure 5.3: 2004 Wind Speed Cubed Frequency Distribution..... | 96 |
| Figure 5.4: 2005 Wind Speed Cubed Frequency Distribution..... | 96 |
| Figure 5.5: 2000 Hourly Electrical Rate and Wind Speed Coincidence..... | 98 |
| Figure 5.6: 2004 Hourly Electrical Rate and Wind Speed Coincidence..... | 98 |
| Figure 5.7: 2005 Hourly Electrical Rate and Wind Speed Coincidence..... | 99 |
| Figure 6.1: Specific Rotor Rating Sensitivity Analysis | 101 |
| Figure 6.2: Generator Capacity Sensitivity Analysis..... | 102 |
| Figure 6.3: Annual Average Wind Speed Sensitivity Analysis | 103 |
| Figure 6.4: Weibull Shape Parameter Sensitivity Analysis | 105 |
| Figure 6.5: Power Law Exponent Sensitivity Analysis with 80 m Hub Height | 106 |
| Figure 6.6: Hub Height Sensitivity Analysis with 1/7 th Power Law Exponent | 107 |

Nomenclature

| | |
|--------------|--|
| A | Area |
| AAR | Annual Average Revenue |
| AEP | Annual Energy Production |
| c | Chord Length |
| C_D | Coefficient of Drag |
| C_L | Coefficient of Lift |
| C_p | Coefficient of Performance |
| COE | Levelized Cost of Energy |
| D | Rotor Diameter |
| D | Drag |
| EES | Engineering Equation Solver |
| FCR | Fixed Charge Rate |
| GE | General Electric Corporation |
| h | Probability |
| H | Height above the Surface of the Earth |
| ICC | Initial Capital Cost |
| IRR | Internal Rate of Return |
| k | Weibull Distribution Shape Parameter |
| kg | Kilogram(s) |
| kW | Kilowatts |
| kW-hr | Kilowatt-hours |
| L | Lift |
| LLC | Land Lease Cost |
| LRC | Levelized Replacement Cost |
| m | Meter(s) |
| \dot{m} | Mass Flow Rate |
| MR | Machine Rating |
| MW | Megawatts |
| MW-hr | Megawatt-hours |
| N_{BLADES} | Number of Rotor Blades |
| NPV | Net Present Value |
| O&M | Operation and Maintenance |
| Q | Torque |
| RPM | Revolutions per Minute |
| s | Second(s) |
| S | Span of Airfoil |
| SPB | Simple Payback |
| t | Time |
| T | Thrust |
| TSR | Tip Speed Ratio |
| u | Change in Swirl Velocity from Upstream to the Plane of the Rotor |
| U | Wind Speed |
| \bar{U} | Annual Average Wind Speed |

| | |
|-------------|--|
| v | Change in Air Velocity from Upstream to the Plane of the Rotor |
| V | Velocity of air |
| V_{in} | Velocity of Incoming Air entering the Plane of the Rotor |
| V_{rot} | Linear Velocity of a Blade Element due to Rotation |
| V_1 | Wind Speed Far Upstream of Turbine |
| V_2 | Wind Speed Far Downstream of Turbine |
| w | Width of a Blade Element |
| \dot{W} | Power |
| α | Angle of Attack |
| Γ | The Gamma Function |
| ω | Angular Velocity of the Rotor |
| ρ | Air Density |
| Φ | Angle between the Plane of the Rotor and V |
| Θ | Angle between the Plane of the Rotor and the Blade Element Chord |
| λ_1 | Thrust Coefficient |
| λ_2 | Torque Coefficient |

Summary

Modern wind turbines have become an economically competitive form of clean and renewable power generation. Optimizing wind turbines for specific sites can further increase their economic competitiveness. A turbine should be optimized for its specific site because wind resource characteristics vary from site to site. This study carries out an economic optimization analysis of a variable speed, three blade, horizontal-axis wind turbine. The turbine design parameters considered are the rotor diameter, hub height, and generator capacity. The lifetime levelized cost of energy and simple payback are the figures of merit minimized. Blade element momentum theory is used to calculate the power produced by the wind turbine rotor. The Weibull distribution is used to model the wind resource.

Increasing the rotor diameter increases the power delivered to the generator at all wind speeds up to the limit of generator capacity. Increasing the generator capacity raises the limit on maximum power output. Increasing the hub height of a wind turbine increases power output due to the higher wind speeds at increased heights. However, all of these design changes involve an increase in capital cost. The cost models and levelized cost of energy (COE) model are taken from the National Renewable Energy Laboratory.

The model developed in this study is used to minimize COE for various scenarios. The base case was defined as a wind resource with an annual average wind speed of 7.5 m/s at a 50 m height, a Weibull shape parameter equal to 2, and a wind shear power law exponent equal to $1/7^{\text{th}}$ in which there is a 3000 kW turbine with an 80 m hub height. The optimum rotor diameter for the base case was found to be 106 m. Specific rotor

rating is defined as the generator capacity relative to the rotor swept area. The optimum specific rotor rating for the base case is 0.34 kW/m^2 . The corresponding optimum COE for the base case is 4.6 cents/kWh.

The turbine design parameters and wind resource characteristics were varied individually to determine their effect on optimal COE and specific rotor rating. Varying the generator capacity from 1500 kW to 4500 kW resulted in the optimal specific rotor rating ranging from 0.31 kW/m^2 to 0.33 kW/m^2 and the optimal COE ranging from 4.3 cents/kWh to 5.2 cents/kWh. Varying the annual average wind speed at 50 m from 6.5 m/s to 8.5 m/s resulted in the optimal specific rotor rating ranging from 0.28 kW/m^2 to 0.39 kW/m^2 and the optimal COE ranging from 5.7 cents/kWh to 4.0 cents/kWh. Varying the Weibull shape parameter from 1.8 to 2.2 resulted in the optimal specific rotor rating ranging from 0.36 kW/m^2 to 0.33 kW/m^2 and the optimal COE ranging from 4.7 cents/kWh to 4.6 cents/kWh. Varying the wind shear power law exponent from 0.1 to 0.2 resulted in the optimal specific rotor rating ranging from 0.33 kW/m^2 to 0.34 kW/m^2 and the optimal COE ranging from 4.7 cents/kWh to 4.5 cents/kWh. Varying the hub height from 70 m to 90 m resulted in the optimal specific rotor rating ranging from 0.33 kW/m^2 to 0.35 kW/m^2 and the optimal COE ranging from 4.7 cents/kWh to 4.6 cents/kWh. These results provide a guideline for the economic optimum wind turbine design in various wind resources.

The model is also used to compare the differences between optimizing a wind turbine located off the coast of Georgia by minimizing the levelized cost of energy, minimizing the simple payback using a time-dependent valuation of electricity, and minimizing the simple payback using an average valuation of electricity. This analysis

was performed over annual periods using several years of historic wind and economic data. The results of this study show that minimizing levelized cost of energy and minimizing simple payback results in similar optimum designs for this particular site. The specific rotor ratings of the optimum designs are within 10% of each other in every year analyzed. The corresponding levelized costs of energy of the optimum designs are within 0.2% of each other. Similarly, the corresponding simple payback values of the optimum designs are equal to each other out to three significant figures. The results show, however, that using an hourly time-dependent valuation of electricity to calculate simple payback results in a different value than when an annual average value of electricity is used to calculate simple payback. These two values differ by as much as 4% at this particular coastal Georgia site. Therefore, the methodology of considering an hourly time-dependent valuation of electricity, as presented in this study, is advantageous to an investor because it provides a more realistic measure of the investment's value.

Chapter 1: Introduction

Modern horizontal axis wind turbines have become an economically competitive form of clean and renewable power generation. As a result, the wind industry has recently experienced tremendous growth. Optimizing wind turbines for specific sites by varying rotor diameter, hub height, and generator capacity can make wind turbines even more economically competitive.

The wind resource characteristics vary from site to site. Therefore, a turbine design must be optimized for the site in which it will be located. This study focuses on the site specific design optimization of a horizontal-axis, variable-speed wind turbine. The design parameters being varied include rotor diameter, hub height, and generator capacity. Increasing any one of these parameters will increase power generation. However, increasing any one of these parameters will increase the capital cost. The typical economic figure of merit used for wind turbine optimization is to minimize the levelized cost of energy (COE). This study analyzes the sensitivity of COE and specific rotor rating on various design parameters and wind resource characteristics. Specific rotor rating is defined as generator capacity over rotor swept area.

This study also considers the hourly time-dependent valuation of electricity and its effect on the optimum design. The demand for electricity fluctuates throughout the day and from season to season. As a result, there is a corresponding fluctuation in the economic value of electricity. This study analyzes a specific site off the Georgia Coast to determine how considering the hourly time-dependent valuation of electricity for that region affects the optimum design, cost of energy, and simple payback of the investment.

1.1 Literature Review

A number of studies have been published concerning the site specific design of wind turbines. These studies are outlined below with a brief summary of their methodology.

1.1.1 Site-Specific Design Optimization of 1.5 – 2.0 MW Wind Turbines [1]

This study minimizes the cost of energy (COE) from a wind turbine located at two specific sites in Denmark, one onshore and one offshore. The turbine design parameters that are investigated include, generator capacity, rotor diameter, hub height, and rotor RPM. This study also models wind turbulence and calculates the resulting fatigue loads exerted on the turbine. This study does not provide a sensitivity analysis of COE on the turbine design parameters or wind resource characteristics. In addition, the turbine being optimized in this study is stall regulated, which means the pitch of the rotor blades is fixed. The vast majority of commercially available large turbines today are equipped with active pitch control.

1.1.2 Wind Turbine Generator Trends for Site-specific Tailoring [2]

This study matches a 1 MW generator with four rotor diameters: 50, 60, 70, and 90 m. Performance is modeled with blade element momentum theory (discussed in Chapter 4) using data from specific wind sites in California. It analyzes both long and short term wind variations - seasonal and time of day - and attempts to match electrical production with electrical demand (for the State of California). A metric called “value factor” is created from the hourly time-dependent valuation of electricity, and a “revenue factor” is defined as the product of the value factor and capacity factor. The

configuration with the highest predicted revenue factor is chosen as the optimum. This study finds the larger rotor diameters to be better. However, the study does not consider the increased capital cost of a larger rotor diameter.

1.1.3 WindPACT Turbine Rotor Design, Specific Rating Study [3]

This study minimizes the COE of a variable speed wind turbine. Four specific rotor ratings are studied by holding the rotor diameter constant at 70 m, while the generator capacity is varied from 1500 kW, to 1000 kW, 1900 kW, and 2300 kW. This study also considers the effect design changes have on fatigue loads and the effect these loads have on operation and maintenance costs. The sensitivity of optimum specific rotor rating and COE on the Weibull shape parameter, annual average wind speed, and maximum tip speed is analyzed. In addition, the study examines the effect of advanced blade designs on the optimum specific rotor rating and COE. The study does not analyze the sensitivity of optimum specific rotor rating and COE on generator capacity, hub height or wind shear power law exponent. It also does not consider the hourly time-dependent valuation of electricity. The results of this study found that the specific rotor rating increases with increasing mean wind speed and with decreasing Weibull shape parameter. The use of advanced blade designs resulted in similar optimum specific rotor ratings as with conventional blade designs but with reduced COE. It was found that increasing the maximum tip speed results in considerable increases in COE but very small changes in optimal specific rotor rating.

1.1.4 Site Specific Optimization of Rotor / Generator Sizing of Wind Turbines [4]

This study optimizes the rotor diameter and generator capacity combination for various wind resources. The turbine modeled in this study has a fixed rotor RPM. Only the capital cost of the generator and rotor blades are considered. This study does not consider the effect a larger rotor would have on the design and cost of other wind turbine components, such as the tower and foundation. A levelized cost of energy is not calculated. Instead, the figure of merit being minimized is capital cost over annual electricity produced. This study also did not consider an hourly time-dependent valuation of electricity. The current study is a continuation of this study by Martin. A more detailed description of the current study's improvements is given in chapter 2.

1.2 Wind Energy Industry Background

Wind energy is a fast growing form of power generation around the world. This is in part due to concerns over global climate change and energy security while demand for electricity continues to grow. Electricity demand is projected to grow at an annual rate of 2.4% globally and 1.5% in North America [5]. In addition, wind energy has proven to be an economically competitive form of power generation.

The global growth in annual installed wind energy capacity for 2006 over 2005 was 32% while the U.S. capacity increased by 27% for 2006 [6,7]. Figure 1.1 lists the ten countries with the most installed wind capacity as well as the ten countries with the most added capacity in 2006. With 2,454 MW of wind capacity added in 2006, the U.S. has the fastest growing wind energy market in the world. The US is now third place for total installed capacity of wind energy. However, wind energy still accounts for less than

one percent of total U.S. power generation. Figure 1.2 shows the wind power production as a percentage of total electricity consumption for several countries as well as the total or global average. With 0.8%, the U.S. is just under the global average of 0.9% electricity consumption coming from wind power.

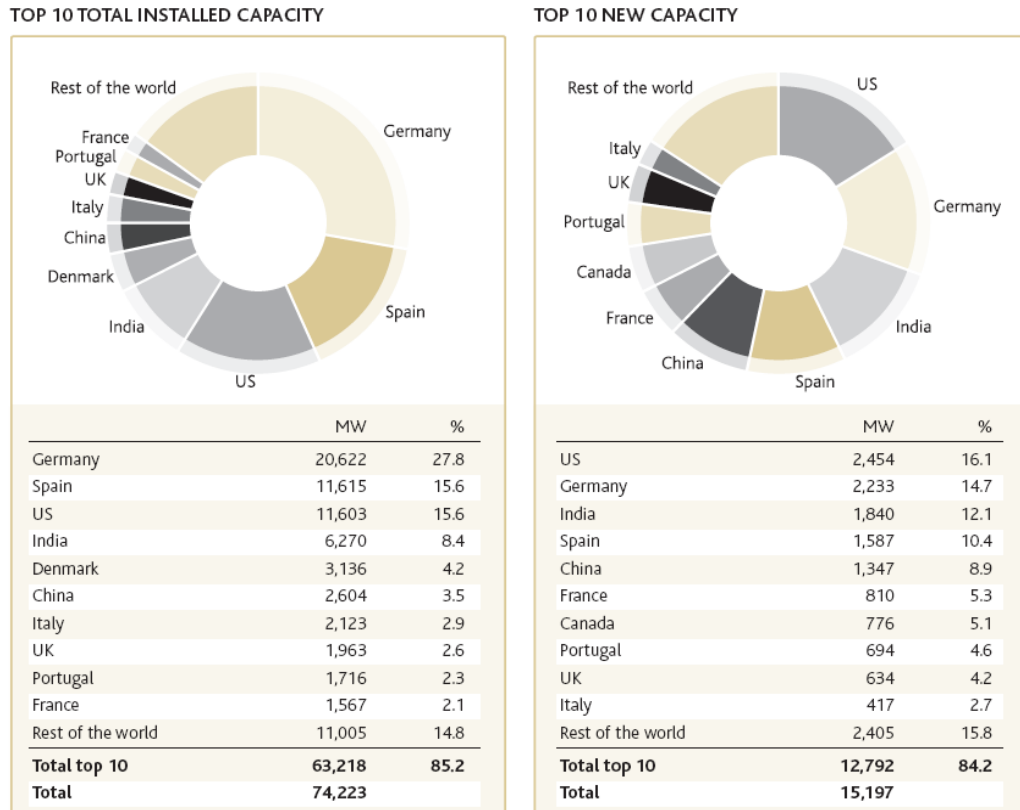


Figure 1.1: Global Ranking of Total Installed Capacity and Added Capacity [6]

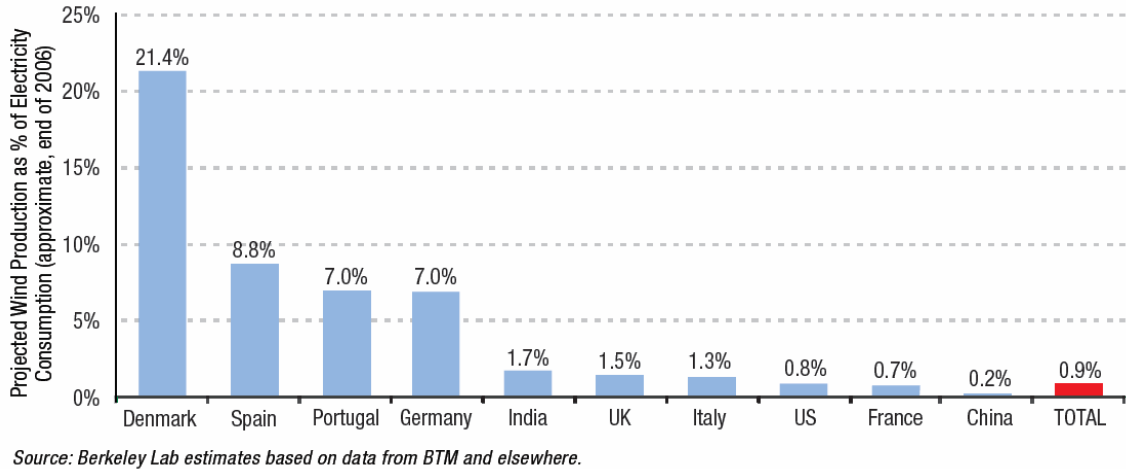


Figure 1.2: Wind Energy Production as % of Electricity Consumption [7]

The U.S. wind industry is not isolated in any one part of the country. Figure 1.3 shows the amount of total installed wind capacity of each state at the end of 2006 as well as the added capacity during 2006. The figure shows that thirty-three out of the fifty US states are currently producing electricity from wind, while Texas and California have the most installed capacity with 2,739 MW and 2,376 MW respectively. The figure also shows the location of wind farms. The wind farms added during 2006 are colored red. This figure demonstrates the large amount of activity in new wind farm development during 2006. It can also be seen that the activity is not isolated in one area, but rather spread out across the country.

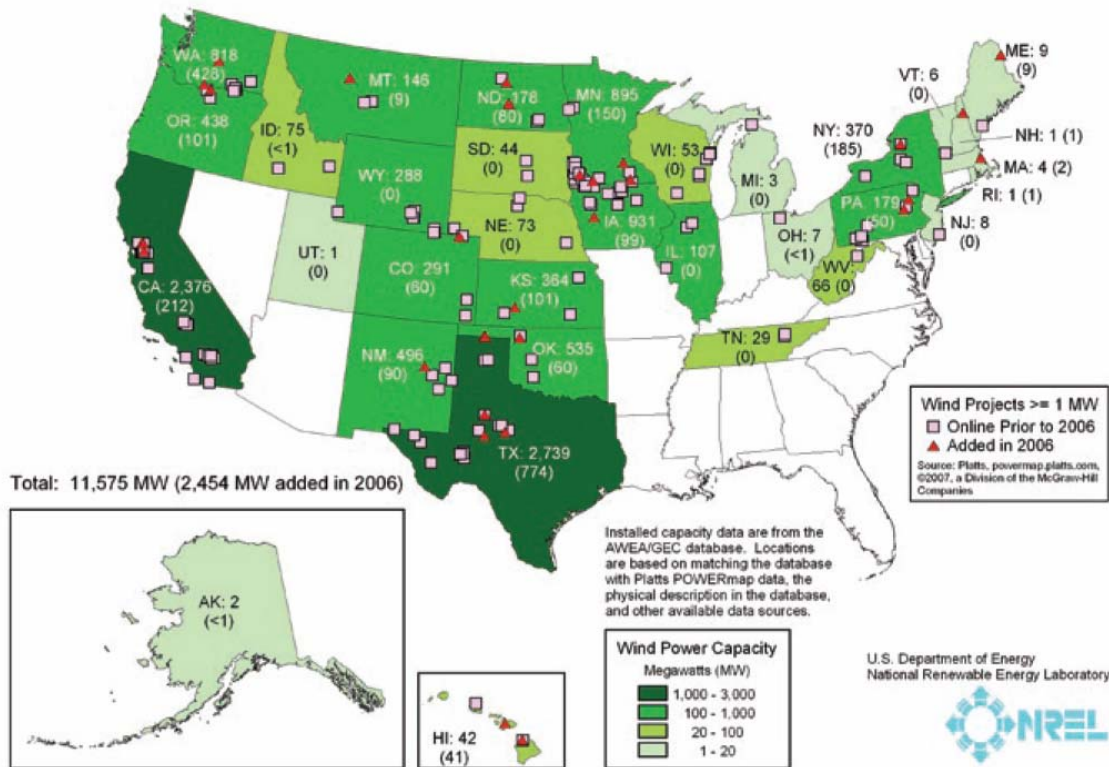
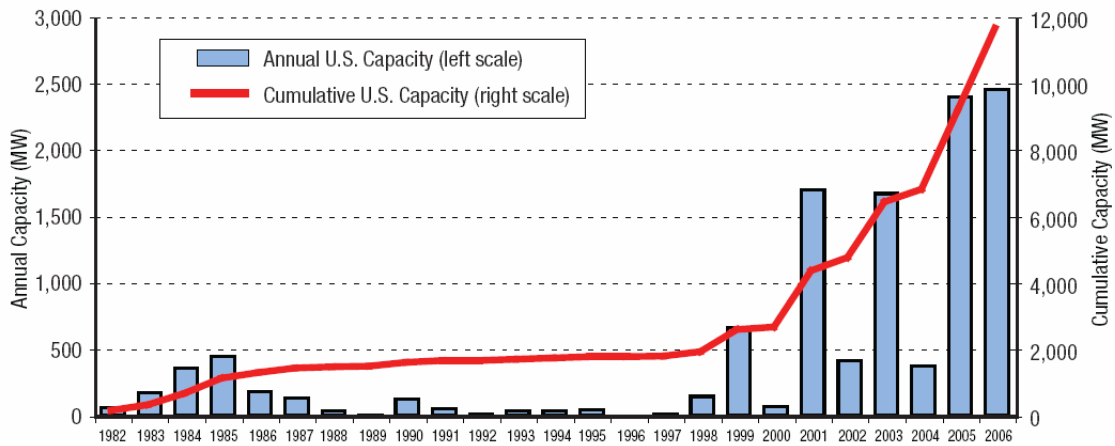


Figure 1.3: Map of U.S. Wind Farm Locations [7]

1.2.1 Factors Affecting Continued Growth of the U.S. Wind Industry

The wind energy industry is growing strong. However, there are some barriers to increased growth in wind energy. One of the main barriers is supply chain bottlenecks. Currently, a developer must wait up to 24 months after ordering to receive shipment of a wind turbine. The bottleneck is with the component suppliers, who have struggled to keep up with an industry that has grown at nearly 30% per year for the past 10 years [6]. Complicating matters is the substantial increase in average turbine size in the past few years. This increase in size has further limited the number of component suppliers, especially for bearings and gearboxes.

Uncertainty related to the production tax credit (PTC) in the U.S. has also affected growth of the U.S. wind industry. The PTC has not always been renewed in a timely manner, which has caused an on-off effect for wind turbine orders. This effect can be seen in Figure 1.4. A large change in wind turbine installations occurred most recently in 2004 after the PTC expired at the end of 2003. The PTC was not renewed until the end of 2004 resulting in only 389 MW of added wind energy capacity in the US. The PTC was then renewed at the end of 2004 which led to record growth in 2005.



Source: AWEA/GEC database.

Figure 1.4: Annual Added and Cumulative Wind Capacity in U.S. [7]

Transmission capacity is also a potential barrier to continued growth of the U.S. wind industry. Figure 1.5 gives a general picture of wind speeds in the U.S. It can be seen that many of the high wind sites are located in the Great Plains region, far from many of the country’s load centers. Developing wind farms in these areas often requires significant investment in transmission lines.



Figure 1.5: Wind Map of the U.S. from 3 Tier [8]

Another factor which will affect wind industry growth is the enactment of renewable portfolio standards (RPS). An RPS requires a certain amount of electricity to be generated from renewable sources. A national RPS does not exist at this time. However, many states have enacted their own RPS's. Currently, 23 states and Washington D.C. have some form of an RPS. Figure 1.6 shows the states which have an RPS and its requirements.

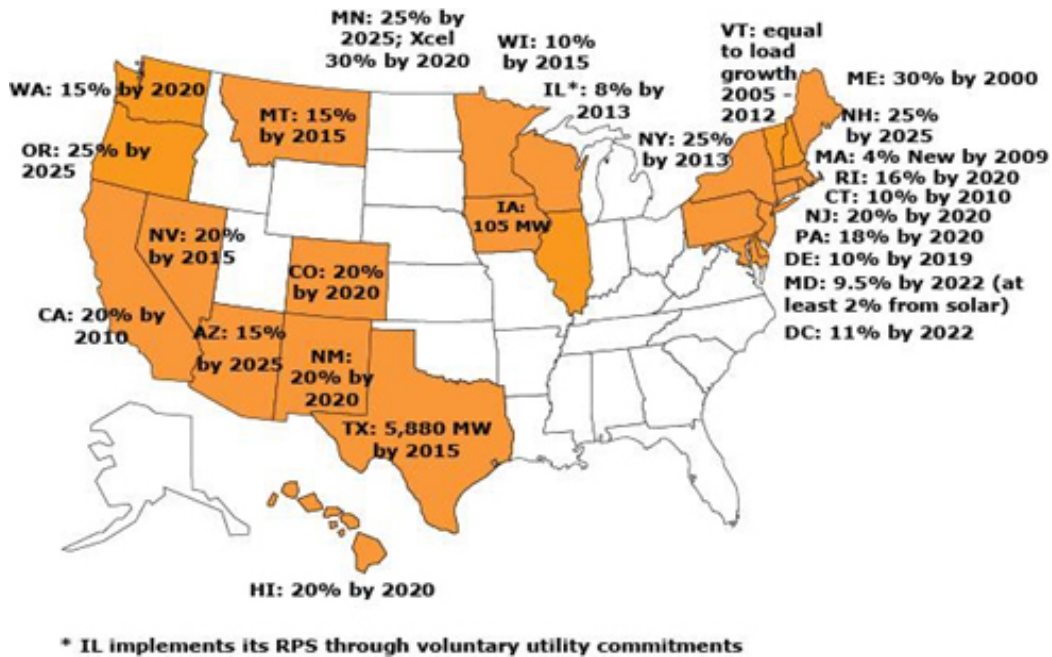


Figure 1.6: Map of States with Renewable Portfolio Standards [9]

1.2.2 Offshore Wind Farms

Offshore sites have many advantages over onshore sites. The average wind speed typically increases substantially when going from onshore to offshore. The quality of wind is also higher offshore. Specifically, the wind is less turbulent, which leads to less fatigue wear of the wind turbine components. In addition, many major U.S. load centers are located in coastal regions, such as the north east U.S. Atlantic coast. These areas could have mediocre wind conditions onshore and limited land availability for a wind farm, while an offshore site could provide superb wind conditions without the land availability issues.

An offshore wind farm has many unique challenges as well. The wind turbine must be protected against the harsher offshore environment. Servicing an offshore

turbine is more difficult and expensive. Foundations for offshore sites with water depths of more than 25 meters are in the development phase.

Europe currently has nearly 900 MW of offshore wind energy installed. Several offshore projects have been proposed in the U.S., but none have been developed. Table 1.1 lists the offshore projects that have been proposed. The table shows that the projects are located off the Atlantic Coast or in the Gulf of Mexico off the coast of Texas.

At this time, permitting of offshore wind farms in federal waters has been frozen while the minerals management service (MMS) defines a permitting process. Federal waters in most states begin 3 nautical miles from the coastline. In most areas it is desirable to develop a wind farm more than 3 nautical miles from the coastline to take full advantage of offshore wind conditions. Texas is in a unique position due to the fact that it is the only state in Table 1.1 whose state controlled waters extend 10 nautical miles offshore. Florida’s waters also extend 10 nautical miles but only on its Gulf Coast [10]. The MMS plans to have a permitting procedure in place by Fall of 2008.

Table 1.1: Potential U.S. Offshore Wind Projects [7]

| State | Proposed Offshore Wind Capacity |
|---------------|--|
| Massachusetts | 735 MW |
| Texas | 650 MW |
| Delaware | 600 MW |
| New Jersey | 300 MW |
| New York | 160 MW |
| Georgia | 10 MW |
| TOTAL | 2,455 MW |

1.3 Wind Turbine Technology

1.3.1 History

Humans have used the power of the wind for many centuries. The first documented windmill was used by the Persians in approximately 900 AD [11]. The windmill appeared in Europe during the middle ages. It was used for many mechanical tasks such as sawing wood, pumping water, grinding grain, and powering tools. The windmill was also widely used in the American west and other rural areas to pump water for cattle and for the steam railroads.

When electrical generators were invented, it was natural for people to turn the generators with windmill rotors. These small wind turbines were popular in rural areas of America. In the 1930s, the Rural Electrification Administration set about to expand the central electrical grid. This was the end of the wind turbine for a few decades. Interest in wind energy reappeared after the oil crisis of the 1970s and 1980s. With lower cost of energy in the 1990s, interest in wind energy subsided in the U.S. However, Europe continued to support wind energy and development continued there.

Various wind turbine designs have been proposed and built over the years. The horizontal axis wind turbine (HAWT) has proven to be the most effective. The closest runner-up to the HAWT is the Darrieus design. Although the Darrieus design has some advantages, such as being able to locate much of the heavy equipment at ground level, it does not capture energy from the wind as efficiently as the HAWT. This can be seen in Figure 1.7. The modern three-blade and high speed two-blade curves are horizontal axis designs. The figure shows that these two designs have the highest efficiencies. For these

reasons, all commercially available large wind turbines of today are a variation of the HAWT.

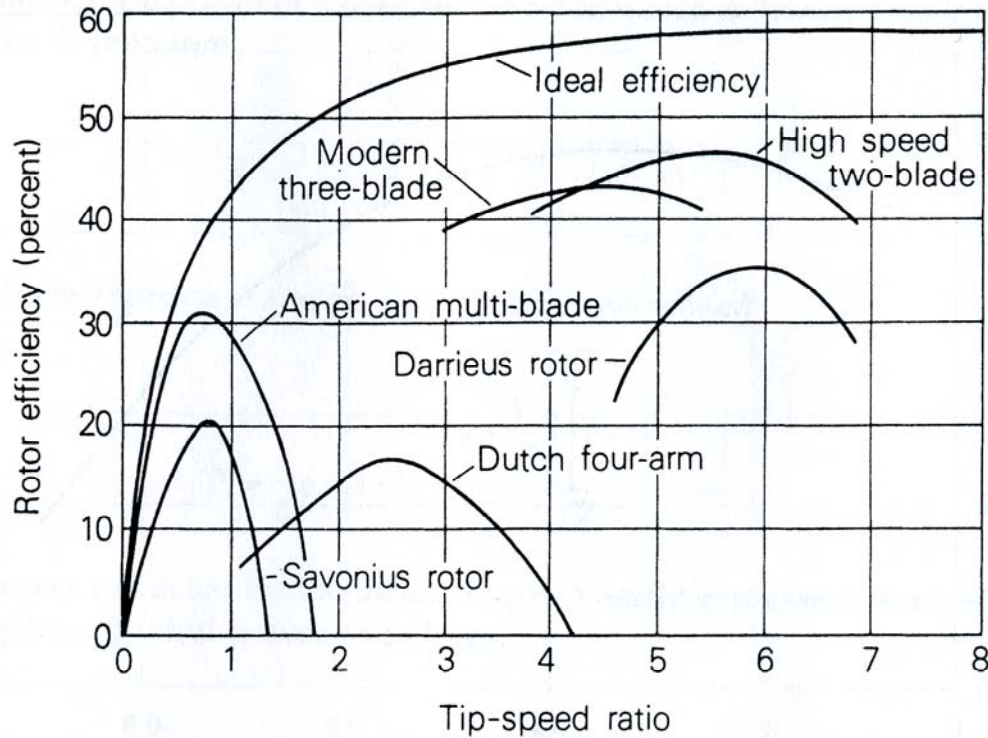


Figure 1.7: Rotor Efficiency versus Tip-Speed Ratio for Various Rotor Types

1.3.2 Modern Wind Turbine

The modern wind turbine is a highly tuned and complicated piece of machinery. The typical modern wind turbine is a three-bladed, variable speed, upwind, horizontal-axis wind turbine with active pitch and yaw control. Variable speed operation allows the rotor RPM to vary, which permits the rotor to operate at its maximum efficiency at every wind speed.

Figure 1.8 shows the general layout of a turbine. The rotor is attached to the nacelle by the hub. The nacelle sits on top of the tower and houses the majority of the wind turbine's functional components. A cut-out view of the nacelle is shown in Figure 1.9. This figure shows the arrangement of the drive train. The rotor turns a low speed shaft which is attached to a gearbox. The gearbox is used to link the low speed shaft to the high speed generator.

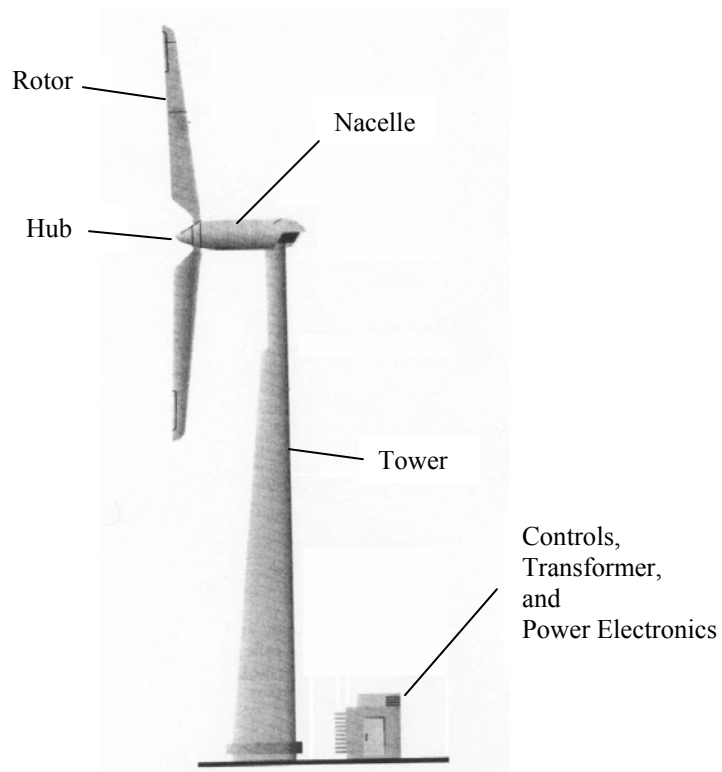


Figure 1.8: Wind Turbine Layout [12]

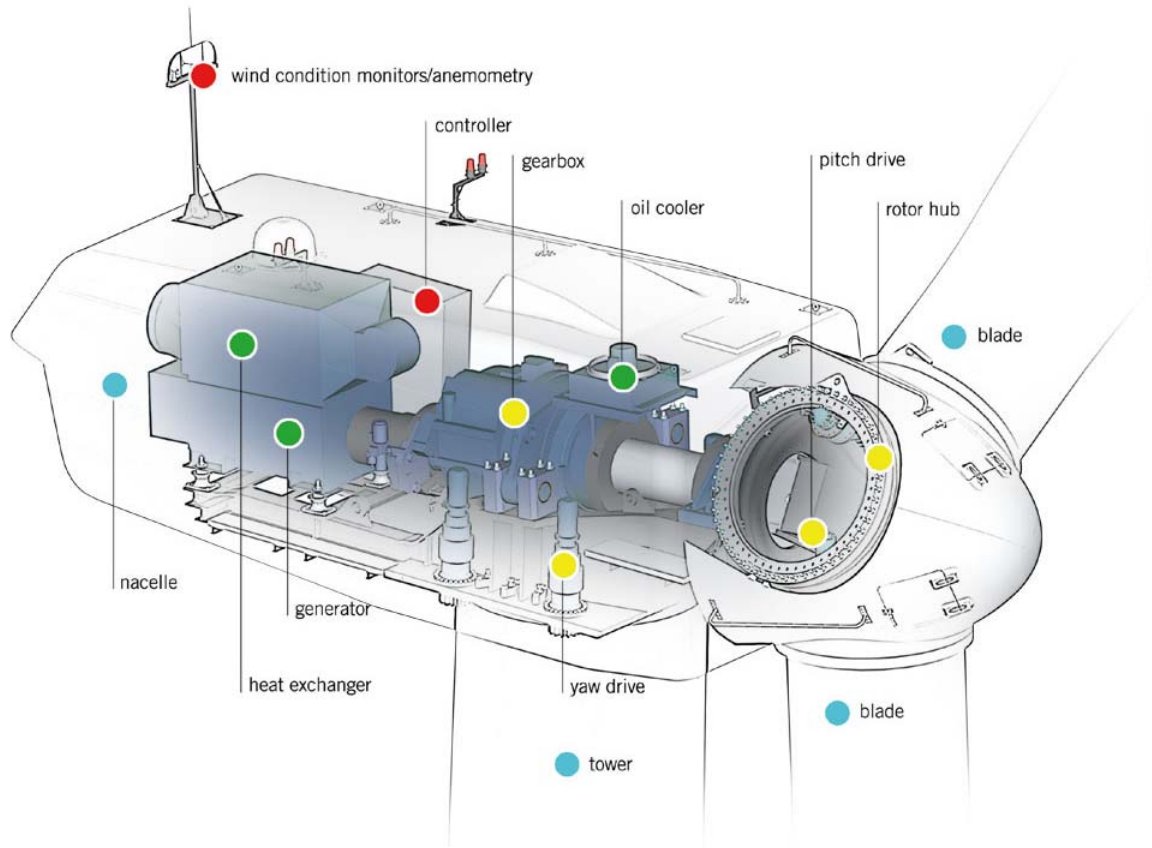


Figure 1.9: Nacelle Layout [13]

1.3.3 U.S. Wind Turbine Market

The wind turbine market has attracted some of the most successful manufacturing companies in the world. Figure 1.10 shows the market share of wind turbines sold in the U.S. during 2006. General Electric has the largest market share with 47%. Siemens and Vestas also have significant U.S. market shares with 23% and 19% respectively.

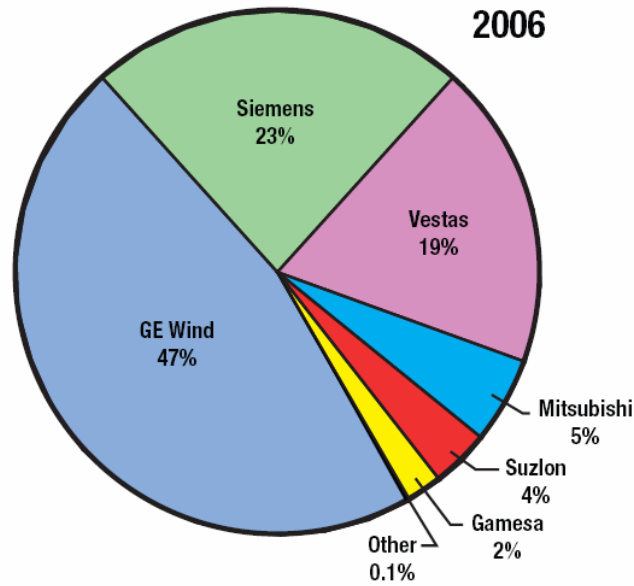
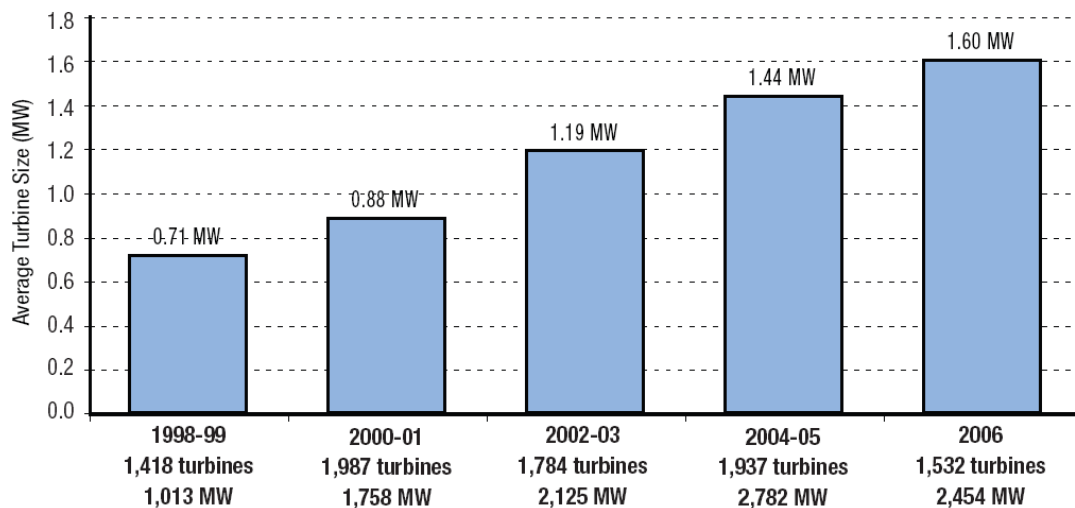


Figure 1.10: U.S. Market Share of Wind Turbine Manufacturers by MW in 2006 [7]

1.3.4 Wind Turbine Size

The size of wind turbines has increased substantially since the 1980's. The size of onshore turbines has reached a point where the levelized cost of energy for even larger machines will be adversely affected by transportation and assembly costs [14]. Offshore wind turbine designs, however, continue to increase in size. A wind turbine manufacturer, REPower Systems, currently offers a 5 MW turbine with a 126 meter rotor diameter, and Clipper Windpower has recently formed a center of excellence for the development of a 7.5 MW offshore wind turbine [15,16].

The increase in wind turbine size over the past few years can be seen in Figure 1.11 and Table 1.2. Figure 1.11 shows the average turbine size from 1998 to 2006. Table 1.2 shows the size distribution from 2000 to 2006. While turbine sizes as large as 3 MW are in operation today, the majority of turbines remain in the 1 to 1.5 MW range.



Source: AWEA/GEC project database.

Figure 1.11: Evolution of Wind Technology [7]

Table 1.2: Size Distribution of Wind Turbines [7]

| | 2000-01 1,758 MW 1,987 turbines | 2002-03 2,125 MW 1,784 turbines | 2004-05 2,782 MW 1,937 turbines | 2006 2,454 MW 1,532 turbines |
|---------------------------|---------------------------------------|---------------------------------------|---------------------------------------|------------------------------------|
| Turbine Size Range | | | | |
| 0.00 to 0.5 MW | 0.4% | 0.5% | 1.9% | 0.7% |
| 0.51 to 1.0 MW | 73.9% | 44.2% | 17.6% | 10.7% |
| 1.01 to 1.5 MW | 25.4% | 42.8% | 56.6% | 54.2% |
| 1.51 to 2.0 MW | 0.4% | 12.3% | 23.9% | 17.6% |
| 2.01 to 2.5 MW | 0.0% | 0.0% | 0.1% | 16.3% |
| 2.51 to 3.0 MW | 0.0% | 0.1% | 0.0% | 0.5% |

1.4 Wind Energy Fundamentals

Wind is fundamentally a form of solar energy. The sun warms the earth unevenly. More solar radiation is absorbed at the equators than the poles, which causes large scale pressure gradients. The heat is distributed to the poles by ocean currents and atmospheric circulation.

1.4.1 Weibull Distribution

At most sites, the wind speed frequency distribution over an annual period can be represented by a Weibull distribution. The Weibull distribution is a function of the average wind speed and the Weibull shape parameter k . The Weibull probability density function is given by:

$$f(U) = k \frac{U^{k-1}}{c^k} \exp\left(-\left(\frac{U}{c}\right)^k\right) \quad (1.1)$$

where:

U = wind speed

k = Weibull shape parameter

c is given by:

$$c = \frac{\bar{U}}{\Gamma\left(1 + \frac{1}{k}\right)} \quad (1.2)$$

where:

\bar{U} = annual average wind speed

Γ represents the Gamma function

A histogram of actual wind data from off the coast of Georgia and its corresponding Weibull distribution is shown in Figure 1.12. The wind resource off the coast of Georgia has an average wind speed of 7.356 m/s and a Weibull shape parameter equal to 2. Figure 1.13 demonstrates how the wind speed frequency distribution varies with the Weibull shape parameter. As the shape parameter becomes larger, the wind speed varies less from the mean wind speed. Most wind resources have a shape parameter equal to or near 2.

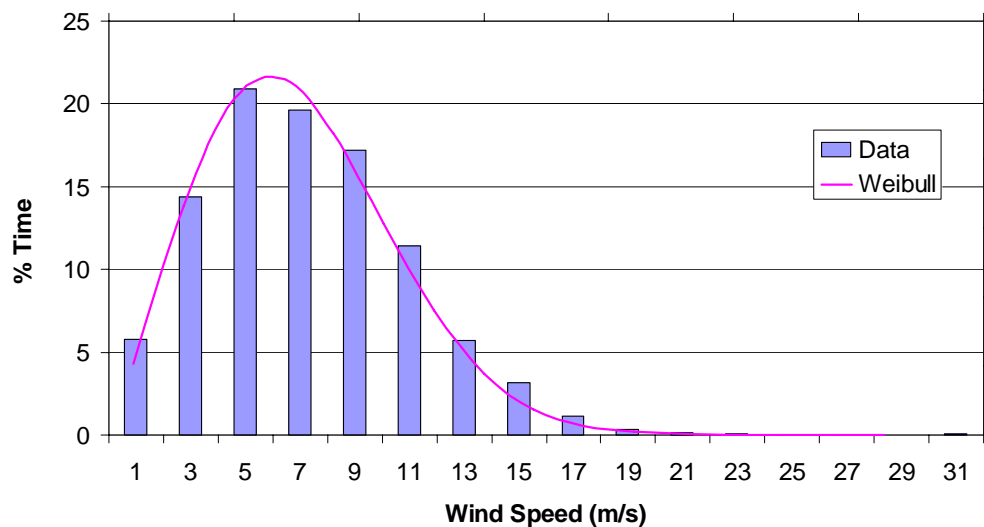


Figure 1.12: Wind speed data histogram and Weibull model at R2 tower in 2000

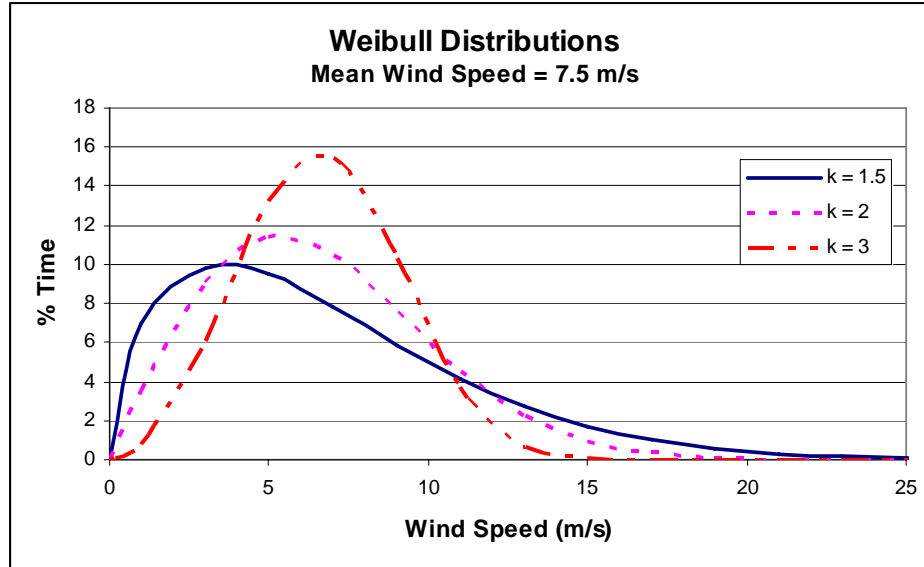


Figure 1.13: Weibull Distributions with Various Shape Parameters

1.4.2 Atmospheric Boundary Layer and Wind Shear

The atmosphere can be divided into several layers. The lowest layer is called the troposphere, which extends upward to an altitude of 10 km. For wind turbine design, this is the part of the atmosphere of interest.

Near ground level, an atmospheric boundary layer is formed by the moving air. The atmospheric boundary layer causes a variation in wind velocity with altitude also known as wind shear. A thorough understanding of the velocity profile at a specific site is necessary for designing the optimum wind turbine at that site. There are two profiles which are commonly used to model wind shear. The first method is the power law profile, which is given by:

$$\frac{U(z)}{U(z_r)} = \left(\frac{z}{z_r} \right)^\alpha \quad (1.3)$$

where:

U = wind speed

z = height

z_r = reference height

α = wind shear power law exponent

The wind shear power law exponent depends on the specific site. It is often equal to or near the value 1/7. The second method is the logarithmic profile law, which is given by:

$$\frac{U(z)}{U(z_r)} = \frac{\ln\left(\frac{z}{z_0}\right)}{\ln\left(\frac{z_r}{z_0}\right)} \quad (1.4)$$

where:

U = wind speed

z = height

z_r = reference height

z_0 = roughness length of the terrain

Both of these methods could be used to model wind shear. This study uses the power law and varies the exponent to model different wind shears.

1.4.3 Wind Power Classes

A wind resource can be divided into different classes depending on its power density expressed in Watts per square meter. Table 1.3 lists the various classes and their corresponding power densities at heights of 10 m and 50 m above the surrounding terrain. The table also shows the corresponding average wind speed for each class. However, these average wind speeds correspond to the power density only if the annual wind speed frequency distribution is a Rayleigh distribution. A Rayleigh distribution is a Weibull distribution with the Weibull shape parameter equal to 2.

Table 1.3: Classes of Wind Power at 10 m and 50 m Above Surface [17]

| Classes of Wind Power Density at 10 m and 50 m Above Surface | | | | |
|--|--|------------------|--|------------------|
| | 10 m Above Surface | | 50 m Above Surface | |
| Wind Power Class | Wind Power Density (W/m ²) | Wind Speed (m/s) | Wind Power Density (W/m ²) | Wind Speed (m/s) |
| 1 | < 100 | < 4.4 | < 200 | < 5.6 |
| 2 | 100 - 150 | 4.4 - 5.1 | 200 - 300 | 5.6 - 6.4 |
| 3 | 150 - 200 | 5.1 - 5.6 | 300 - 400 | 6.4 - 7.0 |
| 4 | 200 - 250 | 5.6 - 6.0 | 400 - 500 | 7.0 - 7.5 |
| 5 | 250 - 300 | 6.0 - 6.4 | 500 - 600 | 7.5 - 8.0 |
| 6 | 300 - 400 | 6.4 - 7.0 | 600 - 800 | 8.0 - 8.8 |
| 7 | > 400 | > 7.0 | > 800 | > 8.8 |

1.5 Introduction to Extracting Energy from the Wind

1.5.1 Kinetic Energy of Wind

Wind turbines convert the kinetic energy of the wind into electricity. It is therefore useful to know how much kinetic energy is available in the wind. The power, \dot{W} , due to the wind velocity relative to the ground is given by:

$$\dot{W} = \frac{1}{2} m V^2 \quad (1.5)$$

where:

$V \equiv$ wind speed

$\dot{m} \equiv$ mass flow rate of wind through column of area A

The mass flow rate through an area A is given by:

$$\dot{m} = \rho AV \quad (1.6)$$

where:

$\rho \equiv$ air density

$A \equiv$ cross-sectional area of column

Combining the two equations above gives:

$$\dot{W} = \frac{1}{2}(\rho AV)V^2 \rightarrow \dot{W} = \frac{1}{2}\rho AV^3 \quad (1.7)$$

This is an important result because it shows that the power available in a cross-sectional area of wind is proportional to the wind speed cubed. Doubling the wind speed will result in an eightfold increase in wind power relative to the ground.

1.5.2 Extractable Energy of Wind

It is not possible, however, to capture 100% of the wind's kinetic energy relative to the ground. Figure 1.14 shows a control volume around a wind turbine. Air enters the control volume at the initial wind speed, V_1 . As the air passes by the turbine, the wind turbine extracts energy from the wind and the air slows. The air exits the control volume at V_2 .

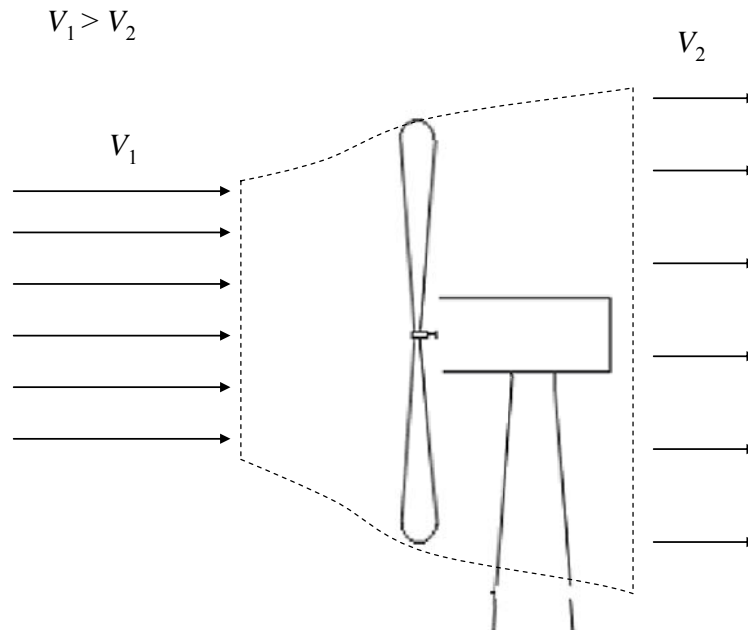


Figure 1.14: Control Volume around Wind Turbine Rotor

The amount of energy extracted by the wind turbine is equal to the loss of energy in the wind, which is equal to the difference in kinetic energy upstream and downstream of the turbine.

$$\dot{W} = \frac{1}{2}\dot{m}V_1^2 - \frac{1}{2}\dot{m}V_2^2 \rightarrow \dot{W} = \frac{1}{2}\dot{m}(V_1^2 - V_2^2) \quad (1.8)$$

The V in the mass flow equation can be determined from actuator disc theory, which shows that half of the wind speed decrease occurs upstream of the turbine rotor and half occurs downstream of the rotor [18]. Therefore, the mass flow rate at the rotor plane is calculated using the average of V_1 and V_2 . Equation 1.8 then becomes:

$$\dot{W} = \frac{1}{2} \left[\rho A \left(\frac{V_1 + V_2}{2} \right) \right] (V_1^2 - V_2^2) \quad (1.9)$$

Equation 1.9 can be rearranged to give:

$$\dot{W} = \frac{1}{2} \rho A V_1^3 \frac{\left(1 + \frac{V_2}{V_1} \right) \left[1 - \left(\frac{V_2}{V_1} \right)^2 \right]}{2} \quad (1.10)$$

or

$$\dot{W} = \frac{1}{2} \rho A V_1^3 C_p \quad (1.11)$$

where:

$$C_p = \frac{\left(1 + \frac{V_2}{V_1} \right) \left[1 - \left(\frac{V_2}{V_1} \right)^2 \right]}{2} \quad (1.12)$$

C_p is the coefficient of performance. It is a function of only V_2/V_1 . In 1919, German physicist Albert Betz showed that the maximum possible coefficient of performance is $16/27$ or approximately 59%. The maximum C_p occurs when V_2 equals $1/3$ the value of V_1 [18]. Figure 1.15 demonstrates the relationship between C_p and V_2/V_1 . It can also be seen that the maximum fraction of the wind's kinetic energy relative to the ground that can be extracted is 59%.

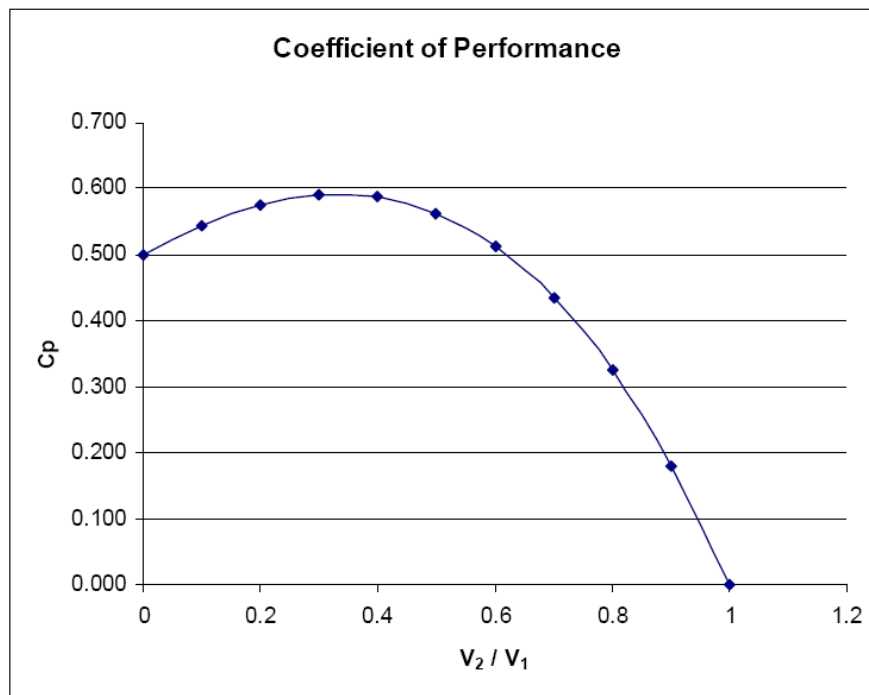


Figure 1.15: Coefficient of Performance as a Function of V_2/V_1

Chapter 2: Research Methodology

2.1 Model Architecture

The wind turbine design optimization model developed for this study is made up of several sub-models. These sub-models include a components cost model, economic evaluation model, electric power model, and a rotor diameter optimization model. Figure 2.1 shows how these various models communicate.

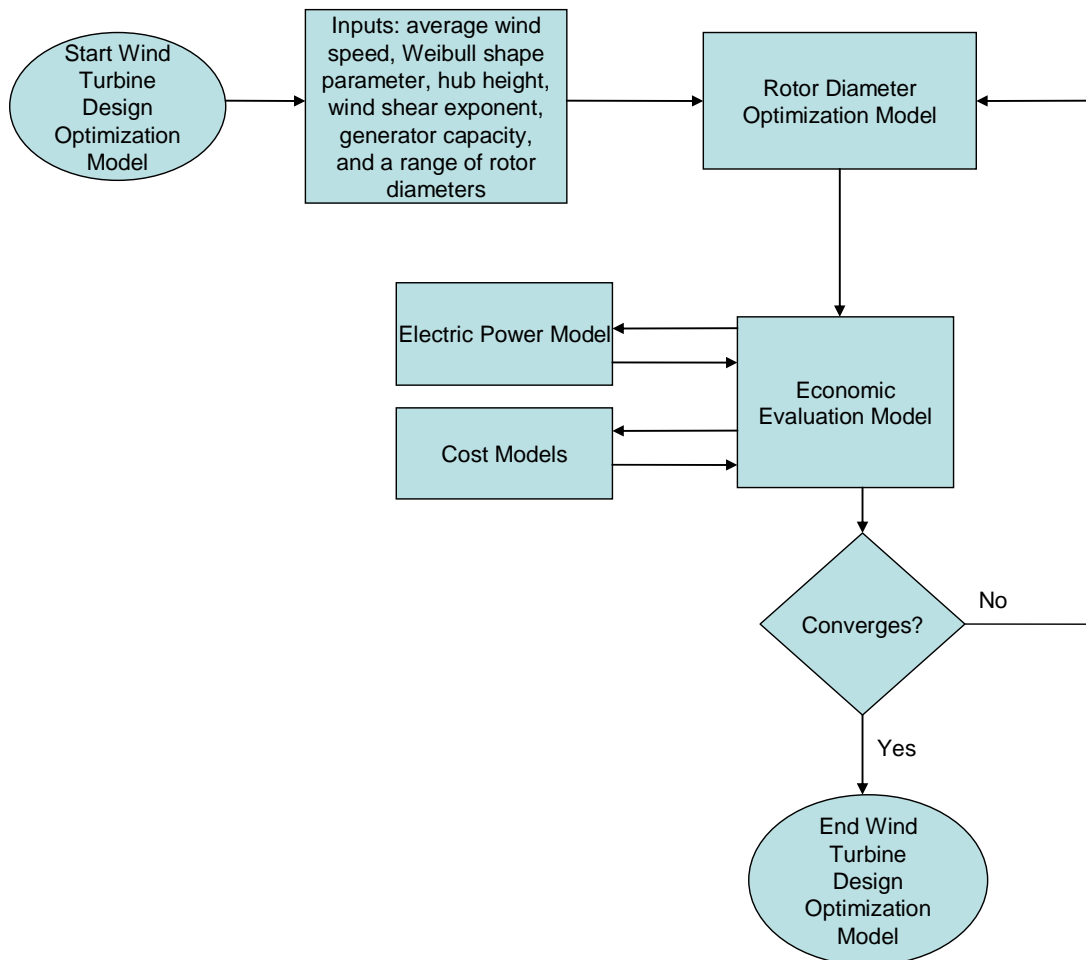


Figure 2.1: Flowchart of Wind Turbine Model

The wind turbine model requires inputs for the average wind speed, Weibull shape parameter k , hub height, wind shear power law exponent, generator capacity, and a range of rotor diameters in which the optimum must lie. The rotor diameter optimization model searches through the range of rotor diameters until it converges. At each rotor diameter, the rotor diameter optimization model calls the economic evaluation model to determine the levelized cost of energy (COE), simple payback (SPB) using a time-dependent valuation of electricity, or SPB using an average valuation of electricity depending on the objective of the optimization. To determine the COE or SPB, the economic evaluation model must call the electric power model to determine how much electricity will be produced over an annual period. The economic evaluation model must also call the components cost model to determine the capital cost of the turbine. The COE or SPB is then returned to the rotor diameter optimization model, which continues to search for the minimum COE or SPB until it converges.

2.2 Rotor Diameter Optimization

The rotor diameter optimization uses a MATLAB algorithm based on the golden section method. Since this is a one dimensional optimization, the golden section method is advantageous because of its simplicity and robustness. However, the golden section method can converge on a local minimum. Figure 2.2 shows that varying the specific rotor rating results in a single minimum COE. Figure 2.3 demonstrates that there is also a single minimum for SPB when varying specific rotor rating. The other second level models are described in the following chapters.

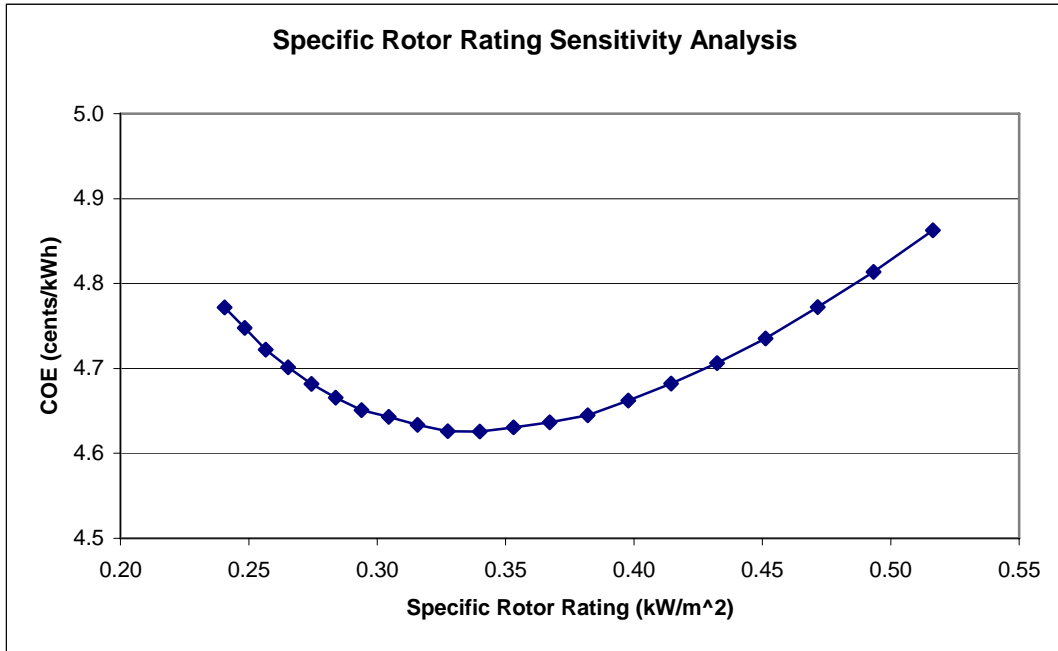


Figure 2.2: Single Minimum Value of COE

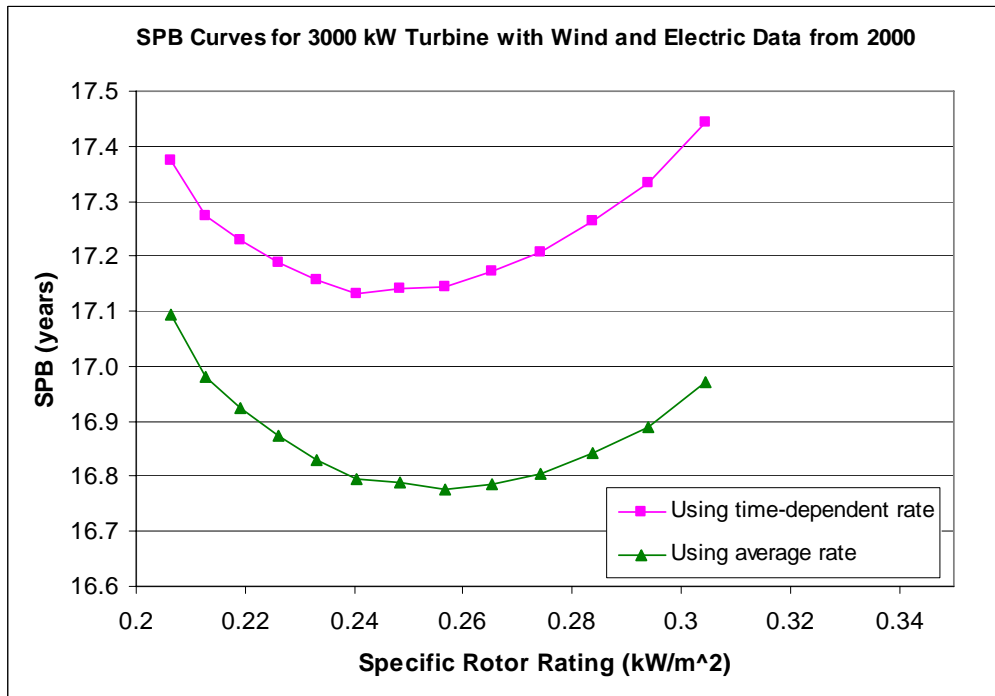


Figure 2.3: Single Minimum Value of SPB

2.3 Improvements over previous model

The wind turbine model used in this study (version 2) was developed from an earlier version (version 1) used in a previous study [4]. The wind turbine model used in this study has many improvements over version 1. These improvements are listed below.

1. Variable speed capability
2. Optimum of pitch and rotor RPM for every wind speed
3. Rotor diameter optimization algorithms used instead of exhaustive search
4. Single step optimization (i.e. no need for creating power tables)
5. More accurate and detailed cost models
6. Able to calculate revenue based on hourly time-dependent valuation of electricity
7. Economic analysis uses levelized cost of energy and simple payback
8. Coded in Matlab instead of Engineering Equation Solver
9. Hub height included as a design parameter
10. Variable drive train efficiency model added

Version 1 of the wind turbine model is only capable of modeling fixed speed wind turbines. Version 2 developed in this study is capable of modeling variable speed turbines as well.

Since version 1 models a fixed speed wind turbine, the blade pitch must be changed for every wind speed. Version 1 simply uses a table of pitch values, which approximate the optimal pitch for each wind speed. Because version 2 models a variable speed turbine, the optimal pitch only needs to be found once. As long as the rotor RPM

remains at the tip speed ratio that results in maximum power production, the pitch that produces the most power will remain the same [18].

Version 1 does not use any optimization algorithms to select the optimum rotor diameter. Instead, it performs an exhaustive search by incrementing the radius by 5 meters. This exhaustive search method involves the creation of many tables and manual manipulation of data in order to find the optimum diameter. Version 2 uses an automated optimization algorithm which more efficiently finds the optimum rotor diameter.

The component cost models used in version 2 are a significant improvement over the cost models used in version 1. Version 1 had only two component models, one model for the blade cost and another for the generator cost. Version 2 contains over 30 component cost models. These models allow the total cost of the turbine as well as the cost of engineering, permitting, civil works, etc. to be calculated.

The figure of merit used in version 1 is simply to maximize annual kWh produced relative to capital cost. The figure of merit used in version 2 is to minimize levelized cost of energy (COE). This allows for easy comparison with other studies as well as a reality check on the accuracy of the model. In addition, version 2 is also capable of calculating a turbine's revenue using historical hourly time-dependent valuations of electricity. In such a case, the figure of merit used is simple payback (SPB) instead of COE.

Version 1 was coded entirely in Engineering Equation Solver (EES). While EES is very good at solving a set of simultaneous equations, Matlab was found to be better suited for optimization and programming general functions. As a result, version 2 was mostly coded in MATLAB. Only the solving of the simultaneous blade element momentum (BEM) equations is performed in EES.

Version 1 did not have a hub height input capability. Version 2 is capable of demonstrating the influence of varying the hub height. This is done by calculating the wind speed according to the vertical wind shear.

Finally, version 1 assumed a drive train efficiency of one. Version 2, however, contains a drive train efficiency model which calculates the efficiency as a function of power output.

Chapter 3: Economic Evaluation Model and Cost Models

3.1 Economic Evaluation Model

3.1.1 Levelized Cost of Energy

The levelized cost of energy (COE) is the real cost of producing one kilowatt-hour (kWh) of electricity. It includes the total cost of building a generating plant, operating the plant over its economic life, financing costs, return on equity, and depreciation. Costs are levelized in real dollars, i.e., adjusted to remove the impact of inflation. The COE is what it would cost the plant owner to produce one kWh. For electricity production, COE is a very convenient method to compare technologies and designs. The COE model used in this study is taken from the National Renewable Energy Laboratory *Wind Turbine Design Cost and Scaling Model* study [19]. The model is given below.

$$COE = \frac{FCR * ICC + LRC}{AEP} + LLC + O \& M \quad (3.1)$$

where:

$FCR \equiv$ fixed charge rate = 0.1185

$ICC \equiv$ initial capital cost in \$

$AEP \equiv$ annual energy production in kWh

$LLC \equiv$ land lease cost = $\frac{\$0.00108}{\text{kWh}}$

$O \& M \equiv$ operations and maintenance = $\frac{\$0.007}{\text{kWh}}$

$$LRC \equiv \text{levelized replacement cost} = \frac{\$10.7}{\text{kW}} MR \quad (3.2)$$

where:

MR \equiv machine rating (same thing as generator capacity)

If LRC were set to zero, minimizing COE would result in the same design as minimizing SPB or maximizing IRR, which are two other economic figures of merit explained below. LRC is not equal to zero, but it is very small compared to ICC . For the economic optimization of a turbine at a Coastal Georgia site, the LRC was approximately 0.7% of the ICC .

The values of LLC , $O\&M$, and LRC are taken directly from the *Wind Turbine Design Cost and Scaling Model* study. The fixed charge rate is the annual amount per dollar of initial capital cost needed to cover the capital cost, i.e. debt payments and return on equity. The *Wind Turbine Design Cost and Scaling Model* study sets FCR to 0.1185, which assumes an independent power producer financial structure with a 30 year lifetime, 70/30 debt/equity ratio, 7% interest on debt, 15 year debt period, 17% return on equity, and a Modified Accelerated Cost Recovery System (MACRS) depreciation structure. The 10-year renewable energy tax credit is not included in the model. These parameters tend to be on the optimistic side, which leads to a lower COE.

It is important to point out, however, that the financial assumptions, which determine the FCR , do not have a large affect on the optimal design. It was observed that, for this study's base case described below, doubling or halving the FCR had a

significant effect on COE, but the optimal specific rotor rating changed by less than 0.02 kW/m².

3.1.2 Simple Payback

One part of this study is to consider the hourly time-dependent valuation of electricity in determining the optimal design. In this case, levelized cost of energy is not a suitable figure of merit. A figure of merit which considers revenue is needed. This study uses the simple payback (SPB). Simple payback is the number of years it takes to recover the initial capital cost of an investment without discounting future profits. SPB is calculated using the following equation:

$$SPB = \frac{ICC}{AAR} \quad (3.3)$$

where:

ICC ≡ initial capital cost

AAR ≡ average annual revenue based on hourly production

It is important to note that this model assumes the wind turbine will produce the same amount of electricity each year. As a result, this analysis assumes a constant revenue stream. Since simple payback does not consider the discount rate or life of the project, the optimal design obtained using simple payback analysis will not be dependent on these values.

SPB is often preferred as a figure of merit because of its simplicity. However, several other economic figures of merit exist. These methods are discussed and

compared below; the discussion is in regard to the needs of this particular study. It is not a general discussion of economic figures of merit.

3.1.3 Net Present Value

The Net Present Value (NPV) is a very popular evaluation method. NPV takes into account the time value of money. The time value of money refers to the fact that \$100 today is worth more than \$100 a year from now. This is because \$100 today could be invested and earn a return higher than the rate of inflation. Therefore, future profits must be discounted. Net present value (also called net present worth) is defined as present value of benefits minus the present value of costs [20]. The present value of costs is the initial capital cost, ICC. It is assumed that the wind speed distribution remains constant from year to year, which would result in a uniform amount of electricity being produced from year to year. Therefore, it is assumed that the annual revenue would be uniform. This uniform cash flow must be discounted since it occurs in the future. NPV for a uniform cash flow is given by the equation below.

$$NPV = AAR \left[\frac{(1+i)^N - 1}{i(1+i)^N} \right] - ICC \quad (3.4)$$

where:

i \equiv discount rate as a decimal value

N \equiv life of the wind turbine in years

ICC \equiv initial capital cost

AAR \equiv average annual revenue based on hourly production

For independent projects, the investment decision is based on NPV being greater than zero. If the investor must decide between two mutually exclusive projects, then the project with the highest NPV should be chosen. In this optimization study, the choice is mutually exclusive. Therefore, the design with the highest NPV should be chosen. It is important to point out that, unlike simple payback, the financial assumptions that go into determining the discount rate and investment life for NPV can change the optimal wind turbine design.

Since rotor diameter is the only design parameter being varied, *AAR* and *ICC* can be generalized as functions of rotor diameter, *D*. Once *i* and *N* are chosen, the value of

$$\left[\frac{(1+i)^N - 1}{i(1+i)^N} \right]$$

will remain constant. Equation 3.8 can then be generalized as:

$$NPV = C * AAR(D) - ICC(D) \quad (3.5)$$

where *C* represents a constant. The maximum net present value is found by differentiating Equation 3.5 with respect to rotor diameter, *D*, and setting it equal to zero as shown below.

$$\frac{dNPV}{dD} = C \frac{dAAR(D)}{dD} - \frac{dICC(D)}{dD} = 0 \quad (3.6)$$

Rearranging the equation above gives:

$$C \frac{dAAR(D)}{dD} = - \frac{dICC(D)}{dD} \quad (3.7)$$

Equation 3.7 shows that the constant, C , has an effect on the rotor diameter that maximizes NPV. Therefore, the financial assumptions that go into determining the discount rate and life of the investment will change the optimum design.

3.1.4 Internal Rate of Return

The internal rate of return (IRR) is the discount rate which sets NPV equal to zero [20]. The IRR for a wind turbine with uniform revenue is found by solving the equation below for IRR. The design with the greatest IRR is chosen as the optimum. If IRR is maximized, the financial assumptions required to determine the life of the project, N , have no effect on the optimal design. Furthermore, maximizing IRR will result in the same design as when SPB is minimized. This is proven below.

$$NPV = AAR \left[\frac{(1 + IRR)^N - 1}{IRR(1 + IRR)^N} \right] - ICC = 0 \quad (3.8)$$

where:

$IRR \equiv$ internal rate of return

$N \equiv$ life of the wind turbine in years

$ICC \equiv$ initial capital cost

$AAR \equiv$ average annual revenue based on hourly production

This equation can be rearranged to give:

$$\left[\frac{(1 + IRR)^N - 1}{IRR(1 + IRR)^N} \right] = \frac{ICC}{AAR} = SPB \quad (3.9)$$

As IRR increases, the left hand side of the above equation decreases for any value of N . The ratio ICC/AAR , which is equivalent to SPB , must then also decrease with increasing IRR. This proves that maximizing IRR will have the same effect as minimizing SPB no matter what the life of the project is assumed to be.

3.1.5 NPV vs. SPB and IRR

NPV is a function of $AAR - ICC$. As a result, maximizing NPV will maximize the absolute wealth created by the investment. Because of this, NPV is biased towards larger investments. As long as the relative return is larger than the discount rate, NPV analysis will push the decision to larger projects even if the relative return is decreasing.

On the other hand, SPB , and IRR are functions of ICC/AAR . Minimizing ICC/AAR will maximize wealth relative to the capital invested. For the purpose of optimizing a wind turbine, it must be decided which objective is more important, to maximize the absolute wealth gained from the turbine or to maximize the relative wealth generated by the turbine. Since a wind turbine is modular, it is more desirable to choose the rotor size that maximizes the turbine's relative ability to generate wealth. Therefore, this study chooses to minimize SPB because it is the simplest method, and as was shown

before, minimizing SPB will result in the same optimal design as maximizing IRR. A case where it would be desirable to maximize absolute wealth would be if land available for wind farm development is limited. In such a case, the absolute wealth generated by the wind farm could be maximized by selecting a turbine with a larger generator capacity.

3.2 Cost Models

Developing accurate component cost models for wind turbines has been made difficult due to the rapid increase in the size of turbines. In the mid to late 1990s, the University of Sunderland developed a set of scaling tools for the wind turbines of that time. However, these tools were quickly out dated as larger turbines were developed. In 1999, DOE began its NREL WindPACT studies, which consisted of several major studies to determine more cost effective wind turbine designs. As part of the WindPACT studies, cost models were developed for each wind turbine component for various designs. The National Renewable Energy Laboratory study, *Wind Turbine Design Cost and Scaling Model*, concisely lists the most up-to-date cost and scaling models for several variations of a three-bladed, upwind, pitch-controlled, variable speed wind turbine [19]. All cost models below were taken from the *Wind Turbine Design Cost and Scaling Model* report.

3.2.1 Land Based Cost Models

Rotor Blade

The blade cost is the cost of a single blade. The blade mass is also given below because it is used in calculating the cost of other components. The figure below shows the blade cost as a function of rotor diameter.

$$Cost_{blade} = 0.5582 * R^3 + 3.8118 * R^{2.5025} - 955.24 \quad (3.10)$$

$$Mass_{blade} = 0.1452 * R^{2.9158} \quad (3.11)$$

where:

R ≡ rotor radius in meters

Cost is in 2002 \$

Mass is in kg

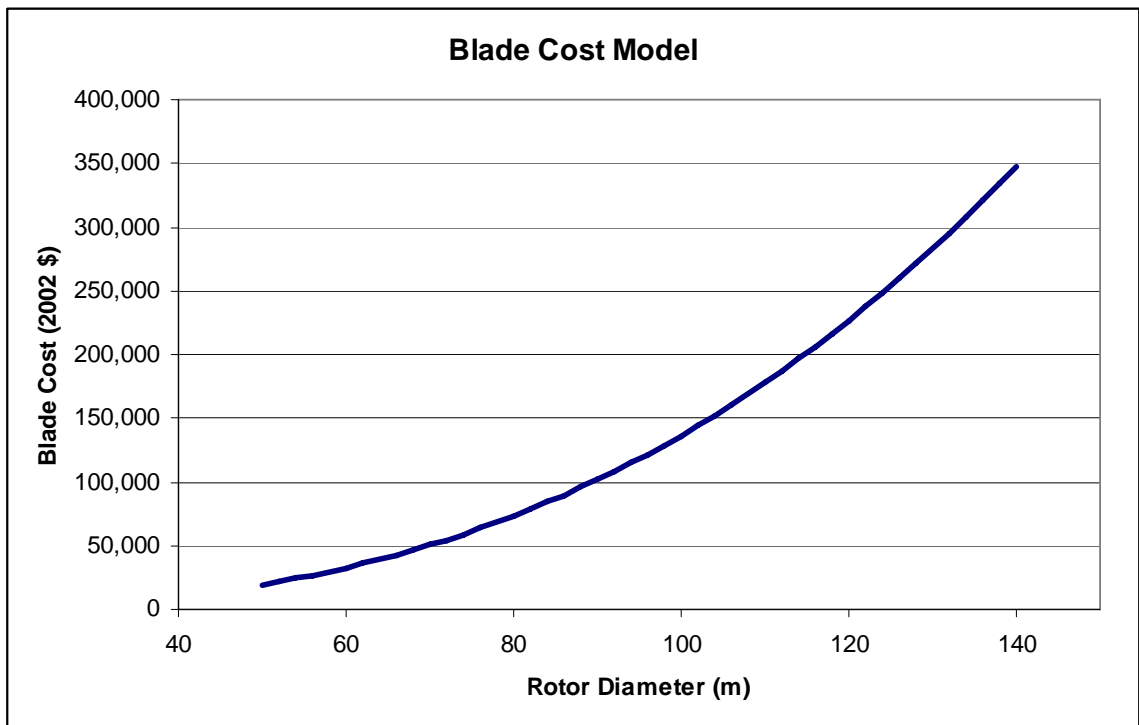


Figure 3.1: Blade Cost as a Function of Rotor Diameter

Rotor Hub

The hub cost is calculated below as a function of blade mass. The figure below shows this relation.

$$Cost_{hub} = 4.05 * Mass_{blade} + 24141 \quad (3.12)$$

where:

Cost is in 2002 \$

Mass is in kg

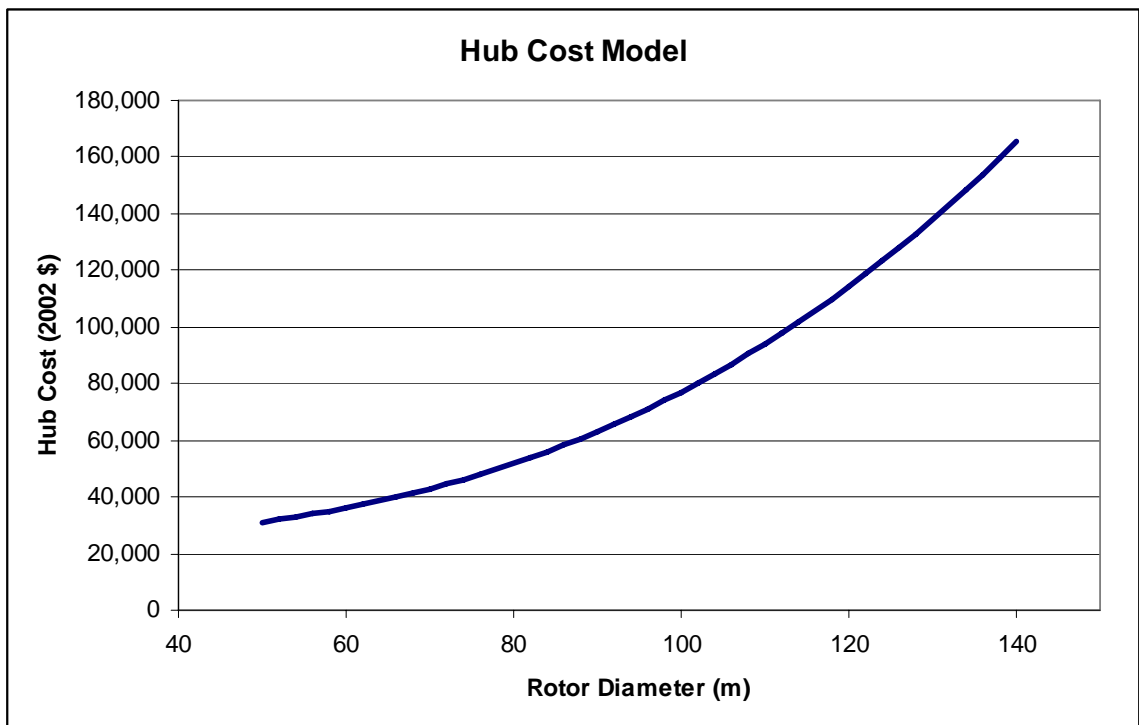


Figure 3.2: Hub Cost as a Function of Rotor Diameter

Pitch System

The total pitch system cost is given below as a function of rotor diameter. This cost is for the pitch mechanisms on all three blades. The figure below shows the pitch system cost as a function of rotor diameter.

$$Cost_{total_pitch_system} = 0.4802 * D^{2.6578} \quad (3.13)$$

where:

$D \equiv$ rotor diameter in meters

Cost is in 2002 \$

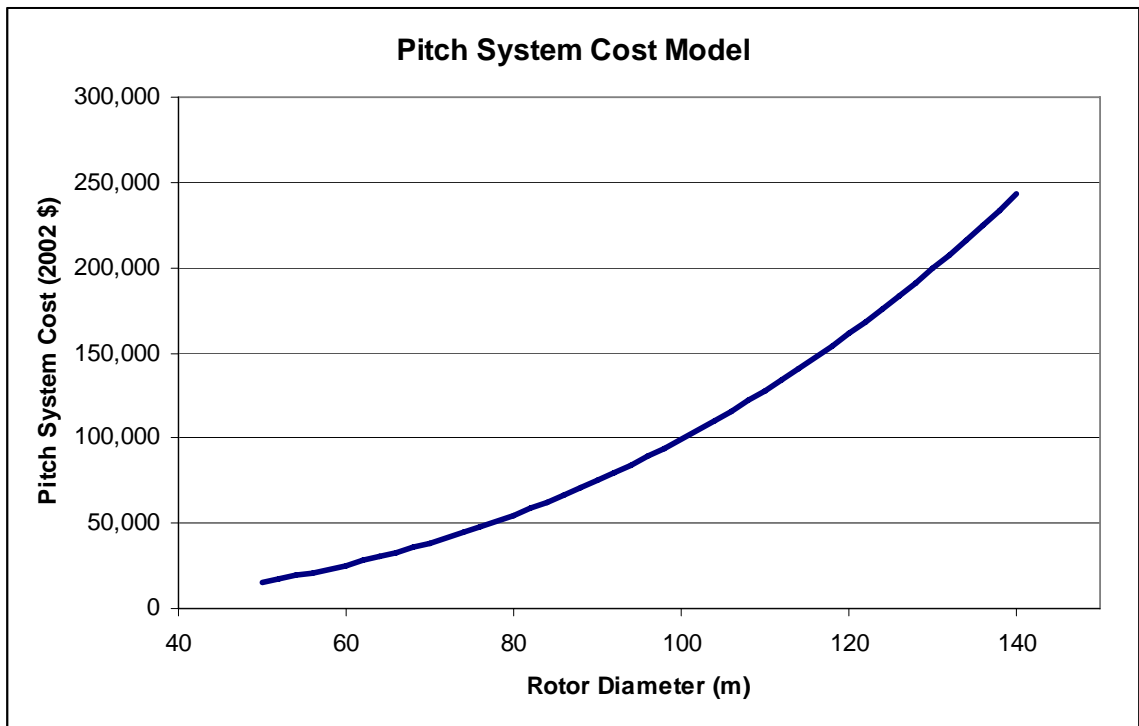


Figure 3.3: Pitch System Cost as a Function of Rotor Diameter

Nose Cone

The nose cone cost is calculated as a function of rotor diameter. The figure below shows the nose cone cost as a function of rotor diameter.

$$Cost_{nose_cone} = 103 * D - 2899 \quad (3.14)$$

where:

$D \equiv$ rotor diameter in meters

Cost is in 2002 \$

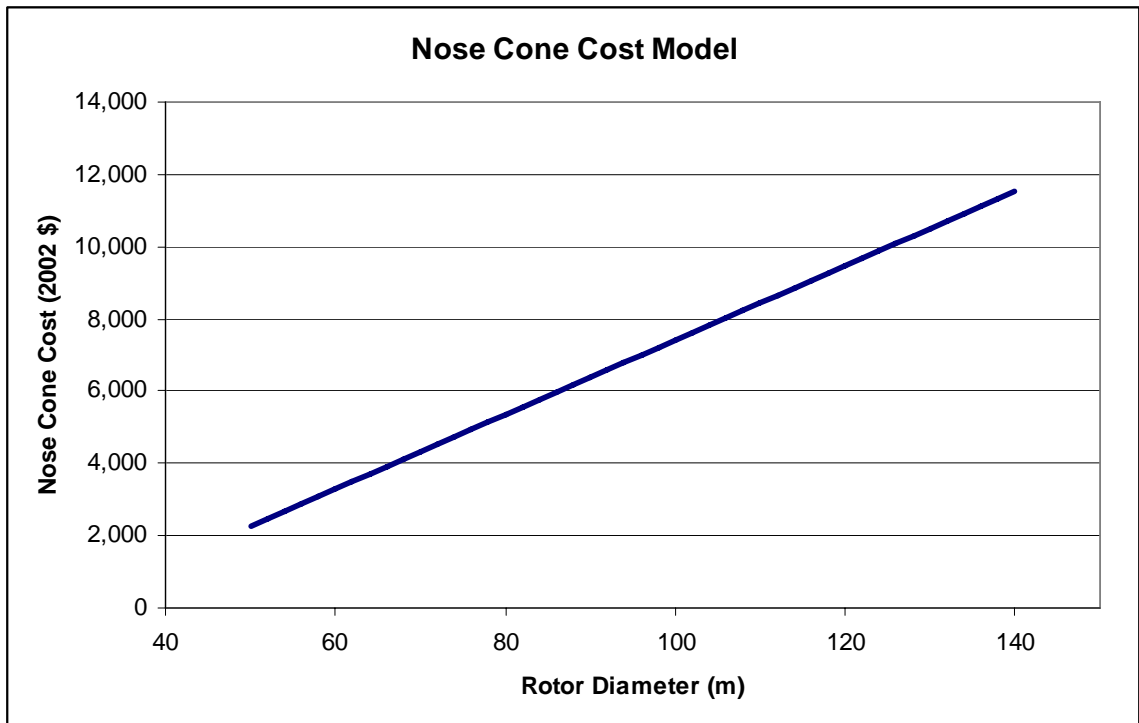


Figure 3.4: Nose Cone Cost as a Function of Rotor Diameter

Low-Speed Shaft

The low speed shaft cost is given below as a function of rotor diameter. The figure below shows the low-speed shaft cost as a function of rotor diameter.

$$Cost_{low-speed_shaft} = 0.1 * D^{2.887} \quad (3.15)$$

where:

D ≡ rotor diameter in meters

Cost is in 2002 \$

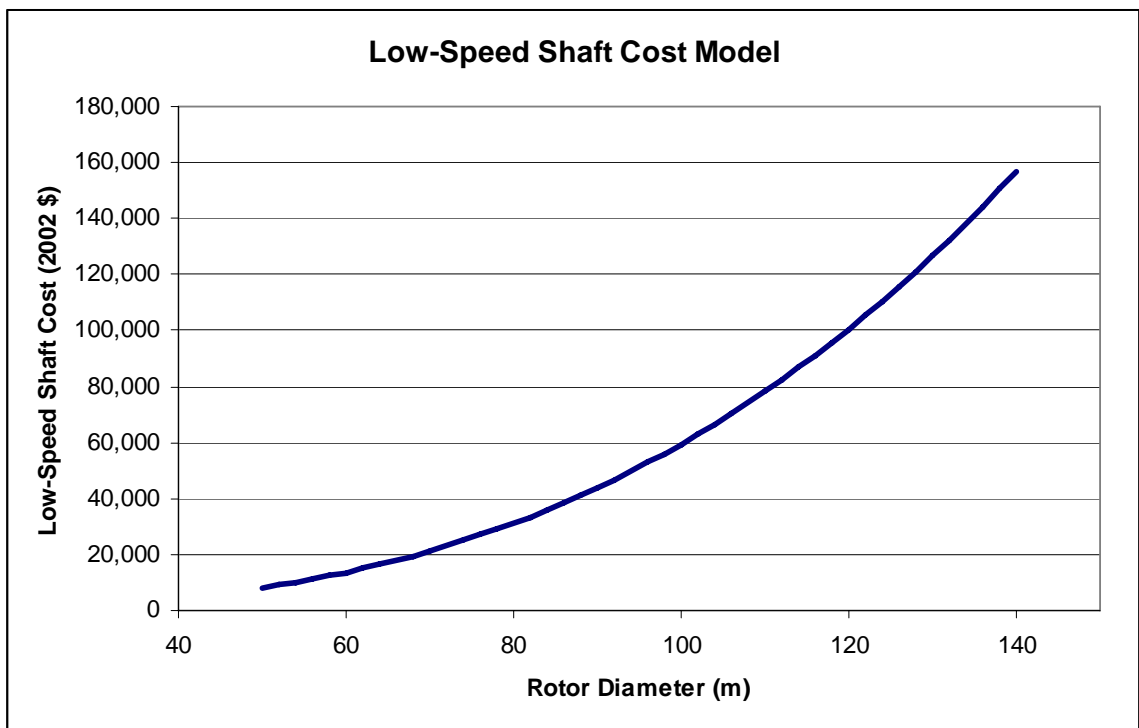


Figure 3.5: Low-Speed Shaft Cost as a Function of Rotor Diameter

Main Bearings

The bearing system cost is calculated as a function of rotor diameter. The figure below shows the main bearing cost as a function of rotor diameter.

$$Cost_{bearing_system} = D^{2.5} (0.0043 * D - 0.011) \quad (3.16)$$

where:

$D \equiv$ rotor diameter in meters

Cost is in 2002 \$

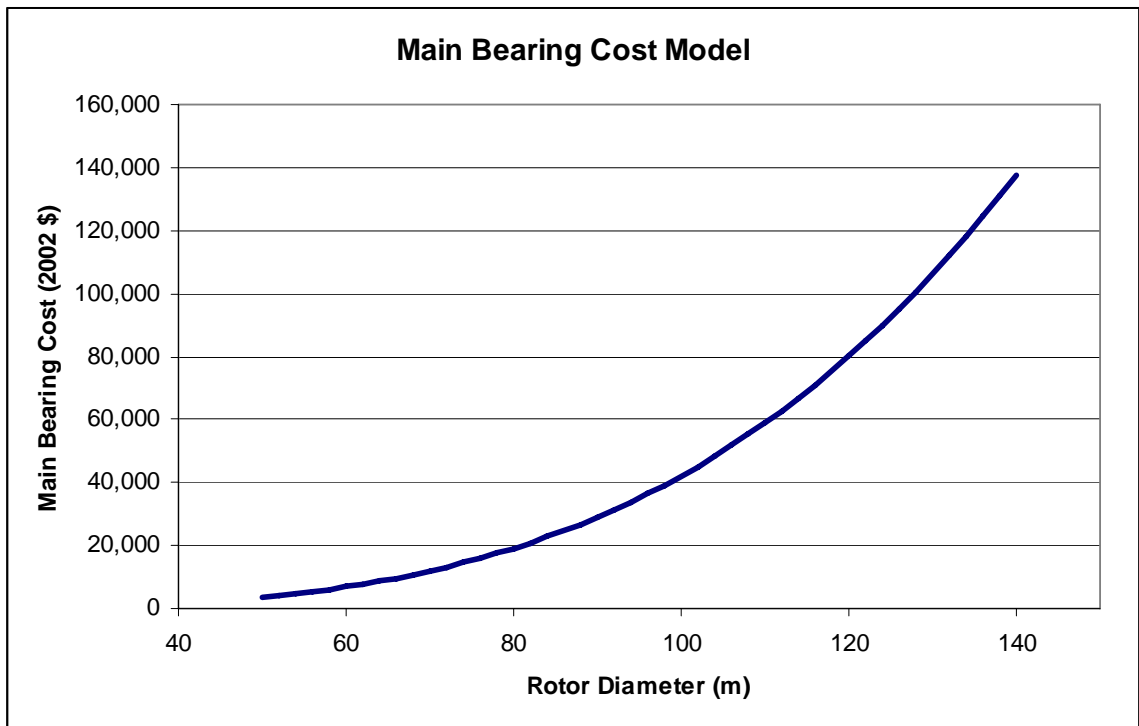


Figure 3.6: Main Bearing Cost as a Function of Rotor Diameter

Gearbox – Three-Stage Planetary/Helical

The gearbox cost is given below as a function of machine rating, which is the same as generator capacity. The gearbox cost given below is only for a three stage planetary/helical gearbox design, which is the most popular design on wind turbines. However, other gearbox designs are used by some manufactures.

$$Cost_{gearbox} = 16.45 * MR^{1.249} \quad (3.17)$$

where:

$MR \equiv$ machine rating in kW
Cost is in 2002 \$

Mechanical Brake, High-Speed Coupling, and Associated Components

The mechanical parking brake and coupling cost are given below as a function of machine rating.

$$Cost_{brake/coupling} = 1.9894 * MR - 0.1141 \quad (3.18)$$

where:

$MR \equiv$ machine rating in kW
Cost is in 2002 \$

Generator – Three-Stage Drive with High-Speed Generator

The generator cost is given below as a function of machine rating. This cost is only applicable for a high-speed wound rotor generator. Other generator/drive train combinations exist but the high-speed wound rotor generator in combination with a three stage gearbox is most common.

$$Cost_{generator} = 65 * MR \quad (3.19)$$

where:

$MR \equiv$ machine rating in kW

Cost is in 2002 \$

Variable-Speed Electronics

The variable-speed electronics cost is given below as a function of machine rating.

$$Cost_{electronics} = 79 * MR \quad (3.20)$$

where:

$MR \equiv$ machine rating in kW

Cost is in 2002 \$

Yaw System

The yaw system cost is given below as a function of rotor diameter. The figure below shows the yaw system cost as a function of rotor diameter.

$$Cost_{yaw_system} = 0.0678 * D^{2.964} \quad (3.21)$$

where:

$D \equiv$ rotor diameter in meters

Cost is in 2002 \$

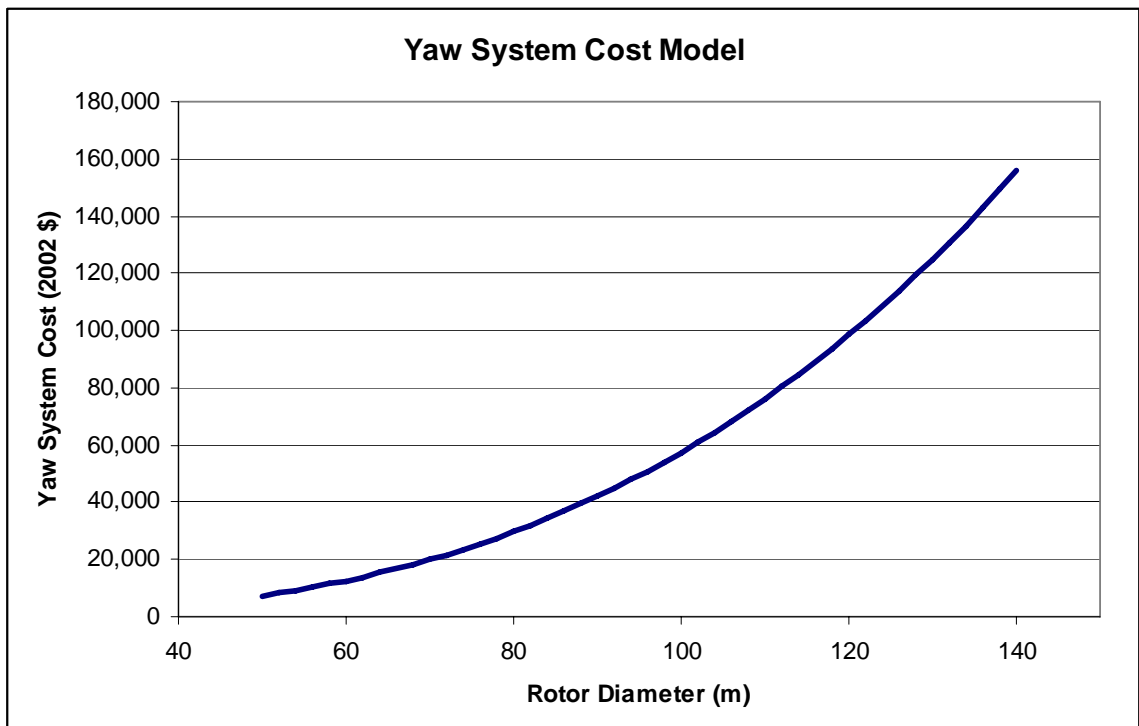


Figure 3.7: Yaw System Cost as a Function of Rotor Diameter

Mainframe – Three-Stage Drive with High-Speed Generator

The mainframe cost is given below as a function of rotor diameter. The mainframe cost depends on the drive train design. The cost function given below is for a three-stage

drive with a high-speed wound rotor generator. The mainframe mass is also given below. The mass is used in other component cost models below. The figure below shows the mainframe cost as a function of rotor diameter.

$$Cost_{mainframe} = 9.489 * D^{1.953} \quad (3.22)$$

where:

$D \equiv$ rotor diameter in meters

Cost is in 2002 \$

$$Mass_{mainframe} = 2.233 * D^{1.953} \quad (3.23)$$

where:

$D \equiv$ rotor diameter in meters

Mass is in kg

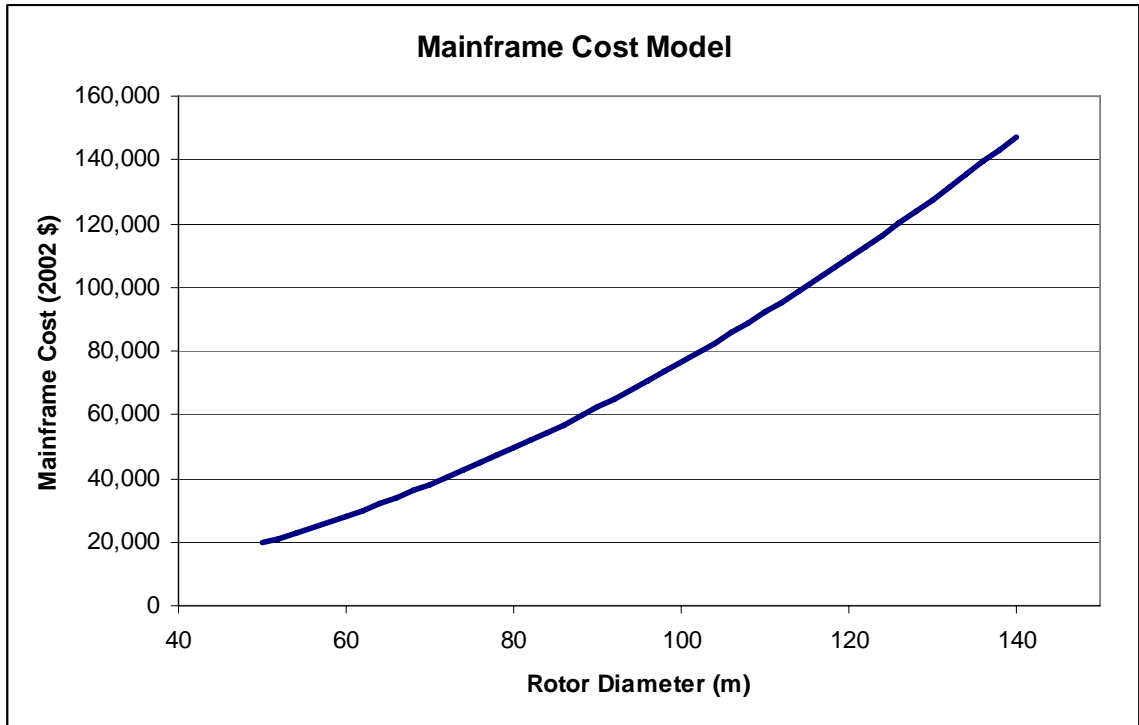


Figure 3.8: Mainframe Cost as a Function of Rotor Diameter

Platforms and Railings

A wind turbine will contain various platforms and railings. The platform and railing cost is calculated as a function of the mainframe mass. The figure below shows the pitch platforms and railings cost as a function of rotor diameter.

$$Cost_{platform_and_railing} = 1.09 * Mass_{mainframe_mass} \quad (3.24)$$

where:

Cost is in 2002 \$

Mass is in kg

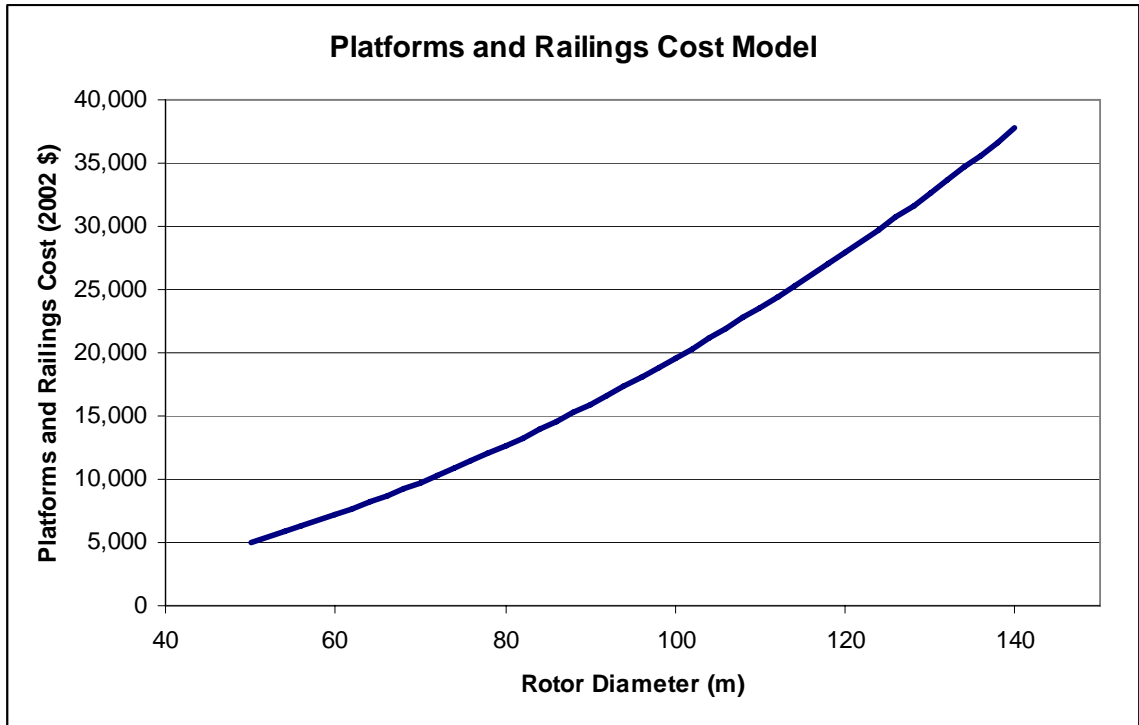


Figure 3.9: Platforms and Railings Cost as a Function of Rotor Diameter

Electrical Connections

The electrical connections cost is the cost of any wiring within the turbine. This includes any tower wiring. The electrical connections cost is given below as a function of machine rating.

$$Cost_{electrical_connection} = 40 * MR \quad (3.25)$$

where:

$MR \equiv$ machine rating in kW

Cost is in 2002 \$

Hydraulic and Cooling Systems

The hydraulic and cooling systems cost is given below as a function of machine rating.

$$Cost_{hydraulic_and_cooling} = 12 * MR \quad (3.26)$$

where:

$MR \equiv$ machine rating in kW

Cost is in 2002 \$

Nacelle Cover

The nacelle cover cost is given below as a function of machine rating.

$$Cost_{nacelle_cover} = 11.537 * MR + 3849.7 \quad (3.27)$$

where:

$MR \equiv$ machine rating in kW

Cost is in 2002 \$

Control, Safety System, and Condition Monitoring

The cost of control, safety system, and condition monitoring equipment is estimated to be \$35,000 per turbine.

$$Cost_{control_safety_monitoring} = \$35,000 \quad (3.28)$$

where:

Cost is in 2002 \$

Tower

The tower cost is given below as a function of rotor swept area and hub height. The figure below shows the tower cost as a function of rotor diameter for various hub heights.

$$Cost_{tower} = 0.596 * A * H - 2121 \quad (3.29)$$

where:

A ≡ rotor swept area

H ≡ hub height

Cost is in 2002 \$

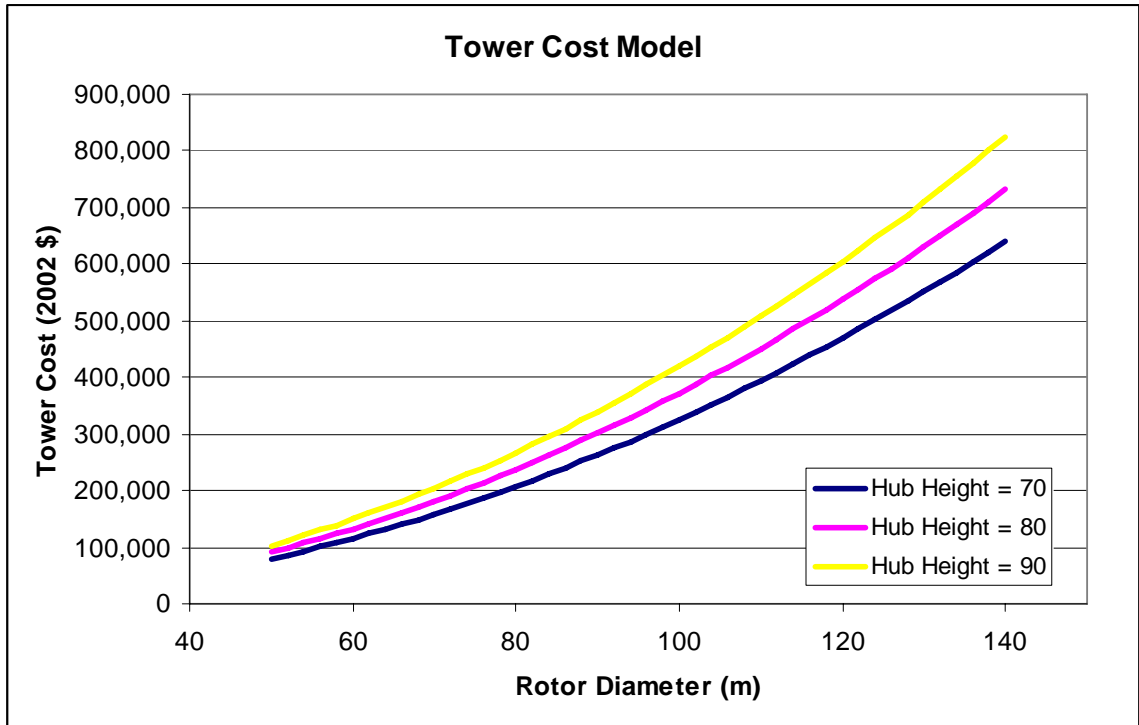


Figure 3.10: Tower Cost as a Function of Rotor Diameter for Different Hub Heights

Foundation

The foundation cost is given below as a function of rotor swept area and hub height. The figure below shows the foundation cost as a function of rotor diameter for various hub heights.

$$Cost_{foundation} = 303.24(A * H)^{0.4037} \tag{3.30}$$

where:

A ≡ rotor swept area

H ≡ hub height

Cost is in 2002 \$

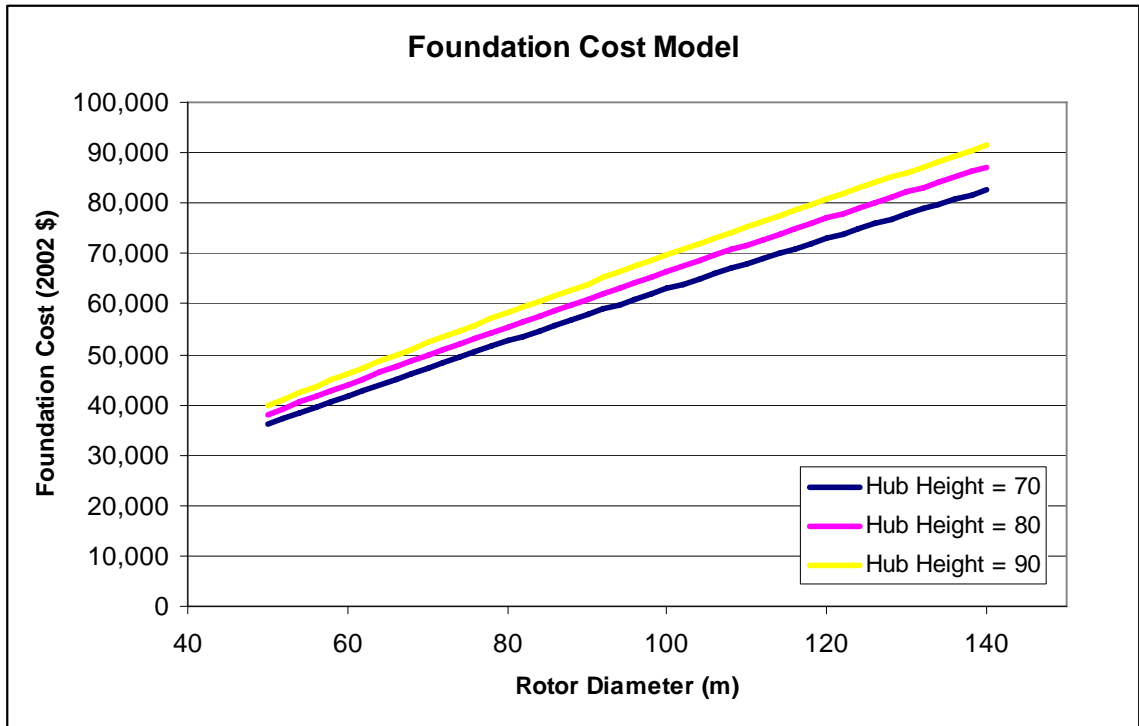


Figure 3.11: Foundation Cost as a Function of Rotor Diameter

Transportation

The transportation cost is calculated as a function of machine rating.

$$Cost_{transportation} = (1.58E-5)*MR^3 - 0.0375*MR^2 + 54.7*MR \quad (3.31)$$

where:

$MR \equiv$ machine rating in kW

Cost is in 2002 \$

Roads and Civil Work

It is often necessary to modify roads and perform other civil works when transporting and erecting a wind turbine. The roads and civil work cost is given below as a function of machine rating.

$$Cost_{roads_civil_work} = (2.17E-6) * MR^3 - 0.0145 * MR^2 + 69.54 * MR \quad (3.32)$$

where:

$MR \equiv$ machine rating in kW

Cost is in 2002 \$

Assembly and Installation

The assembly and installation cost of the wind turbine is given below as a function of hub height and rotor diameter. The figure below shows the assembly and installation cost as a function of rotor diameter for various hub heights.

$$Cost_{assembly_and_installation} = 1.965 * (H * D)^{1.1736} \quad (3.33)$$

where:

$H \equiv$ hub height

$D \equiv$ rotor diameter

Cost is in 2002 \$

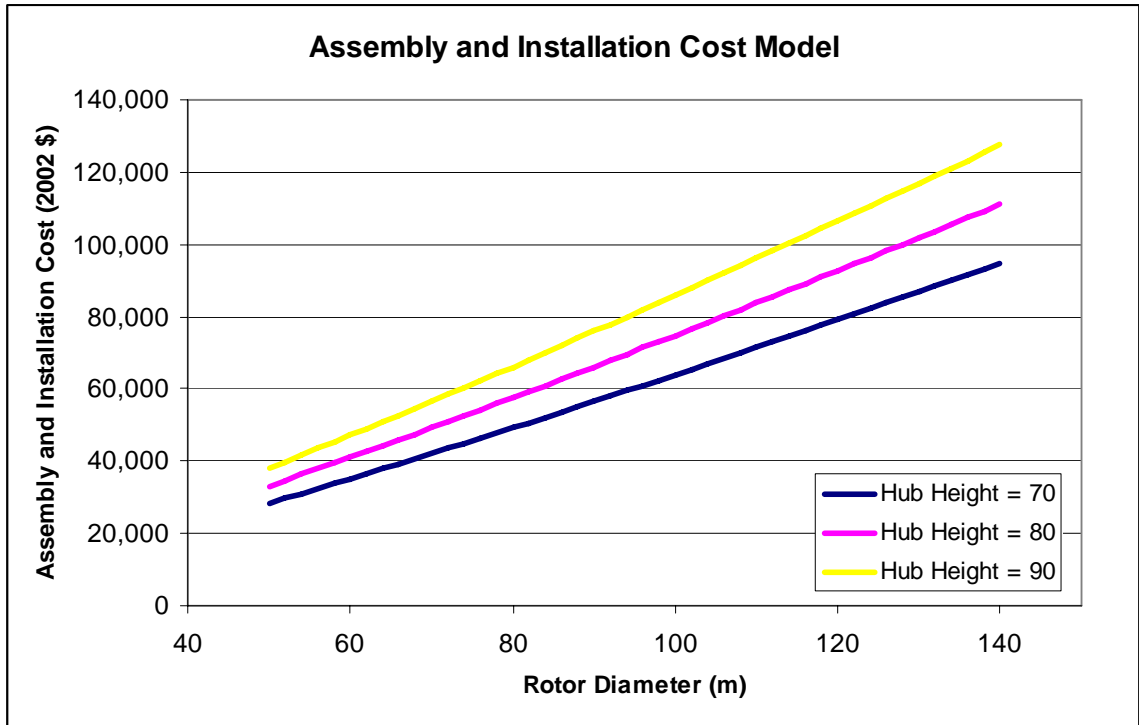


Figure 3.12: Assembly and Installation Cost as a Function of Rotor Diameter

Electrical Interface

The electrical interface cost includes the turbine transformer and the individual turbines share of cables used to connect the turbine to the substation. The electrical interface cost is given below as a function of machine rating.

$$Cost_{electrical_interface} = (3.49E - 6) * MR^3 - 0.0221 * MR^2 + 109.7 * MR \quad (3.34)$$

where:

$MR \equiv$ machine rating in kW

Cost is in 2002 \$

Engineering and Permitting

The engineering and permitting cost is given below as a function of machine rating.

$$Cost_{engineering_permitting} = (9.94E - 4) * MR^2 + 20.31 * MR \quad (3.35)$$

where:

$MR \equiv$ machine rating in kW

Cost is in 2002 \$

Levelized Replacement Cost (LRC)

The levelized replacement cost (LRC) is to cover long-term replacements and overhaul of major turbine components. The LRC is given below as a function of machine rating.

$$LRC = 10.7 * MR \quad (3.36)$$

where:

$MR \equiv$ machine rating in kW

LRC is in 2002 \$

Operations and Maintenance

The operations and maintenance (O&M) cost covers day-to-day scheduled and unscheduled maintenance. The O&M cost is given below as a function of annual energy production.

$$Cost_{O\&M} = 0.007 \quad (3.37)$$

where:

Cost is in 2002 \$ per kWh

Land Lease Cost (LLC)

A wind farm developer typically must lease the land on which the turbines will stand. The land lease cost varies widely from site to site depending on the value of the land and the potential market price for the wind. The *Wind Turbine Design Cost and Scaling Model* report estimates the land lease cost to be a function of annual energy production.

$$LLC = 0.00108 \quad (3.38)$$

where:

LLC is in 2002 \$ per kWh

3.2.2 Additional Offshore Cost Models

The cost models given below for an offshore wind farm are only rough estimates. These models are for shallow water only, which is defined as a water depth of less than 25 meters. It is assumed that the wind farm would be located 8 kilometers offshore. The models are based on a wind farm of 167 turbines with 3 MW ratings.

Marinization Cost

An offshore wind turbine is subjected to a harsh environment. Therefore, the turbine must be maritized. The cost of maritization is estimated to be 13.5% of the turbine cost, which is the cost of all equipment from the tower up.

Offshore Control, Safety System, and Condition Monitoring

Offshore systems are expected to be more sophisticated and extensive. Therefore, the cost of control, safety system, and condition monitoring equipment for an offshore turbine is estimated to be \$55,000 per turbine.

$$Cost_{\text{offshore_control_safety_monitoring}} = \$55,000 \quad (3.39)$$

where:

Cost is in 2002 \$

Offshore Support Structure

While land based turbines are placed on a concrete foundation, offshore turbines require a different support structure. The offshore support structure must extend from the sea bed to sea level. Several offshore support structure types exist. The model below is for the most common type, a steel pile driven into the sea bed. The model includes the cost of installation of the pile as well. The offshore support structure cost replaces the foundation cost for an offshore wind turbine. The offshore support structure cost is given below as a function of machine rating.

$$Cost_{\text{offshore_support_structure}} = 294 * MR \quad (3.40)$$

where:

$MR \equiv$ machine rating in kW

Cost is in 2002 \$

Offshore Transportation

The transportation cost for an offshore turbine is taken to be the same as a land based turbine. In the case of an offshore turbine, the components are being transported to the port and staging area.

Port and Staging Equipment

The port and staging equipment costs cover the facilities required to install and maintain an offshore wind farm. Such facilities would include ships and barges for installation of piles and installing underwater electrical lines. The port and staging equipment cost is given below as a function of machine rating.

$$Cost_{\text{port_and_staging_equipment}} = 20 * MR \quad (3.41)$$

where:

$MR \equiv$ machine rating in kW

Cost is in 2002 \$

Offshore Turbine Installation

The installation of an offshore turbine involves higher costs than a land based turbine. The offshore turbine installation cost also include transporting the turbine from the port to the wind farm. The offshore turbine installation cost is given below as a function of machine rating.

$$Cost_{\text{offshore_turbine_installation}} = 98 * MR \quad (3.42)$$

where:

$MR \equiv$ machine rating in kW

Cost is in 2002 \$

Offshore Electrical Interface and Connection

The power created by an offshore wind farm must be transferred back to shore. In addition, cabling is required between the individual turbines in the wind farm. All of these cables are underwater and buried beneath the sea bed. The offshore electrical interface and connection cost is given below as a function of machine rating.

$$Cost_{\text{offshore_electrical_interface_and_connection}} = 255 * MR \quad (3.43)$$

where:

$MR \equiv$ machine rating in kW

Cost is in 2002 \$

Offshore Permits, Engineering, and Site Assessment

The offshore engineering and permitting cost is higher for an offshore site. The offshore engineering and permitting cost is given below as a function of machine rating.

$$Cost_{\text{offshore_engineering_and_permits}} = 36 * MR \quad (3.44)$$

where:

$MR \equiv$ machine rating in kW

Cost is in 2002 \$

Personal Access Equipment

A turbine located offshore requires special access equipment for maintenance operations. The access equipment cost is given below.

$$Cost_{\text{access_equipment}} = 58800 \quad (3.45)$$

where:

Cost is in 2002 \$

Scour Protection

The sea floor around the foundation of an offshore wind farm must be protected from erosion. This is referred to as scour protection. The scour protection cost is given below as a function of machine rating. This cost is a component of the initial capital cost.

$$Cost_{scour_protection} = 54 * MR \quad (3.46)$$

where:

$MR \equiv$ machine rating in kW

Cost is in 2002 \$

Surety Bond

If an offshore wind farm is decommissioned, the wind turbines and foundations must be removed to prevent them from becoming navigation hazards. As a result, a surety bond guarantees funds will be available to remove these structures. The surety bond cost is given below as a function of the initial capital cost and offshore warranty cost. This cost is a component of the initial capital cost.

$$Cost_{surety_bond} = 0.03 * (ICC - Cost_{offshore_warranty}) \quad (3.47)$$

where:

$ICC \equiv$ the initial capital cost of the installed turbine

$Cost_{offshore_warranty} \equiv$ the offshore warranty cost calculated below

Offshore Warranty

Wind turbines located offshore will be subject to more extreme environments than those located onshore. Therefore, an additional warranty is required for offshore wind turbines. The offshore warranty is given below as a function of offshore turbine cost, where

offshore turbine cost includes the cost of tower and all the components above it. This cost is a component of the initial capital cost.

$$Cost_{\text{offshore_warranty}} = 0.15 * Cost_{\text{offshore_turbine}} \quad (3.48)$$

Offshore Levelized Replacement Cost

Since turbines located offshore will be subject to a more extreme environment, the risk of wear and damage is higher. Therefore, a larger levelized replacement cost (LRC) is needed. The offshore LRC is given below as a function of machine rating. LRC is an annual cost.

$$LRC_{\text{offshore}} = 16.7 * MR \quad (3.49)$$

where:

$MR \equiv$ machine rating in kW

LRC is in 2002 \$

Offshore Bottom Lease Cost

The offshore bottom lease cost is taken to be the same as the onshore land lease cost.

Offshore O&M

Since turbines located offshore will be subject to a more extreme environment, the risk of wear and damage is higher. Therefore, a larger O&M cost is needed. The offshore O&M

cost is given below as a function of annual energy production. The cost is taken to be per kWh produced.

$$Cost_{offshore_O\&M} = 0.0196 \quad (3.50)$$

where:

Cost is in 2002 \$ per kWh

3.2.3 Summary of Cost Models

The cost models described above have been summarized in this section. Tables 3.1 and 3.2 list the cost models needed to calculate the initial capital cost of a land based wind turbine and the initial capital cost of an offshore wind turbine respectively. As stated above, all of these cost models are taken directly from the NREL *Wind Turbine Design Cost and Scaling Model* study. Additionally, the cost models for a land based turbine have been condensed below. Equation 3.51 splits the initial capital cost of a land based turbine into two parts, the turbine cost and the supporting cost. The turbine cost includes the rotor, the nacelle, and all components housed inside the nacelle (i.e. the cost of everything sitting on top of the tower). The supporting cost includes the tower, foundation, transportation, roads and civil work, assembly and installation, electrical interface with grid, and engineering/permitting. The supporting cost is sensitive to the particular site in which the turbine will be installed.

$$ICC_{land_based} = Cost_{turbine} + Cost_{supporting} \quad (3.51)$$

$$\begin{aligned}
Cost_{turbine} = & 0.0043D^{3.5} + 0.209D^3 + 0.0678D^{2.964} + 0.0779D^{2.9158} + \\
& 0.1D^{2.887} + 0.48D^{2.6578} + 2.02D^{2.5025} - 0.011D^{2.5} + \\
& 11.9D^{1.953} + 103D + 16.5(MR)^{1.249} + 210MR + 57200
\end{aligned} \tag{3.52}$$

$$\begin{aligned}
Cost_{supporting} = & (2.1E-5)*MR^3 - 0.0731MR^2 + 254MR + \\
& 0.468D^2H + 275(D^2H)^{0.4037} + 1.97(DH)^{1.1736} - \\
& 2121
\end{aligned} \tag{3.53}$$

where:

D \equiv rotor diameter

MR \equiv machine rating in kW

H \equiv hub height

Cost is in 2002 \$

Table 3.1: Summary of Initial Capital Cost Components for Land Based Turbine

| |
|--|
| $Cost_{blade} = 0.5582 * R^3 + 3.8118 * R^{2.5025} - 955.24$ |
| $Mass_{blade} = 0.1452 * R^{2.9158}$ |
| $Cost_{hub} = 4.05 * Mass_{blade} + 24141$ |
| $Cost_{total_pitch_system} = 0.4802 * D^{2.6578}$ |
| $Cost_{nose_cone} = 103 * D - 2899$ |
| $Cost_{low-speed_shaft} = 0.1 * D^{2.887}$ |
| $Cost_{bearing_system} = D^{2.5} (0.0043 * D - 0.011)$ |
| $Cost_{gearbox} = 16.45 * MR^{1.249}$ |
| $Cost_{brake/coupling} = 1.9894 * MR - 0.1141$ |
| $Cost_{generator} = 65 * MR$ |
| $Cost_{electronics} = 79 * MR$ |
| $Cost_{yaw_system} = 0.0678 * D^{2.964}$ |
| $Cost_{mainframe} = 9.489 * D^{1.953}$ |
| $Mass_{mainframe} = 2.233 * D^{1.953}$ |
| $Cost_{platform_and_railing} = 1.09 * Mass_{mainframe_mass}$ |
| $Cost_{electrical_connection} = 40 * MR$ |
| $Cost_{hydraulic_and_cooling} = 12 * MR$ |
| $Cost_{nacelle_cover} = 11.537 * MR + 3849.7$ |
| $Cost_{control_safety_monitoring} = \$35,000$ |
| $Cost_{tower} = 0.596 * A * H - 2121$ |
| $Cost_{foundation} = 303.24 (A * H)^{0.4037}$ |
| $Cost_{transportation} = (1.58E-5) * MR^3 - 0.0375 * MR^2 + 54.7 * MR$ |
| $Cost_{roads_civil_work} = (2.17E-6) * MR^3 - 0.0145 * MR^2 + 69.54 * MR$ |
| $Cost_{assembly_and_installation} = 1.965 * (H * D)^{1.1736}$ |
| $Cost_{electrical_interface} = (3.49E-6) * MR^3 - 0.0221 * MR^2 + 109.7 * MR$ |
| $Cost_{engineering_permitting} = (9.94E-4) * MR^2 + 20.31 * MR$ |

Table 3.2: Summary of Initial Capital Cost Components for Offshore Turbine

| |
|--|
| $Cost_{blade} = 0.5582 * R^3 + 3.8118 * R^{2.5025} - 955.24$ |
| $Mass_{blade} = 0.1452 * R^{2.9158}$ |
| $Cost_{hub} = 4.05 * Mass_{blade} + 24141$ |
| $Cost_{total_pitch_system} = 0.4802 * D^{2.6578}$ |
| $Cost_{nose_cone} = 103 * D - 2899$ |
| $Cost_{low-speed_shaft} = 0.1 * D^{2.887}$ |
| $Cost_{bearing_system} = D^{2.5} (0.0043 * D - 0.011)$ |
| $Cost_{gearbox} = 16.45 * MR^{1.249}$ |
| $Cost_{brake/coupling} = 1.9894 * MR - 0.1141$ |
| $Cost_{generator} = 65 * MR$ |
| $Cost_{electronics} = 79 * MR$ |
| $Cost_{yaw_system} = 0.0678 * D^{2.964}$ |
| $Cost_{mainframe} = 9.489 * D^{1.953}$ |
| $Mass_{mainframe} = 2.233 * D^{1.953}$ |
| $Cost_{platform_and_railing} = 1.09 * Mass_{mainframe_mass}$ |
| $Cost_{electrical_connection} = 40 * MR$ |
| $Cost_{hydraulic_and_cooling} = 12 * MR$ |
| $Cost_{nacelle_cover} = 11.537 * MR + 3849.7$ |
| $Cost_{control_safety_monitoring} = 55,000$ |
| $Cost_{tower} = 0.596 * A * H - 2121$ |
| $Cost_{marinization} = 13.5 \% \text{ of all costs above}$ |
| $Cost_{offshore_support_structure} = 294 * MR$ |
| $Cost_{offshore_transportation} = (1.58E - 5) * MR^3 - 0.0375 * MR^2 + 54.7 * MR$ |
| $Cost_{port_and_staging_equipment} = 20 * MR$ |
| $Cost_{offshore_turbine_installation} = 98 * MR$ |
| $Cost_{offshore_electrical_interface_and_connection} = 255 * MR$ |
| $Cost_{offshore_engineering_and_permits} = 36 * MR$ |
| $Cost_{access_equipment} = 58800$ |
| $Cost_{scour_protection} = 54 * MR$ |
| $Cost_{surety_bond} = 0.03 * (ICC - Cost_{offshore_warranty})$ |
| $Cost_{offshore_warranty} = 0.15 * Cost_{offshore_turbine}$ |

3.3 Base Case Cost Analysis

The base case is defined as a turbine with a 3000 kW generator and 80 m hub height placed in a wind resource with an annual average wind speed of 7.5 m/s, Weibull shape parameter of 2, and wind shear power law exponent of 0.14. The optimum specific rotor rating for these conditions was found to be 0.34 kW/m². The component costs of the initial capital cost for the base case turbine design with minimum COE is given in the table below. The total initial capital cost of the base case is \$3,307,310. This is a very low value for a 3000 kW turbine. The reason for this is that the cost models do not represent actual pricing of wind turbines, which is a function of market factors. The cost models are designed to provide reliable scaling of cost with turbine size. In addition, the cost models are in 2002 dollars. Many of the raw materials needed in a wind turbine have significantly increased in price since 2002.

Table 3.3: Component Cost of Base Case Design with Minimum COE

| Component | Cost in 2002 \$ |
|---|------------------------|
| 3 Rotor Blades | 494,250 |
| Rotor Hub | 88,623 |
| Pitch System | 118,870 |
| Nose Cone | 8,127 |
| Low-Speed Shaft | 72,249 |
| Main Bearings | 53,450 |
| Gearbox | 362,320 |
| Brake and Coupling | 5,968 |
| Generator | 195,000 |
| Variable-Speed Electronics | 237,000 |
| Yaw System | 70,198 |
| Mainframe | 87,218 |
| Platforms and Railings | 22,321 |
| Electrical Connections | 120,000 |
| Hydraulic and Cooling Systems | 36,000 |
| Nacelle Cover | 38,461 |
| Control, Safety, and Monitoring Systems | 35,000 |
| Tower | 426,580 |
| Foundation | 70,184 |
| Transportation | 253,470 |
| Roads and Civil Work | 136,710 |
| Assembly and Installation | 81,005 |
| Electrical Interface | 224,430 |
| Engineering and Permitting | 69,876 |
| ICC | 3,307,310 |

A breakdown of the base case costs is shown below. The costs are divided into a rotor, nacelle, tower and foundation. The rotor group includes the blades, rotor hub, pitch system, and nose cone costs. The nacelle group includes the low-speed shaft, main bearings, gearbox, brake and coupling, generator, variable-speed electronics, yaw system, mainframe, platforms and railings, electrical connections, hydraulic cooling systems, nacelle cover, and control, safety, and monitoring systems. The tower and foundation group includes only the tower and foundation. The balance of station group includes transportation, roads and civil work, assembly and installation, electrical interface with grid, and engineering and permitting.

It can be seen from Figure 3.13 that the largest cost is for the Nacelle. The rotor cost and balance of station costs are nearly equal. The breakdown of costs for each group is shown below in Figures 3.14, 3.15, 3.16, and 3.17. Figure 3.14 shows the breakdown of rotor costs for the base case. It can be seen that nearly 70% of the rotor costs is for the rotor blades.

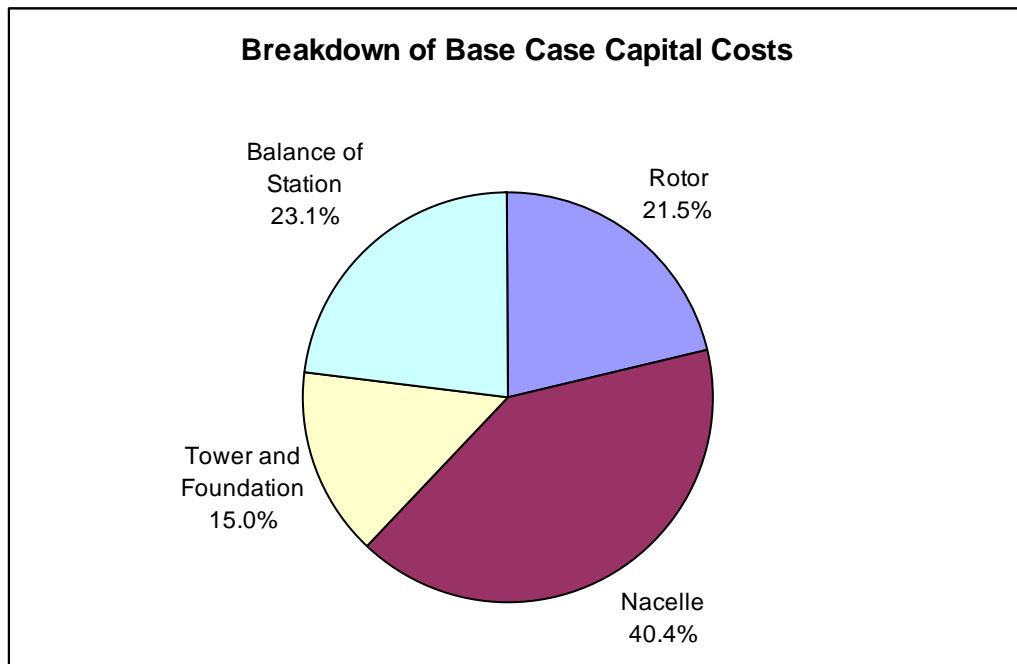


Figure 3.13: Breakdown of Base Case Capital Costs

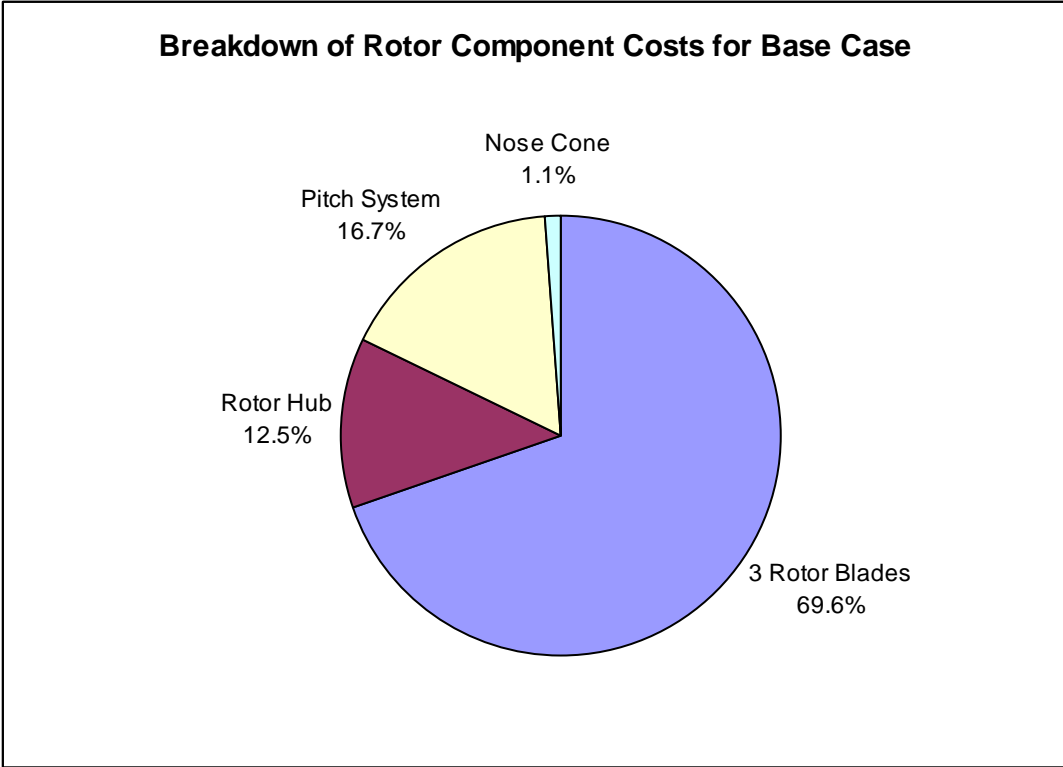


Figure 3.14: Breakdown of Rotor Component Costs for Base Case

Figure 3.15 shows the breakdown of the nacelle cost for the base case. With 27.1% of the nacelle cost, the gearbox makes up the largest percentage of the nacelle cost. The generator and variable speed electronics also make-up large percentages of the nacelle cost with 14.6% and 17.8% respectively. The breakdown of tower and foundation costs is shown below. With 86% of the tower and foundation cost, the tower cost is several times larger than the foundation cost.

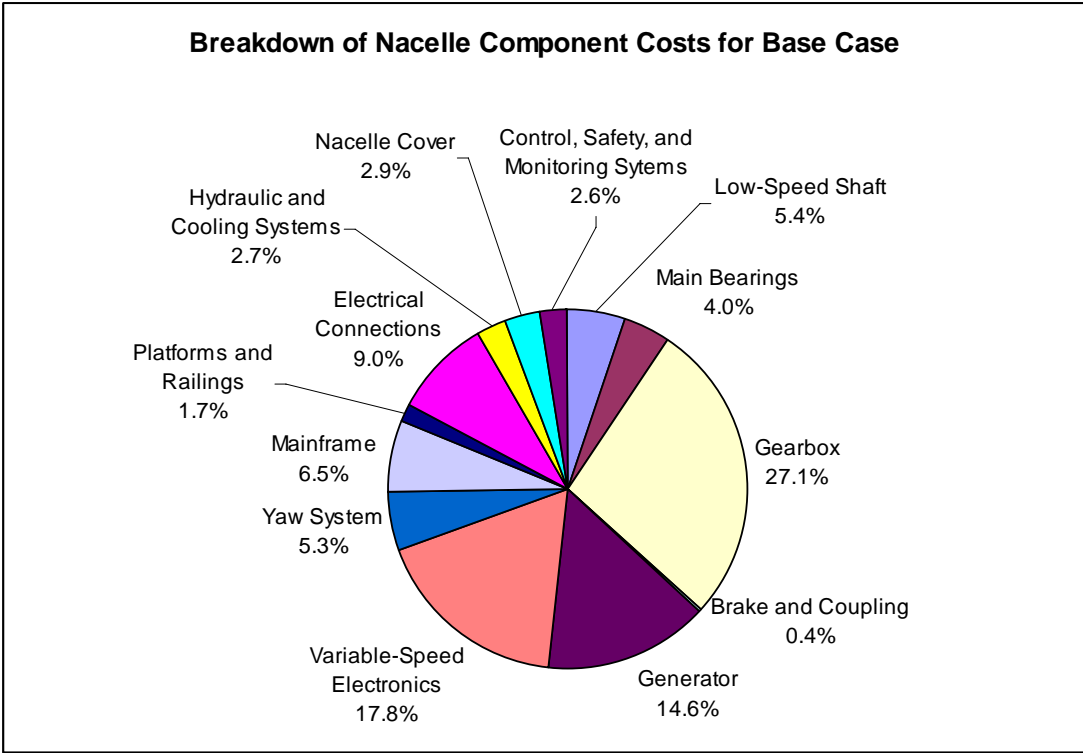


Figure 3.15: Breakdown of Nacelle Component Costs for Base Case

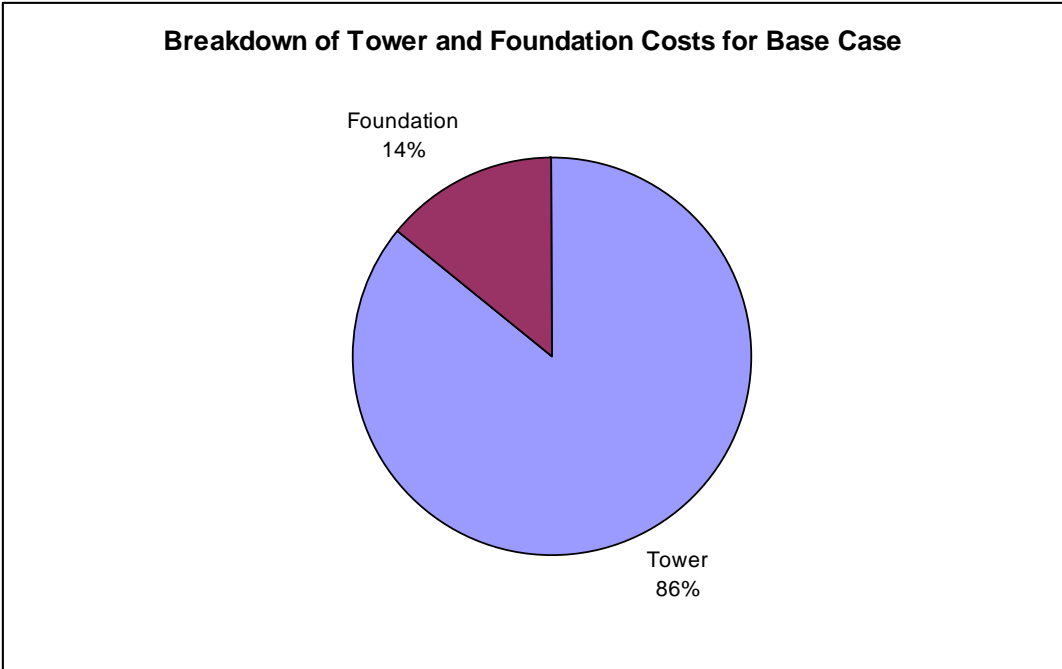


Figure 3.16: Breakdown of Tower and Foundation Costs for Base Case

The breakdown of balance of station cost is shown below. Transportation makes up the largest portion with 33% of balance of station cost. Transportation costs also begin to increase very fast as turbine size increases. The electrical interface with the grid also makes up a large percentage of the balance of station cost.

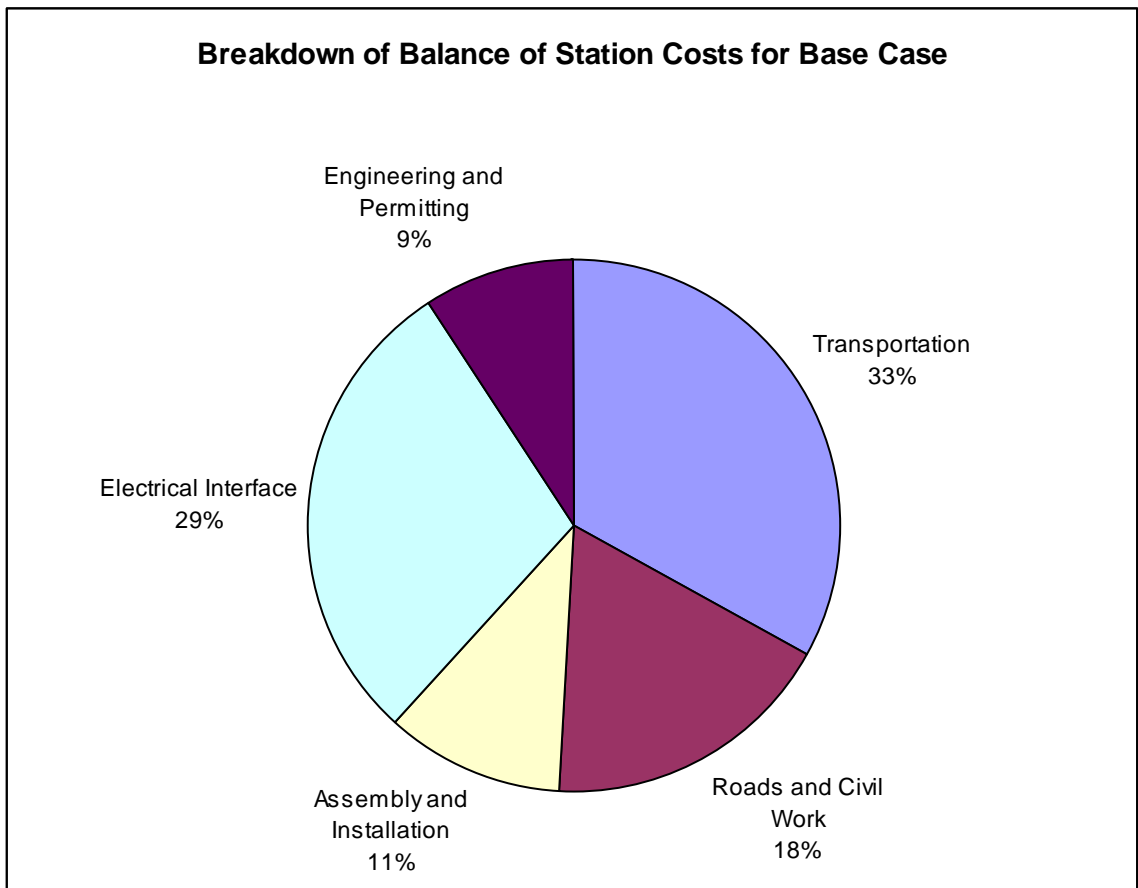


Figure 3.17: Breakdown of Balance of Station Costs for Base Case

The initial capital cost (ICC) of a 1500 kW turbine and a 4500 kW turbine are shown below in Table 3.4 and Table 3.5 respectively. The cost shown is for a turbine

with an optimal specific rating for the base case wind resource, which is an annual average wind speed of 7.5 m/s and a Weibull shape parameter equal to 2.

Table 3.4: ICC of an Optimal 1500 kW Turbine with Base Case Wind Resource

| Component | Cost in 2002 \$ |
|--|------------------------|
| 3 Rotor Blades | 206,445 |
| Rotor Hub | 49,986 |
| Pitch System | 51,660 |
| Nose Cone | 5,159 |
| Low-Speed Shaft | 29,221 |
| Main Bearings | 17,682 |
| Gearbox | 152,440 |
| Brake and Coupling | 2,984 |
| Generator | 97,500 |
| Variable-Speed Electronics | 118,500 |
| Yaw System | 27,714 |
| Mainframe | 47,277 |
| Platforms and Railings | 12,099 |
| Electrical Connections | 60,000 |
| Hydraulic and Cooling Systems | 18,000 |
| Nacelle Cover | 21,155 |
| Control, Safety, and Monitoring Sytems | 35,000 |
| Tower | 226,860 |
| Foundation | 54,486 |
| Transportation | 51,034 |
| Roads and Civil Work | 79,009 |
| Assembly and Installation | 56,066 |
| Electrical Interface | 126,600 |
| Engineering and Permitting | 32,701 |
| ICC | 1,579,578 |

Table 3.5: ICC of an Optimal 4500 kW Turbine with Base Case Wind Resource

| Component | Cost in 2002 \$ |
|--|------------------------|
| 3 Rotor Blades | 882,660 |
| Rotor Hub | 142,560 |
| Pitch System | 206,870 |
| Nose Cone | 10,682 |
| Low-Speed Shaft | 131,890 |
| Main Bearings | 111,360 |
| Gearbox | 601,210 |
| Brake and Coupling | 8,952 |
| Generator | 292,500 |
| Variable-Speed Electronics | 355,500 |
| Yaw System | 130,210 |
| Mainframe | 131,040 |
| Platforms and Railings | 33,536 |
| Electrical Connections | 180,000 |
| Hydraulic and Cooling Systems | 54,000 |
| Nacelle Cover | 55,766 |
| Control, Safety, and Monitoring Sytems | 35,000 |
| Tower | 648,340 |
| Foundation | 83,048 |
| Transportation | 927,460 |
| Roads and Civil Work | 217,050 |
| Assembly and Installation | 103,460 |
| Electrical Interface | 364,150 |
| Engineering and Permitting | 111,520 |
| ICC | 5,818,764 |

The total initial capital costs of the three turbines described above are plotted below in Figure 3.18. The turbines range in generator capacity from 1500 kW to 4500 kW. All three turbines have a rotor diameter which results in the minimum levelized cost of energy for the base case wind resource. As described above, the base case wind resource is an annual average wind speed of 7.5 m/s and a Weibull shape parameter equal to 2. It can be seen that the total initial capital cost increases significantly as the generator capacity increases. Specifically, for each kW increase in generator capacity, the total capital cost increases approximately \$1400.

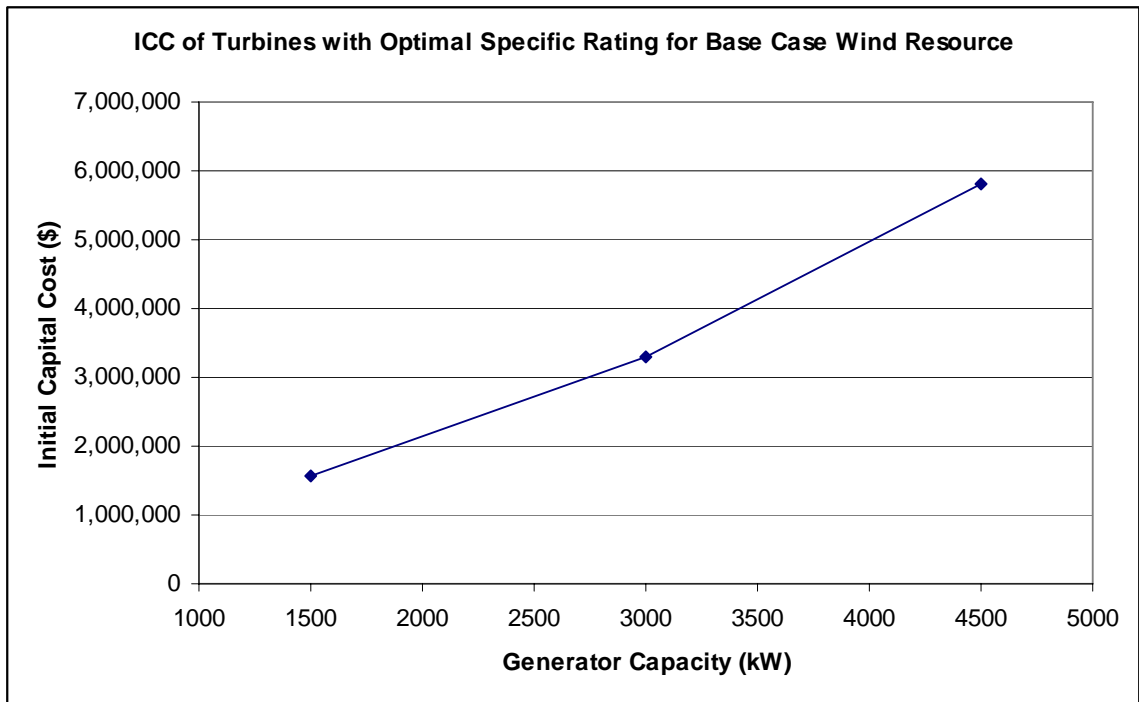


Figure 3.18: Initial Capital Cost of Turbines with Optimal Specific Ratings

Chapter 4: Electric Power Model

The electric power model calculates the power generated by the turbine over an annual period. To do this, the model calculates the power produced by the turbine over multiple wind speeds from the cut-in wind speed of the turbine, 4 m/s, to the cut-out wind speed, 27 m/s. This power is then multiplied by the amount of time the wind blows at each of those wind speeds, which is given by the Weibull distribution for that particular wind resource. However, the increments in wind speed from the cut-in speed to the cut-out speed are not constant. Instead, the increments are set such that the cube of the wind speed increments at 15 (m/s)³. Because power is a function of velocity cubed, smaller bin sizes are needed at higher wind speeds to obtain the same accuracy in annual electricity produced. Incrementing the wind speed cubed instead of wind speed results in the fewest number of power calculations, which significantly reduces the overall computation time.

In order to calculate the power at each wind speed, the model first calculates the power extracted from the wind by the rotor using blade element momentum theory. It then calculates the drive train efficiency to determine the power entering the electrical grid.

4.1 Blade Element Momentum Theory

Blade element momentum (BEM) theory is used to calculate the power transferred from the wind to the wind turbine rotor shaft. BEM theory was first developed to determine the performance of airplane propellers where energy is transferred from the rotor to the surrounding air. The same methods can be used to

determine the performance of a wind turbine rotor where energy is transferred from the surrounding air to the rotor.

BEM theory divides each blade into multiple elements along the radial axis of the blade as shown in Figure 4.1. Each element is treated as a separate airfoil. The thrust and torque on each element is then derived using lift and drag. In addition, thrust and torque equations are derived from a momentum balance through the annulus formed by the blade elements as the rotor rotates. This gives four transcendental equations which can be solved numerically.

As air passes over an airfoil, both lift and drag forces are generated. Figure 4.2 shows an airfoil cross-section with the lift force, drag force, and angle of attack. Equations 4.1 and 4.2 give the lift and drag force per unit of chord length.

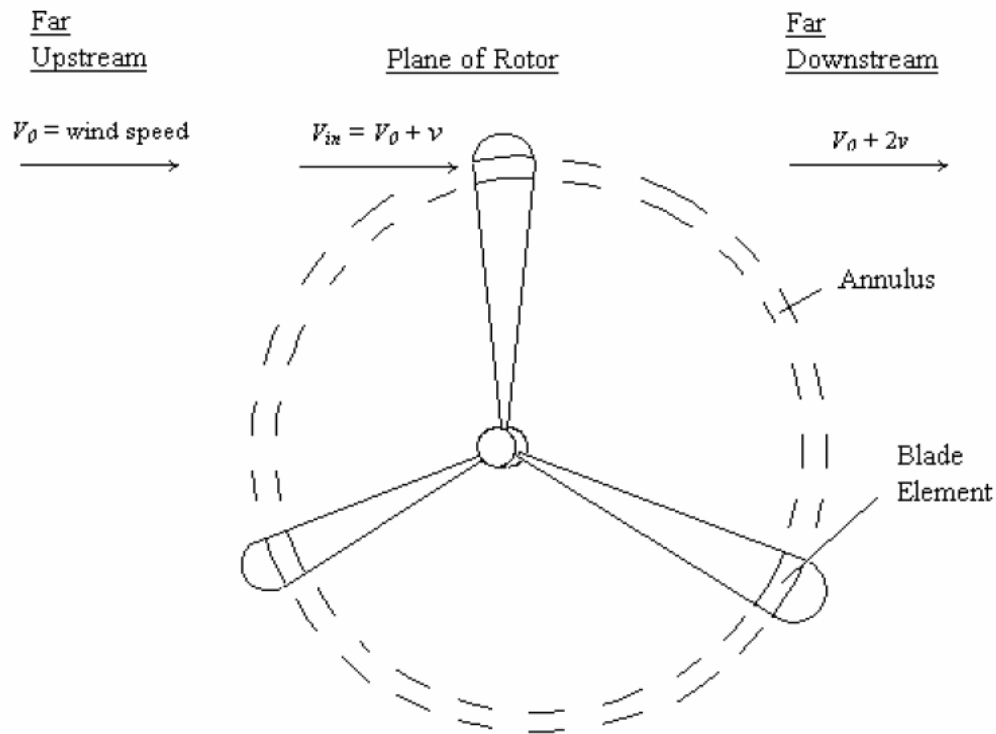


Figure 4.1: Annulus Created by Blade Element as the Rotor Rotates

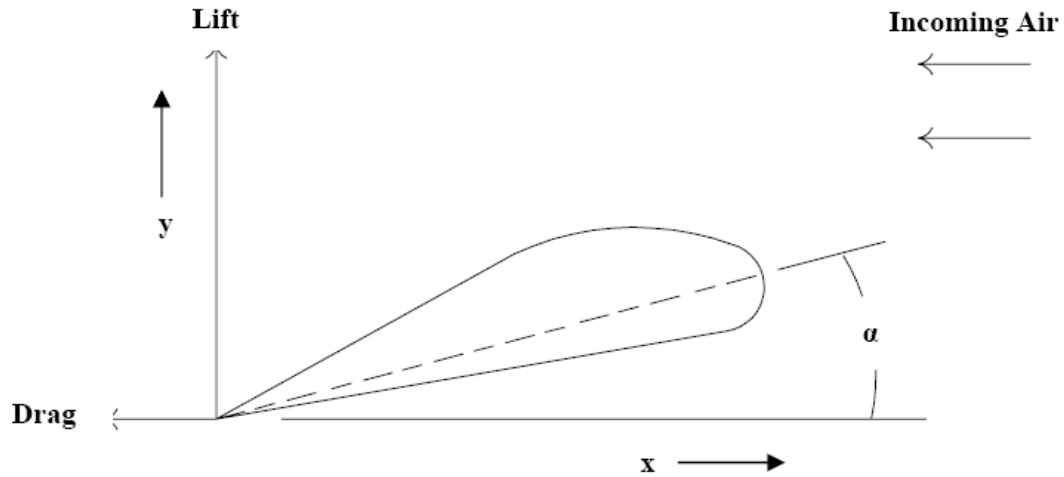


Figure 4.2: Lift and drag forces on an airfoil section

$$L = C_L \frac{1}{2} \rho V^2 S \quad (4.1)$$

$$D = C_D \frac{1}{2} \rho V^2 S \quad (4.2)$$

where:

$L \equiv$ lift force on the airfoil (per unit of chord length)

$D \equiv$ drag force on the airfoil (per unit of chord length)

$\rho \equiv$ density of air

$V \equiv$ velocity of air over the airfoil

$S \equiv$ span (length) of airfoil

$C_L \equiv$ coefficient of lift

$C_D \equiv$ coefficient of drag

The coefficients of lift and drag are functions of the angle of attack, α . Data for the S809 airfoil was used in this study. The S809 airfoil has been used for research by NREL and closely approximates the airfoils of commercially available wind turbines [4]. The C_L and C_D versus angle of attack, α , for the S809 airfoil are shown in Figure 4.3. These values are from a 2004 wind tunnel test.

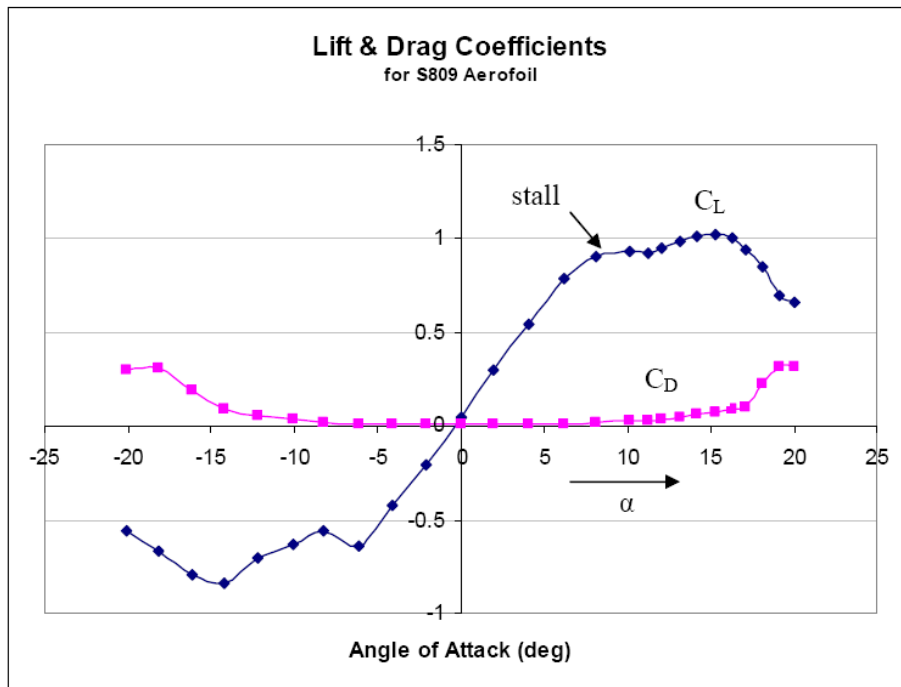


Figure 4.3: Lift and drag coefficients versus angle of attack for S809 airfoil [21]

When using BEM theory, equations 4.1 and 4.2 can be applied to each segment as follows:

$$L_i = C_L \frac{1}{2} \rho V_i^2 c_i w_i \quad (4.3)$$

$$D_i = C_D \frac{1}{2} \rho V_i^2 c_i w_i \quad (4.4)$$

where:

$L_i \equiv$ lift force on the i *th* segment

$D_i \equiv$ drag force on the i *th* segment

$c_i \equiv$ chord length of the i *th* segment

$w_i \equiv$ width of i *th* segment

$V_i \equiv$ velocity air passing over the airfoil

As can be seen in Figure 4.4, V_i is not the horizontal wind speed from wind data. It is rather a summation of two velocity vectors, V_{in} and V_{rot} . V_i is found using the equations below.

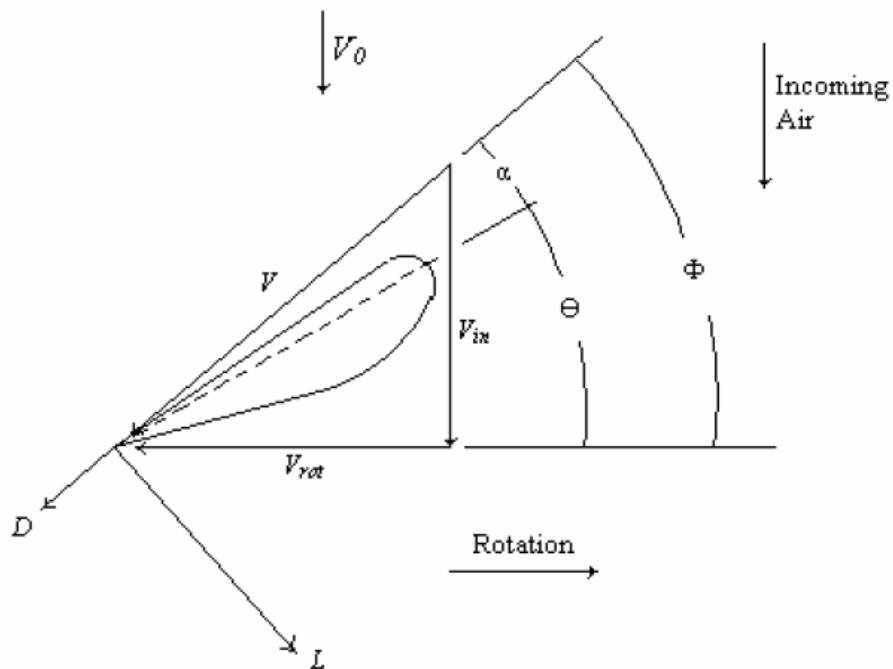


Figure 4.4: Cross section of wind turbine airfoil showing velocity relationships

$$V_{in,i} = V_0 + v_i \quad (4.5)$$

$$V_{rot,i} = \Omega R_i - u_i \quad (4.6)$$

$$V_i = \sqrt{V_{in,i}^2 + V_{rot,i}^2} \quad (4.7)$$

where:

$V_0 \equiv$ wind speed

$v_i \equiv$ change in wind speed from far upstream to plane of rotor through i *th* anulus

$u_i \equiv$ change in swirl from far upstream to plane of rotor

$R_i \equiv$ radial distance of blade segment from rotor hub

$\Omega \equiv$ angular velocity of rotor

4.1.1 Thrust and Torque from Lift and Drag

Equations 4.8 and 4.9 provide the transformations needed to determine the thrust and torque of each blade segment on the rotor. The thrust and torque of each segment on the rotor are then given by Equations 4.10 and 4.11 below. These values are then multiplied by 3 since there are three blades.

$$\lambda_{1,i} = C_{L,i} \cos \phi_i - C_{D,i} \sin \phi_i \quad (4.8)$$

$$\lambda_{2,i} = C_{L,i} \sin \phi_i - C_{D,i} \cos \phi_i \quad (4.9)$$

$$T_i = \lambda_{1,i} \frac{1}{2} \rho V_i^2 c_i w_i \quad (4.10)$$

$$Q_i = \lambda_{2,i} \frac{1}{2} \rho V_i^2 c_i w_i R_i \quad (4.11)$$

where:

T_i \equiv thrust on i *th* blade element

Q_i \equiv torque on i *th* blade element

ρ \equiv air density

c_i \equiv chord length of i *th* blade element

w_i \equiv width of i *th* blade element

R_i \equiv radial distance of i *th* blade element from rotor hub

4.1.2 Thrust and Torque from Momentum

A second set of thrust and torque equations are derived from a momentum balance across the annulus created by the rotating blade segments. The thrust exerted on the rotor by each annulus is given by Equation 4.12. As was mentioned in chapter 1, the wind speed far downstream will be lower than the wind speed far upstream. Furthermore, half of the total change in wind speed will occur upstream of the turbine and half will occur downstream [18]. The following momentum balance can be written for each segment.

$$T_i = \dot{m}_i (V_{upstream} - V_{downstream}) = \dot{m} [V_0 - (V_0 + 2v_i)] = \dot{m}_i \cdot 2v_i \quad (4.12)$$

where:

$T_i \equiv$ thrust on i th blade element

$V_0 \equiv$ wind speed

$v_i \equiv$ change in wind speed from far upstream to plane of rotor through i th annulus

$\dot{m}_i \equiv$ mass flow rate through the i th annulus

The mass flow rate through each annulus can be calculated as follows:

$$\dot{m}_i = \rho A_i (V_0 + v_i) = \rho (2\pi R_i w_i) (V_0 + v_i) \quad (4.13)$$

where:

$\rho \equiv$ air density

$A_i \equiv$ area of i th annulus

$R_i \equiv$ radial distance of i th blade element from rotor hub

$w_i \equiv$ width of i th blade element

The torque exerted on the rotor by each annulus is given by Equation 4.14. In addition to the decrease in wind speed from far upstream to far downstream of a wind turbine, the rotor also creates a swirl (rotational) velocity. As with the change in wind speed, half of the change in swirl velocity occurs upstream of the turbine and half occurs downstream [18].

$$Q_i = \dot{m}_i \cdot 2u_i R_i \quad (4.14)$$

where:

$Q_i \equiv$ torque on i th blade element

$u_i \equiv$ change in swirl speed from far upstream (zero) to the rotor plane through the i th annulus

4.1.3 Solving Torque and Thrust Equations

Blade element momentum theory produces the two sets of transcendental equations for the rotor torque and thrust derived above. These equations are solved using engineering equation solver (EES). The mechanical power of the rotor is then calculated by:

$$\dot{W} = \omega \sum Q_i \quad (4.15)$$

where:

$\omega \equiv$ angular velocity of the rotor

4.1.4 Pitch and Rotor RPM Optimization

The mechanical power produced by a wind turbine rotor depends on the angular velocity of the rotor and the pitch of the rotor blades. The pitch of the rotor blades and rotor RPM can be optimized at each wind speed for maximum power. This optimization is simplified when modeling a variable speed turbine. Every wind turbine blade has an optimum tip speed ratio at which it will produce the maximum power [18]. Tip speed ratio (TSR) is the ratio of the blade tip speed to the wind speed and is given below in Equation 4.16. In addition, the pitch that results in maximum power will remain the same if the rotor's angular velocity remains at the optimum tip speed ratio [18]. Analysis was carried out to determine that the optimum tip speed ratio for the rotor used in this study is 5.8. When the rotor operates at this tip speed ratio, the optimum pitch is 1.7 degrees. Therefore, in this study the tip speed and pitch are held constant at those optimum values.

$$TSR = \frac{\omega R}{V_0} \quad (4.16)$$

where:

$\omega \equiv$ angular velocity of rotor

$R \equiv$ rotor radius

$V_0 \equiv$ wind speed far upstream

It should be noted that this study does not model the actual dynamic situation seen by a real wind turbine. It is not always possible to operate at the optimum tip speed ratio under dynamic conditions. An actual wind turbine will be subject to constant changes in wind speed as well as turbulence. The rotor angular velocity cannot change instantaneously due to its inertia. In addition, a wind turbine rotor has a limited range of angular velocities over which it can operate. In order to maximize power under these dynamic conditions, a wind turbine will constantly vary the rotor blade pitch.

4.2 Drive Train Efficiency Model

Now that the mechanical power of the rotor is known, it must be determined how much of this power makes it to the electrical grid. A simplified overview of the energy transfer from wind to electrical grid is shown in Figure 4.5. The rotor absorbs energy from the wind as described above. This energy is transferred through a gearbox to increase the shaft speed. This is done so that a smaller generator can be used for the same output. The energy is then converted from mechanical to electrical energy with an

AC generator. Due to the variable speed operation of the turbine, the electricity has a variable frequency. Power electronics are necessary to first rectify the electricity to DC current and then invert the electricity to 60 Hz (in the U.S.) so that it is at the frequency of the electrical grid. The electrical energy is then passed to the electrical grid.

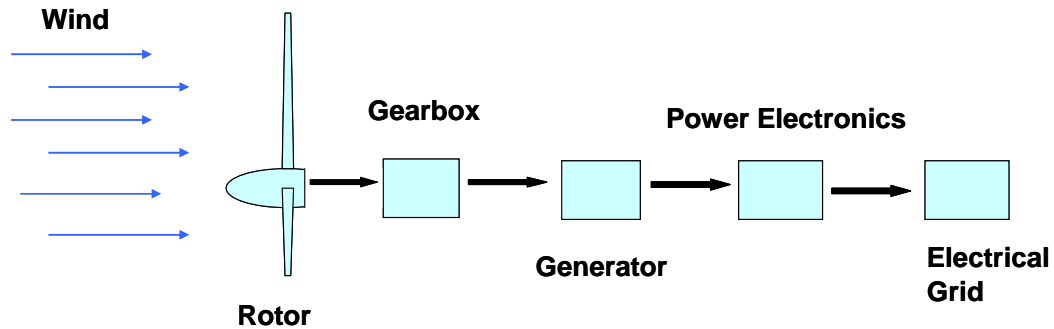


Figure 4.5: Energy Transfer from Wind to Electrical Grid

Each transfer of energy has an associated energy loss. Therefore, it is necessary to calculate the efficiency of the drive train. The drive train efficiency model includes the efficiencies of the gearbox, generator, and power electronics. The drive train efficiency model used in this study was taken from the *WindPACT Advanced Wind Turbine Drive Train Designs Study* [22]. The drive train efficiency is a function of the power being generated relative to the generator capacity. Figure 4.6 shows the drive train efficiency versus power output as a percentage of generator capacity. The efficiency ranges from approximately 80% at low power to 95% at rated power.

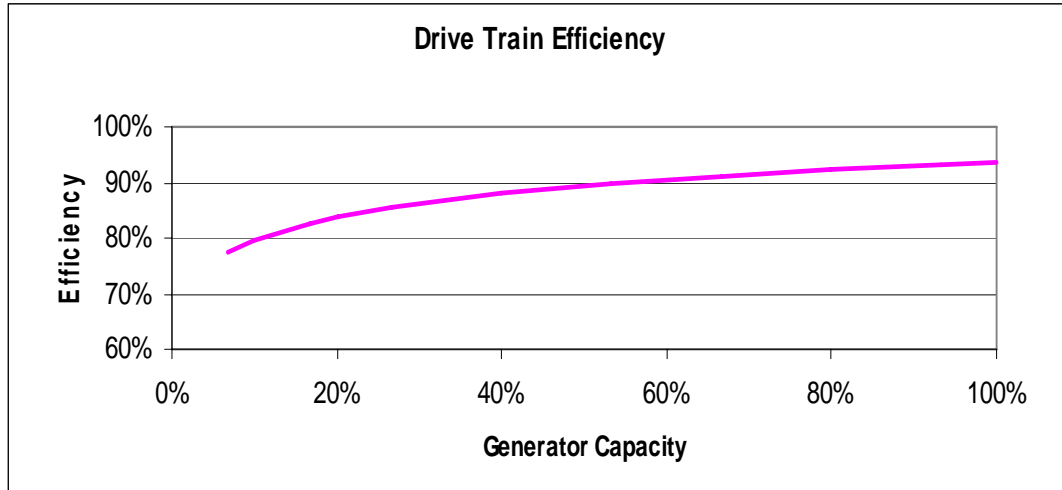


Figure 4.6: Drive Train Efficiency

4.3 Model Validation

The electric power model was validated against the General Electric 3.6s wind turbine power curve [13]. Figure 4.7 shows that the model replicates the power curve well. There is a difference between the model and actual power curve in the area where output approaches its rated capacity. In the figure below this occurs at a wind speed near 12 m/s. This discrepancy between the model and actual power curve is a result of controls on the actual wind turbine, which feather the turbine blades as the power output approaches the generator capacity. The model used in this study assumes a perfect control system where the power output of the turbine is allowed to increase at maximum efficiency until it reaches the generator capacity. In a real turbine, this could produce overshoot above rated power.

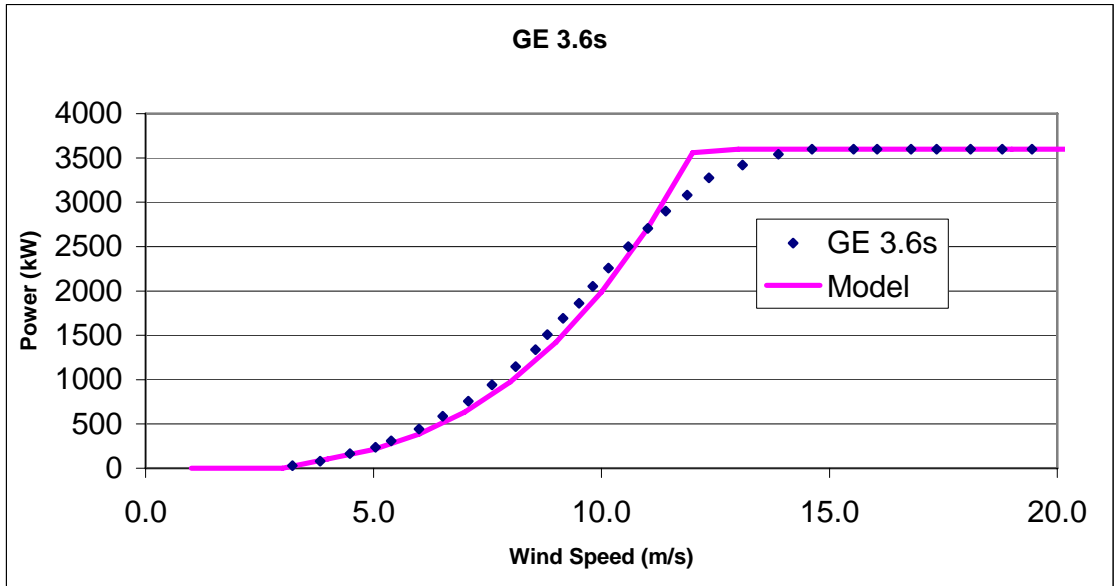


Figure 4.7: Model Validation Using GE 3.6 MW Turbine Power Curve

Chapter 5: Economic Data Analysis

As discussed in chapter 1, the second objective of this study is to determine the turbine generator capacity per swept rotor area design that results in the minimum COE and SPB for a 3000 kW turbine with an 80 m hub height at an offshore coastal Georgia site. Therefore, it is necessary to determine the wind speed distribution as well as the economic value of electricity at this site. This requires the analysis of wind speed and electric rate data. The following sections describe the wind and rate data used in this study as well as the analysis performed on them.

5.1 Wind Data

The wind data used in this study was recorded at the Navy R2 tower located in the Atlantic off coast of Georgia. The R2 tower is shown in Figure 3. As the figure shows, the tower stands 50 m above sea level. This allows the wind to be measured at a height close to that of a wind turbine hub height, which results in more accurate data. due to the shorter distance over which the wind speeds has to be adjusted for wind shear. Specifically, the measurements are taken at 50 m above sea level. The wind shear power law exponent was found to be 0.1 at this location in previous studies [10].

The R2 tower has been recording wind speeds since 1999. However, there are gaps in the available data due to equipment failures on the tower. Several years are missing large amounts of data. A large amount of missing data in any one year could alter the results of this study. Only the data from 2000, 2004, and 2005 were found to be more than 90% complete. Therefore, these are the only years that are analyzed in this study.

The wind speed data recorded at R2 are 6 minute averages of the actual wind. An average of the 6 minute data was calculated for every hour in the year to give an average wind speed for every hour in the year.



Figure 5.1: R2 Navy Tower off the Coast of Georgia

5.2 Rate Data

The Georgia hourly time-dependent electricity rate is an accurate estimate of the value of electricity. Specifically, this is the avoided cost of power generation. Avoided cost is how much it costs at any time to produce one more kWh of electricity. The data used in this study for years 2000, 2004, and 2005 provides an electrical rate for every hour in the year for the Coastal Georgia region.

5.3 Electrical Rate and Wind Data Analysis

In order to calculate the actual simple payback of a wind turbine, it is necessary to know how much the electricity is worth at the time it is being produced. As described in chapter 2, the methodology of the model used in this study is to calculate the power generated by the turbine for multiple wind speed bins and multiply that by the amount of time in a year the wind blows at the speed for that bin. As described in chapter 4, the bin size is 15 (m/s)^3 giving bins from 4 m/s to 27 m/s . Each year of wind data was analyzed to determine the percentage of time the wind speed is in each bin. The results are shown in Figures 5.2, 5.3, and 5.4.

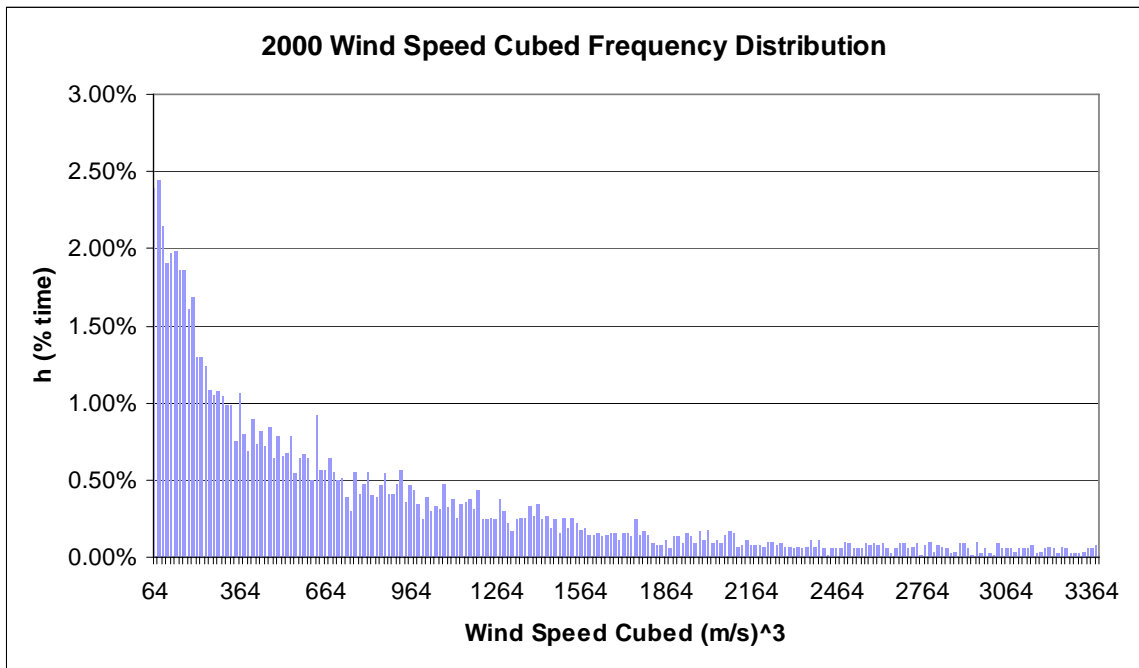


Figure 5.2: 2000 Wind Speed Cubed Frequency Distribution

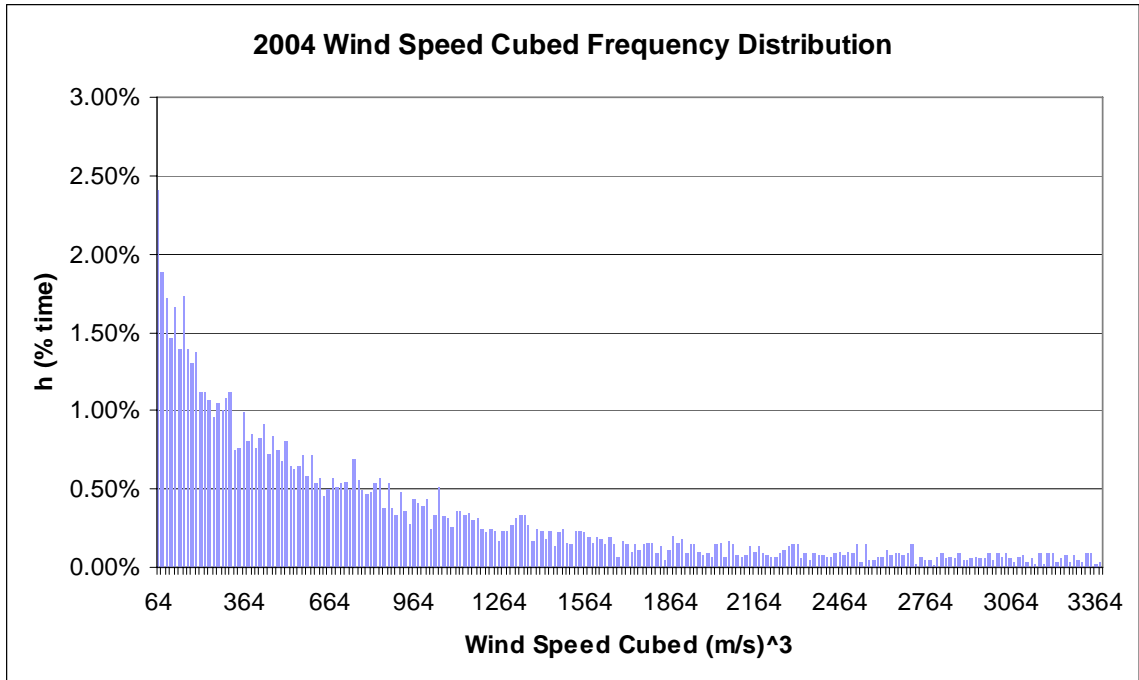


Figure 5.3: 2004 Wind Speed Cubed Frequency Distribution

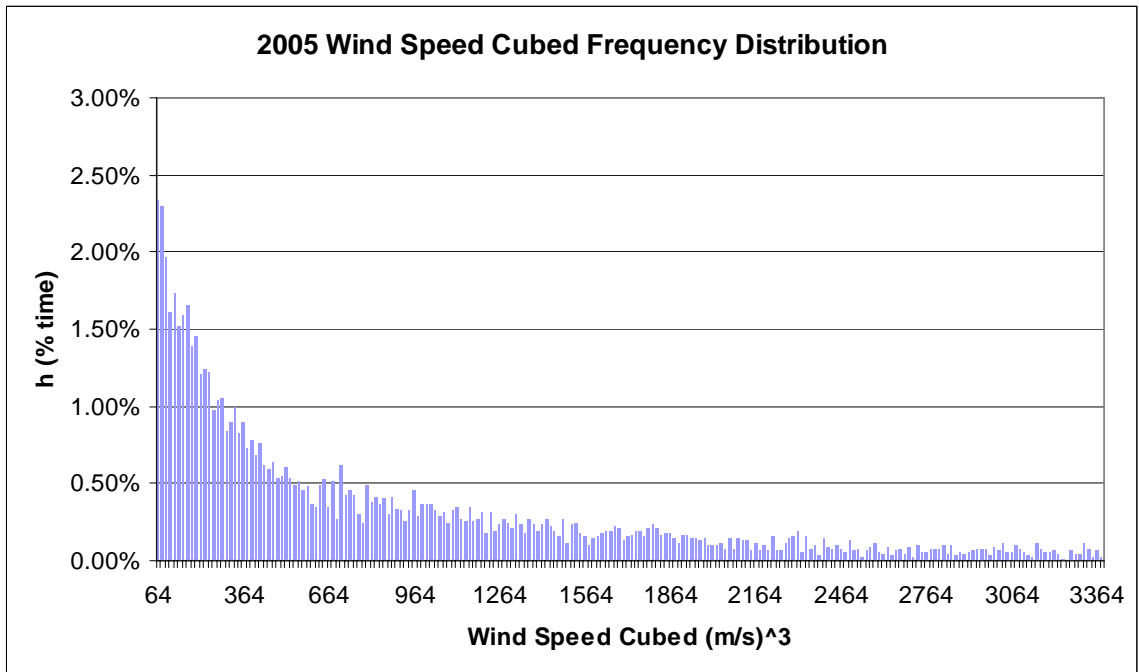


Figure 5.4: 2005 Wind Speed Cubed Frequency Distribution

To calculate the revenue earned by the turbine, it is necessary to know the value of electricity for each of the wind speed bins. This was determined by performing a coincidence analysis of wind speed data and the RTP rate data for every hour in the year. For each wind speed bin, an average RTP rate was calculated from the rates that coincide with the wind speeds that were within the bin range. The results of the coincidence analysis are shown in Figures 5.5, 5.6, and 5.7. These figures also contain a linear trend line of the average rates versus wind speed cubed. The results show that there is a negative trend in the average rate as wind speed increases. This means that while the turbine will produce more electricity at higher wind speeds, the electricity it produces is worth less. This trend is most pronounced in 2000. In 2004, there is only a very slight negative trend. In 2005, the results again show a clear negative trend in the average rate versus wind speed. It should be noted, however, that the change in value of electricity is small in comparison to the cubic relation of wind speed and power generation. The results of this analysis show a large increase in electrical rate from 2004 to 2005. This rate increase has continued since 2005.

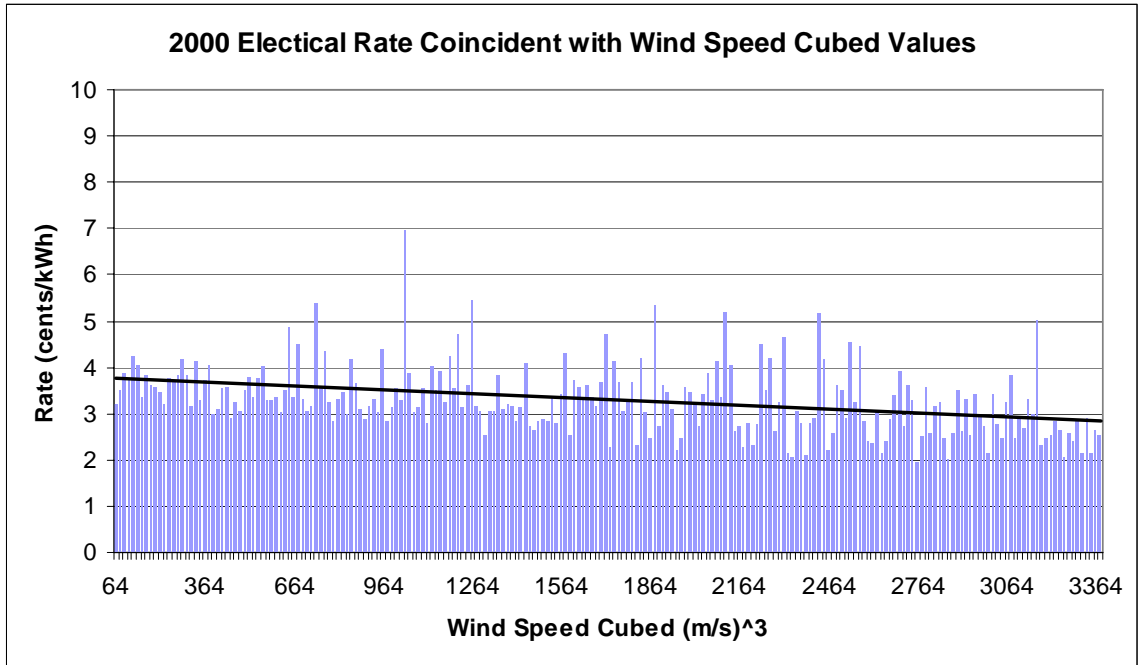


Figure 5.5: 2000 Hourly Electrical Rate and Wind Speed Coincidence

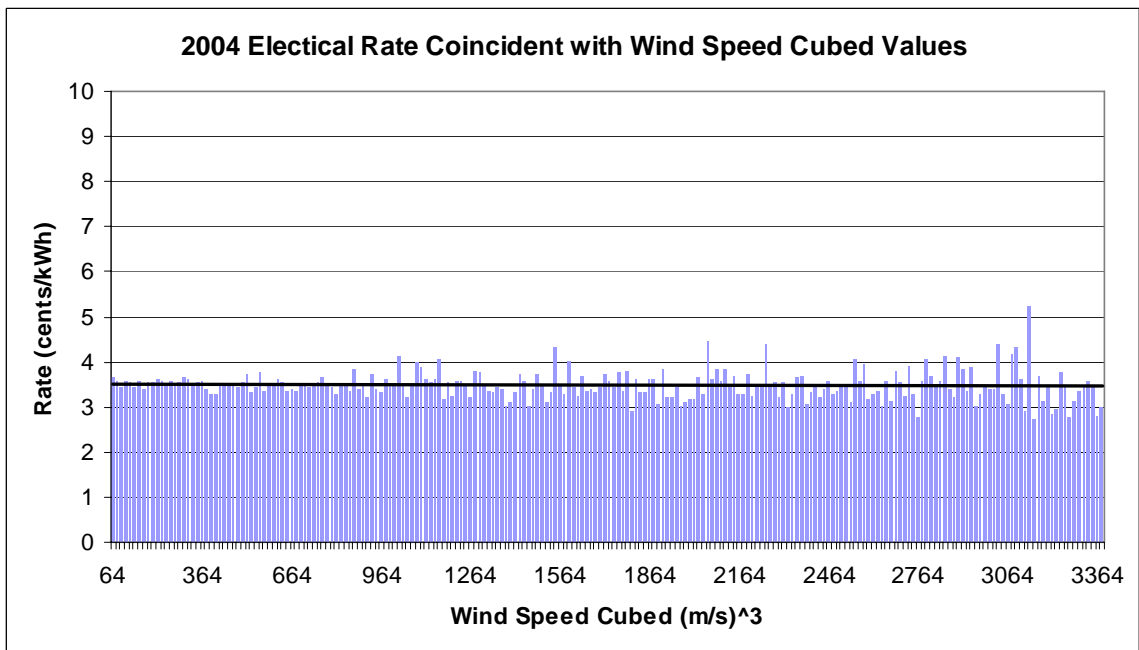


Figure 5.6: 2004 Hourly Electrical Rate and Wind Speed Coincidence

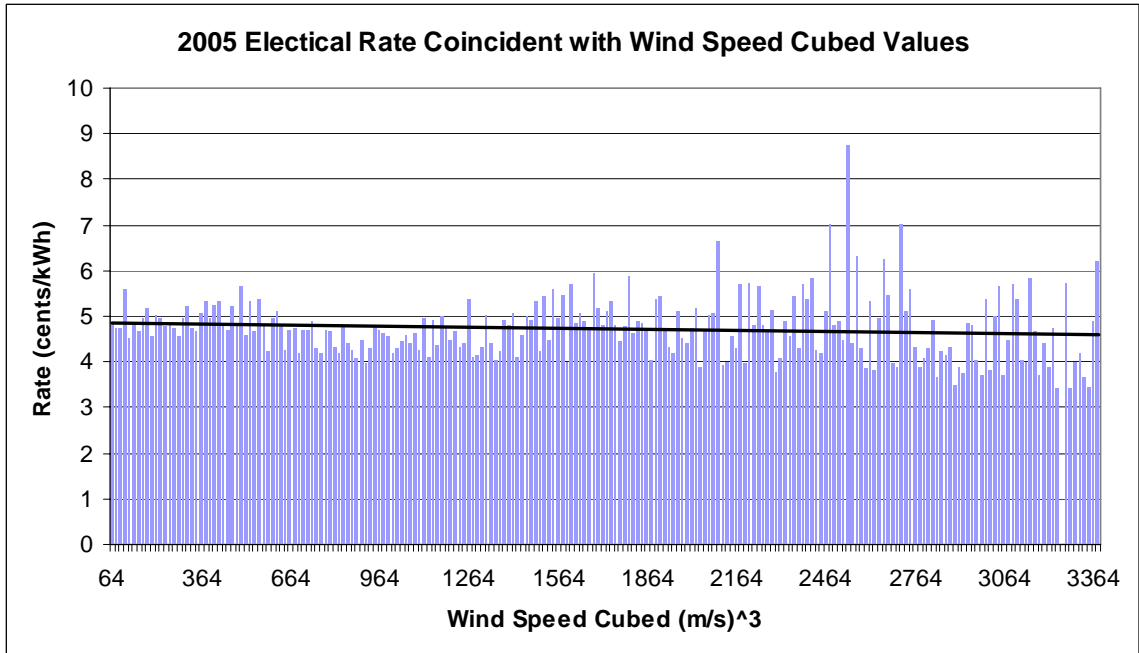


Figure 5.7: 2005 Hourly Electrical Rate and Wind Speed Coincidence

Chapter 6: Results, Discussion, and Conclusions

6.1 Results and Discussion

6.1.1 Sensitivity Analysis of Specific Rotor Rating and COE

The results of the sensitivity analysis are presented below. Figure 6.1 shows the sensitivity of the COE on specific rotor rating for the base case, which is a generator capacity equal to 3000 kW, annual average wind speed equal to 7.5 m/s at a 50 m anemometer height, Weibull shape parameter equal to 2, hub height equal to 80 m, and wind shear power law exponent equal to 0.14. A 3000 kW turbine was chosen for the base case because currently available, large scale wind turbines range from 1000 kW to 5000 kW. A 3000 kW turbine is in the center of this range. Figure 6.1 shows that it is advantageous for a turbine's specific rotor rating to be within 0.05 kW/m^2 of the optimal specific rotor rating for its specific site. A specific rotor rating outside of that range could result in a COE more than 0.1 cents/kWh higher than the optimum COE. These results also show that there is a single minimum COE, which means there is only one optimum design. The optimum rotor diameter for the base case was found to be 106 m. The corresponding optimum specific rotor rating for the base case is 0.34 kW/m^2 . The high sensitivity of COE on specific rotor rating found in this study is in agreement with the results of the *WindPACT Turbine Rotor Design, Specific Rating Study* [3]. The results of the WindPACT study also found there to be a single minimum COE.

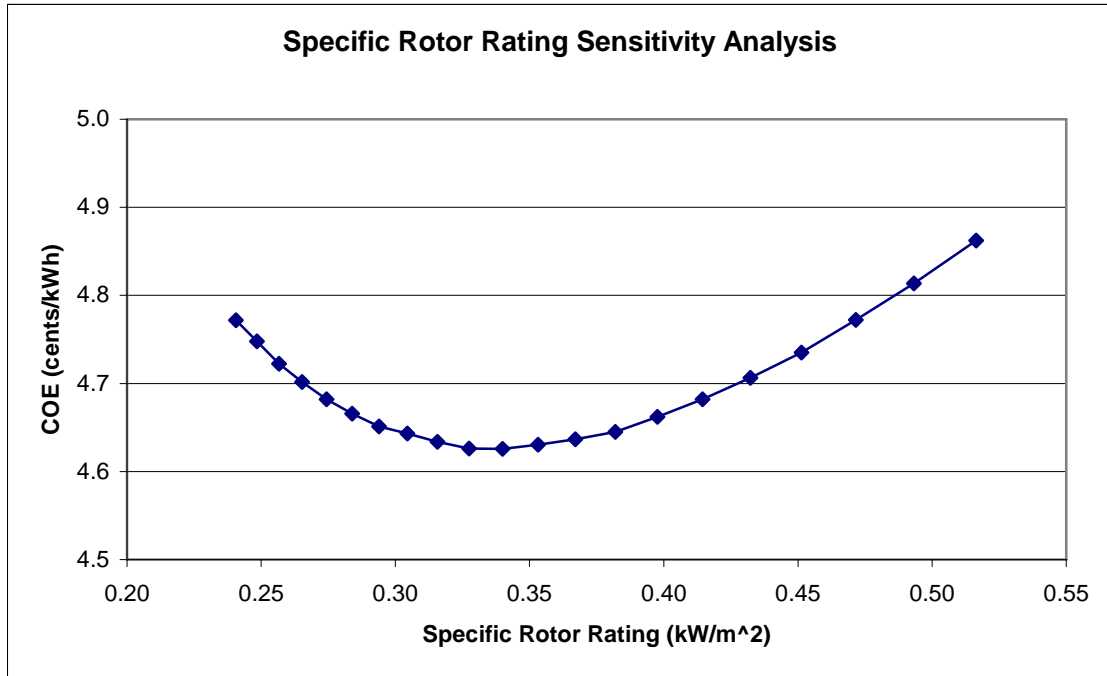


Figure 6.1: Specific Rotor Rating Sensitivity Analysis

Figure 6.2 shows the sensitivity of the optimal specific rotor rating and the optimal COE on varying the generator capacity from the base case. Varying the generator capacity from 1500 kW to 4500 kW resulted in the optimal specific rotor rating ranging from 0.31 kW/m² to 0.33 kW/m² and the optimal COE ranging from 4.3 cents/kWh to 5.2 cents/kWh. The results show that the specific rotor rating increases when the generator capacity increases from 1500 kW to 3000 kW, but the specific rotor rating remains nearly constant when the generator capacity increases from 3000 kW to 4500 kW. This means that the optimal rotor area increases at a faster rate between 3000 kW and 4500 kW than between 1500 kW and 3000 kW.

The results also show that the optimal COE is lowest for the 1500 kW generator capacity and highest for the 4500 kW generator capacity. These results demonstrate that, despite the industry trend of increasing turbine sizes, larger turbines do not always result

in a lower optimal COE. This is because as the turbine increases in size, the capital cost of the turbine begins to increase faster than the increase in energy production. This study did not attempt to find an optimum turbine size, but the results show that an optimum turbine size would be smaller than 3000 kW. These results are only applicable to onshore turbines. Larger turbines might be more economical for offshore applications.

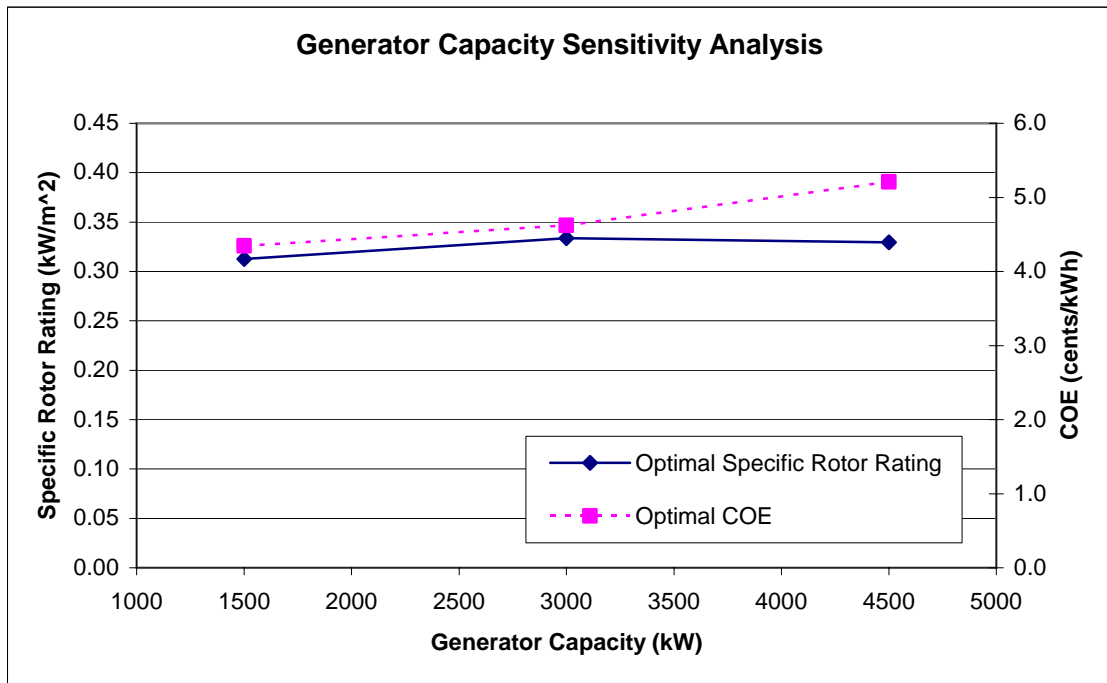


Figure 6.2: Generator Capacity Sensitivity Analysis

Figure 6.3 shows the sensitivity of the optimal specific rotor rating and the optimal COE on varying the annual average wind speed. As the annual average wind speed increases, the optimal specific rotor rating increases and the optimal COE decreases. Varying the annual average wind speed at 50 m from 6.5 m/s to 8.5 m/s resulted in the optimal specific rotor rating ranging from 0.28 kW/m² to 0.39 kW/m² and

the optimal COE ranging from 5.7 cents/kWh to 4.0 cents/kWh. These results show that the annual average wind speed has a large effect on the optimal specific rotor rating and optimal COE. This is expected because of the cubic relationship between velocity and power. An increase in the optimal specific rotor rating for a fixed generator capacity means the optimal rotor diameter is decreasing. This is expected since a higher wind speed means the wind has a higher power density and therefore does not need as much rotor swept area for a given generator capacity. The sensitivity of optimal COE shown in the figure is in general agreement with the *WindPACT Rotor Design, Specific Rating Study* [3]. It is difficult to compare the optimum specific rotor ratings found in this study to the WindPACT Study because the specific rotor rating resolution in the WindPACT Study is low and the base cases are different.

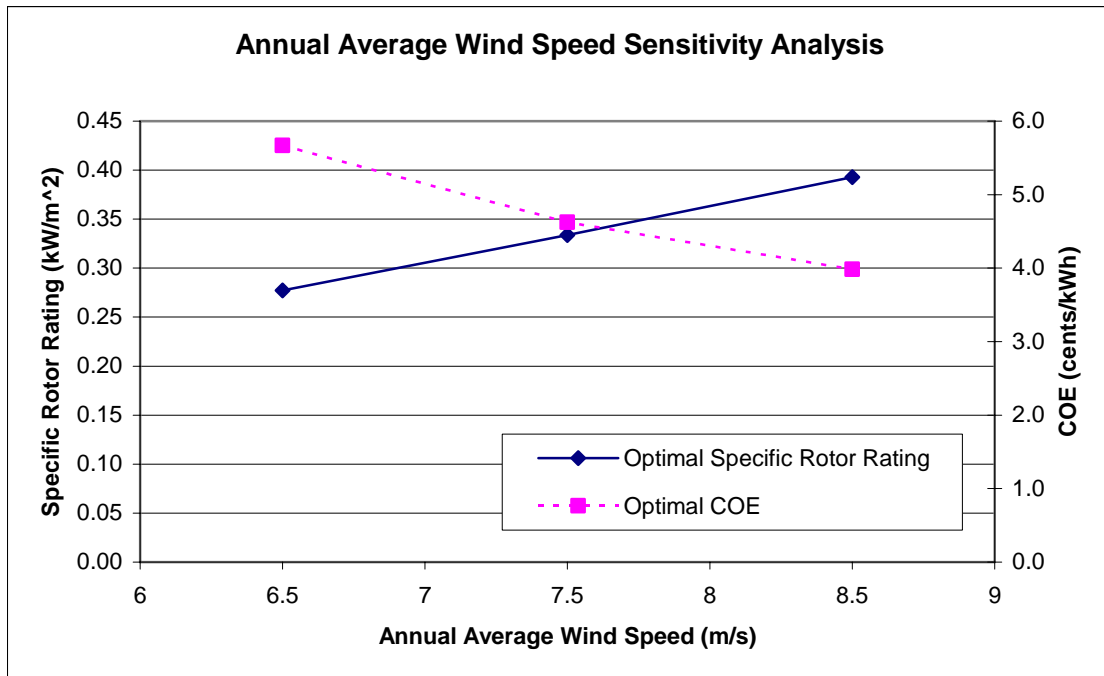


Figure 6.3: Annual Average Wind Speed Sensitivity Analysis

Figure 6.4 shows the sensitivity of the optimal specific rotor rating and the optimal COE on the Weibull shape parameter. Varying the Weibull shape parameter from 1.8 to 2.2 resulted in the optimal specific rotor rating ranging from 0.36 kW/m² to 0.33 kW/m² and the optimal COE ranging from 4.7 cents/kWh to 4.6 cents/kWh. The results show that a larger Weibull shape parameter results in a decrease in the optimal specific rotor rating and optimal COE. The results also show that the optimal specific rotor rating and optimal COE are not very sensitive to the shape parameter. The *WindPACT Rotor Design, Specific Rating Study* agrees with the low sensitivity of optimal COE on the Weibull shape parameter and with the trend of decreasing optimal COE with increasing Weibull shape parameter [3].

These results are expected because as the Weibull shape parameter increases, the wind speed varies less from the annual average wind speed (see Figure 1.13). This means that there will be a smaller percentage of very low wind speeds and a smaller percentage of very high wind speeds. A smaller percentage of very low wind speeds will lower the optimal COE. A smaller percentage of very high wind speeds will raise the optimal COE. However, at the very high wind speeds, the power output is limited by the generator capacity. At very high wind speeds, the power no longer increases with the cube of wind speed. Therefore, the lower percentage of very low wind speeds causes a greater decrease in the optimal COE than the increase in optimal COE caused by the smaller percentage of very high wind speeds. As expected, this effect is very subtle, which results in the low sensitivity of optimal COE on Weibull shape parameter.

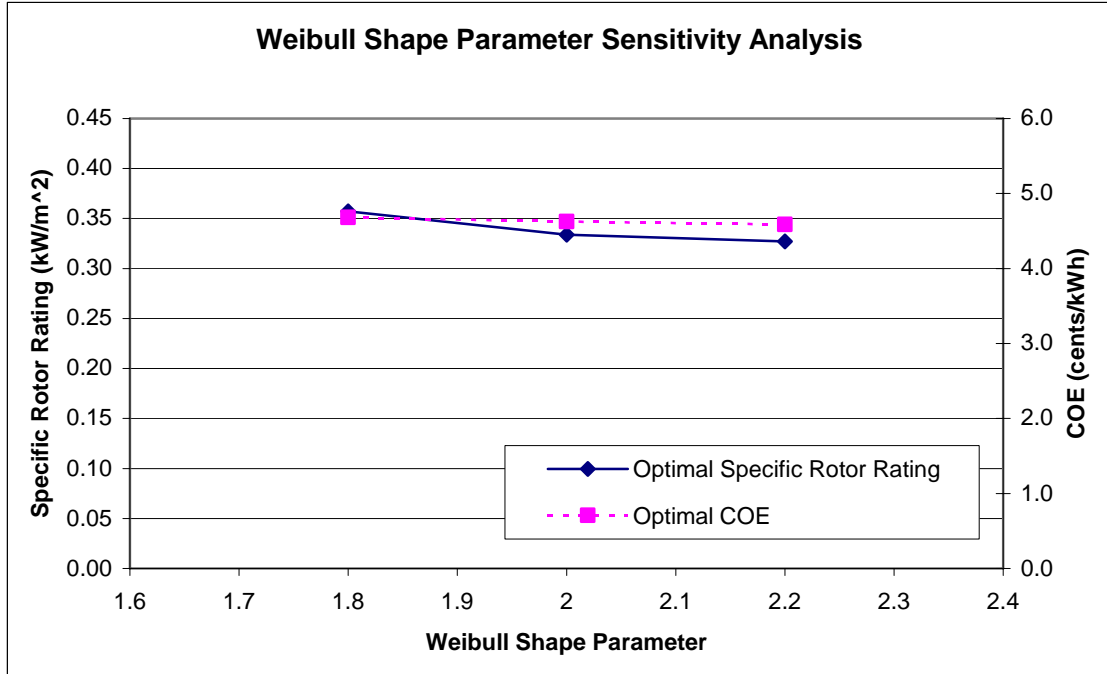


Figure 6.4: Weibull Shape Parameter Sensitivity Analysis

Figure 6.5 shows the sensitivity of the optimal specific rotor rating and optimal COE on the wind shear power law exponent. As the wind shear power law exponent increases, the COE decreases and the specific rotor rating increases slightly. Varying the wind shear power law exponent from 0.1 to 0.2 resulted in the optimal specific rotor rating ranging from 0.33 kW/m² to 0.34 kW/m² and the optimal COE ranging from 4.7 cents/kWh to 4.5 cents/kWh. Increasing the wind shear power law exponent has a smaller but similar effect on optimal specific rotor rating and optimal COE as increasing the annual average wind speed. This is expected since increasing the wind shear power law exponent increases the wind shear. Since the wind speed input is held constant at 7.5 m/s at a 50 meter anemometer height and the hub height is held constant at 80 m, an increased wind shear will result in slightly higher wind speeds at the hub height of the turbine.

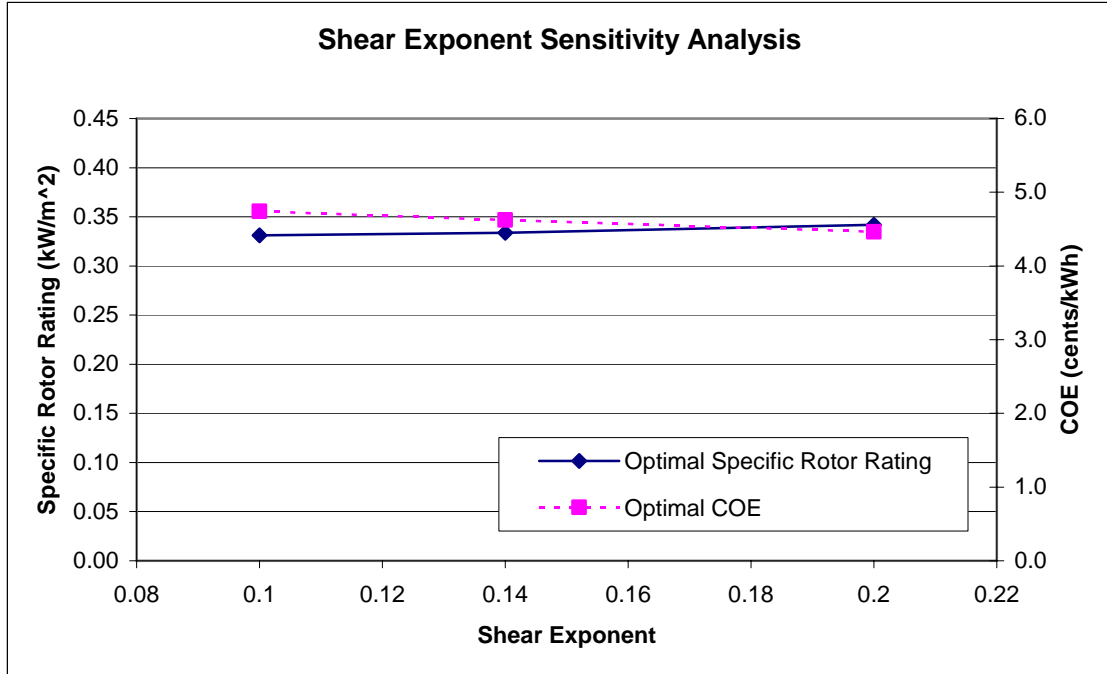


Figure 6.5: Power Law Exponent Sensitivity Analysis with 80 m Hub Height

Figure 6.6 shows the sensitivity of the optimal specific rotor rating and optimal COE on hub height. Varying the hub height from 70 m to 90 m resulted in the optimal specific rotor rating ranging from 0.33 kW/m² to 0.35 kW/m² and the optimal COE ranging from 4.7 cents/kWh to 4.6 cents/kWh. The increase in optimal specific rotor rating for a fixed generator capacity with increased hub height means the optimal rotor diameter decreases with hub height. This is expected since wind speed increases with hub height due to wind shear. However, because of the added cost of the tower and foundation, increasing the hub height from 70 m to 90 m decreases the optimal COE only slightly.

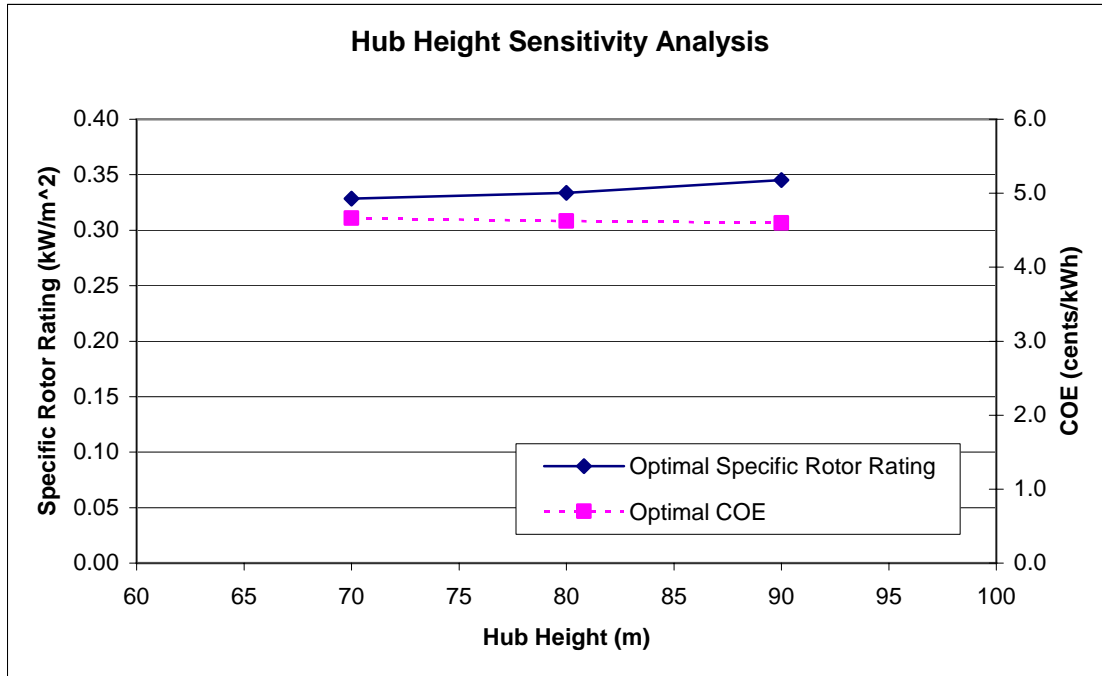


Figure 6.6: Hub Height Sensitivity Analysis with 1/7th Power Law Exponent

6.1.2 Minimizing COE and SPB for a Coastal Georgia Site

The results of the economic optimization of a wind turbine design located off the Georgia coast are shown in Table 6.1. The optimization was run for a 3000 kW turbine with an 80 m hub height for the three years of acceptable available data, 2000, 2004, and 2005. As stated above, a 3000 kW turbine was chosen because it is in the middle of the range of currently available, large scale wind turbines. Three figures of merit were used, i.e. levelized cost of energy, simple payback using an hourly time dependent rate to calculate revenue, and simple payback using an annual average electrical rate to calculate revenue.

The results show that the revenue calculated from the hourly time dependent rate per kWh of electricity produced is slightly less than the average electricity rate. This means that, on average, electricity is produced when its economic value is below average.

The results of this study also show that minimizing any of the three figures of merit results in similar optimum designs for this particular site. The specific rotor rating of the three optimum designs for each year were within 10% of each other. The corresponding levelized costs of energy of the three optimum designs for each year are within 0.2% of each other. The corresponding simple payback values of the three optimum designs for each year are equal out to three significant figures. These results demonstrate that the three figures of merit used will result in small differences between the optimum designs, and these small differences have almost no effect on COE or simple payback. The results demonstrate, however, that using an hourly time-dependent valuation of electricity to calculate simple payback results in a different value than when an annual average value of electricity is used to calculate simple payback. These two values differ by as much as 4% at this particular coastal Georgia site.

Table 6.1: Results of Minimizing COE and SPB for a Coastal Georgia Site

| Minimizing COE | | | |
|---|-------------|-------------|-------------|
| Year | 2000 | 2004 | 2005 |
| Gen Cap (kW) | 3000 | 3000 | 3000 |
| Hub Height (m) | 80 | 80 | 80 |
| Specific Rating (kW/m ²) | 0.24 | 0.25 | 0.27 |
| COE (\$/kWh) | 0.0935 | 0.0917 | 0.0941 |
| SPB Using Time Dependent Rate(years) | 17.1 | 16.1 | 12.3 |
| SPB Using Average Rate (years) | 16.8 | 15.8 | 11.8 |
| Revenue(time-dependent)/Electricity (\$/kWh) | 0.0338 | 0.0350 | 0.0473 |
| Average Rate (\$/kWh) | 0.0345 | 0.0356 | 0.0491 |
| Minimizing SPB Using Time Dependent Rate | | | |
| Year | 2000 | 2004 | 2005 |
| Gen Cap (kW) | 3000 | 3000 | 3000 |
| Hub Height (m) | 80 | 80 | 80 |
| Specific Rating (kW/m ²) | 0.24 | 0.27 | 0.29 |
| COE (\$/kWh) | 0.0935 | 0.0918 | 0.0942 |
| SPB Using Time Dependent Rate(years) | 17.1 | 16.1 | 12.3 |
| SPB Using Average Rate (years) | 16.8 | 15.8 | 11.8 |
| Revenue(time-dependent)/Electricity (\$/kWh) | 0.0338 | 0.0350 | 0.0473 |
| Average Rate (\$/kWh) | 0.0345 | 0.0356 | 0.0491 |
| Minimizing SPB Using Average Rate | | | |
| Year | 2000 | 2004 | 2005 |
| Gen Cap (kW) | 3000 | 3000 | 3000 |
| Hub Height (m) | 80 | 80 | 80 |
| Specific Rating (kW/m ²) | 0.25 | 0.26 | 0.28 |
| COE (\$/kWh) | 0.0935 | 0.0918 | 0.0941 |
| SPB from Time-dependent Rate(years) | 17.1 | 16.1 | 12.3 |
| SPB from Avg Rate (years) | 16.8 | 15.8 | 11.8 |

6.2 Conclusions

This study has demonstrated the importance of site specific wind turbine design optimization. It has been shown that a change in the turbine specific rotor rating (generator capacity relative to rotor swept area) as small as 0.05 kW/m² can have a significant effect on the levelized cost of energy (COE). For a 3000 kW turbine, a 0.05 kW/m² change in specific rotor rating is equivalent to changing the rotor diameter from 100 m to 107 m. It has also been shown that there is a single minimum COE with respect to specific rotor rating for a fixed generator capacity, which means there is only one optimum design.

It has been shown that the optimal specific rotor rating varies in a non-linear fashion with generator capacity. The optimal rotor area increases at a faster rate as the turbine generator capacity increases. The results demonstrate that larger turbines do not always result in lower COE. The industry trend to develop even larger turbines is largely for offshore applications. An optimum turbine size was not found in this study, but the results show that it would be smaller than 3000 kW.

The annual average wind speed has the largest effect on the optimal specific rotor rating and optimal COE. The optimal COE decreases by as much as 1 cent/kWh with a 1 m/s increase in annual average wind speed. This is expected since wind power increases with the cube of wind speed; doubling the wind speed will increase its power eight fold. The trends of optimal COE on the wind resource characteristics (annual average wind speed and Weibull shape parameter) found in this study agree with the results of the *WindPACT Rotor Design, Specific Rating Study* [3]. It has been shown that a wind resource with a larger Weibull shape parameter will have a smaller optimal specific rotor rating and a slightly lower optimal COE. Additionally, a variation in wind shear with a fixed hub height of 80 m has only a moderate effect on the optimal specific rotor rating and COE. Increasing a turbine's hub height with a fixed wind shear had only a moderate effect on the optimal specific rotor rating and COE. However, wind shear and hub height sensitivities are interconnected. If the wind shear increases, the sensitivity of COE on hub height will increase.

This study has demonstrated the importance of considering the hourly time-dependent valuation of electricity by comparing the simple payback calculated from an hourly time-dependent valuation of electricity and simple payback calculated from an

annual average valuation of electricity. The two values differed by as much as 4% at the specific coastal Georgia site studied. Therefore, the methodology of considering an hourly time-dependent valuation of electricity, as presented in this study, is advantageous to an investor because it provides a more realistic measure of the investment's value. For this reason alone, the hourly time-dependent valuation of electricity in addition to the wind resource characteristics should be considered in site specific studies.

Considering the hourly time-dependent valuation did not change the optimal design much for the specific site analyzed in this study. The difference between minimizing COE (ignoring the value of electricity) and minimizing simple payback with an hourly time-dependent valuation of electricity resulted in less than a 0.02 kW/m² difference in the optimum specific rotor ratings. However, there could be a difference between the optimal designs at other sites.

This study did not consider how wind turbine design changes affect the fatigue loads on the turbine components and the resulting change in costs. Incorporating this aspect into a future study would provide further valuable information for site specific wind turbine design optimization.

Appendix A: Rotor Data

Table A.1: Published C_L and C_D Values for the S809 Aerofoil [21]

| Angle of Attack (deg) | S809 Published C_L | S809 Published C_D |
|-----------------------|----------------------|----------------------|
| -20.1 | -0.56 | 0.3027 |
| -18.1 | -0.67 | 0.3069 |
| -16.1 | -0.79 | 0.1928 |
| -14.2 | -0.84 | 0.0898 |
| -12.2 | -0.7 | 0.0553 |
| -10.1 | -0.63 | 0.039 |
| -8.2 | -0.56 | 0.0233 |
| -6.1 | -0.64 | 0.0131 |
| -4.1 | -0.42 | 0.0134 |
| -2.1 | -0.21 | 0.0119 |
| 0.1 | 0.05 | 0.0122 |
| 2 | 0.3 | 0.0116 |
| 4.1 | 0.54 | 0.0144 |
| 6.2 | 0.79 | 0.0146 |
| 8.1 | 0.9 | 0.0162 |
| 10.2 | 0.93 | 0.0274 |
| 11.3 | 0.92 | 0.0303 |
| 12.1 | 0.95 | 0.0369 |
| 13.2 | 0.99 | 0.0509 |
| 14.2 | 1.01 | 0.0648 |
| 15.3 | 1.02 | 0.0776 |
| 16.3 | 1 | 0.0917 |
| 17.1 | 0.94 | 0.0994 |
| 18.1 | 0.85 | 0.2306 |
| 19.1 | 0.7 | 0.3142 |
| 20.1 | 0.66 | 0.3186 |
| 30 | 0.705 | 0.4784 |
| 40 | 0.729 | 0.6743 |
| 50 | 0.694 | 0.8799 |
| 60 | 0.593 | 1.0684 |
| 70 | 0.432 | 1.2148 |
| 80 | 0.227 | 1.2989 |
| 90 | 0 | 1.308 |

Table A.2: Blade Element Specifications [21]

| Blade Element Number | Radial Distance / Radius (Dimensionless) | Chord Length / Radius (Dimensionless) | Twist Angle (deg) |
|-----------------------------|---|--|--------------------------|
| 1 | 0 | 0.039 | 0 |
| 2 | 0.144 | 0.059 | 0 |
| 3 | 0.167 | 0.082 | 30 |
| 4 | 0.192 | 0.133 | 27.59 |
| 5 | 0.25 | 0.128 | 20.05 |
| 6 | 0.303 | 0.123 | 14.04 |
| 7 | 0.357 | 0.118 | 9.67 |
| 8 | 0.413 | 0.113 | 6.75 |
| 9 | 0.468 | 0.108 | 4.84 |
| 10 | 0.522 | 0.103 | 3.48 |
| 11 | 0.578 | 0.098 | 2.4 |
| 12 | 0.632 | 0.093 | 1.51 |
| 13 | 0.687 | 0.088 | 0.76 |
| 14 | 0.743 | 0.083 | 0.09 |
| 15 | 0.75 | 0.078 | 0 |
| 16 | 0.797 | 0.073 | -0.55 |
| 17 | 0.852 | 0.068 | -1.11 |
| 18 | 0.908 | 0.063 | -1.55 |
| 19 | 0.962 | 0.057 | -1.84 |
| 20 | 1 | 0.052 | -2 |

References

1. Fuglsang, Peter, and Kenneth Thomsen. "Site-Specific Design Optimization of 1.5-2.0 MW Wind Turbines." *Journal of Solar Energy Engineering*, Vol. 123, pp. 296-303, 2001.
2. Jackson, K., C.P. van Dam, and D. Yen-Nakafuji. "Wind Turbine Generator Trends for Site-specific Tailoring." *Wind Energy*, 8, pp. 443-455, 2005.
3. Malcolm, D.J., and A.C. Hansen. "WindPACT Turbine Rotor Design, Specific Rating Study." National Renewable Energy Laboratory, <http://www.nrel.gov/docs/fy04osti/34794.pdf> (Accessed March 2007)
4. Martin, Kirk. "Site Specific Optimization of Rotor/Generator Sizing of Wind Turbines." Master's Thesis in the Woodruff School of Mechanical Engineering, Georgia Institute of Technology, August 2006.
5. Energy Information Agency. "International Energy Outlook 2007." [http://www.eia.doe.gov/oiaf/ieo/pdf/0484\(2007\).pdf](http://www.eia.doe.gov/oiaf/ieo/pdf/0484(2007).pdf) (Accessed October 2007)
6. Global Wind Energy Council. "Global Wind 2006 Report." http://www.gwec.net/fileadmin/documents/Publications/gwec-2006_final_01.pdf (Accessed June 2007)
7. Wisner, Ryan, and Mark Bolinger. "Annual Report on U.S. Wind Power Installation, Cost, and Performance Trends: 2006." National Renewable Energy Laboratory, <http://www.nrel.gov/wind/pdfs/41435.pdf> (Accessed June 2007)
8. 3Tier. "Firstlook Wind Map of U.S." <http://firstlook.3tiergroup.com> (Accessed October 2007)
9. Pew Center on Global Climate Change. "States with Renewable Portfolio Standards." http://www.pewclimate.org/what_s_being_done/in_the_states/rps.cfm (Accessed June 2007)
10. National Oceanic and Atmospheric Administration. "Drawing Lines in the Water." <http://aquaculture.noaa.gov/pdf/uscopgrapocbnd.pdf> (Accessed October 2007)
11. Manwell, J.F., J.G. McGowan, and A.L. Rogers. "Wind Energy Explained – Theory, Design, and Application." John Wiley & Sons Ltd, West Sussex, England, 2002.
12. Patel, Mukund R. "Wind and Solar Power Systems." CRC Press, Boca Raton, FL, 1999

-
13. GE Energy. "3.6 MW Offshore Series Wind Turbine."
http://www.gepower.com/prod_serv/products/wind_turbines/en/downloads/ge_36_brochure_new.pdf (Accessed August 2006)
 14. Malcolm, D.J. and A.C. Hansen. "WindPACT Turbine Rotor Design Study" National Renewable Energy Laboratory, <http://www.nrel.gov/wind/pdfs/32495.pdf>
 15. REpower Systems. "REpower 5M." <http://www.repower.de/index.php?id=237&L=1> (Accessed August 2006)
 16. Clipper Establishes Development Center for 7.5 MW Turbine. "North American Wind Power, 09 October 2007,
http://www.nawindpower.com/naw/e107_plugins/content/content.php?content.1313 (Accessed October 2007)
 17. American Wind Energy Association (AWEA). "Basic Principles of Wind Resource Evaluation." <http://www.awea.org/faq/basicwr.html> (Accessed October 2007)
 18. Burton, Tony, David Sharpe, Nick Jenkins, and Ervin Bossanyi. "Wind Energy Handbook." John Wiley & Sons Ltd, West Sussex, England, 2001
 19. Fingersh, L., M. Hand, and A. Laxson. "Wind Turbine Design Cost and Scaling Model." National Renewable Energy Laboratory,
<http://www.nrel.gov/wind/pdfs/40566.pdf> (Accessed June 2006)
 20. Newnan, Donald G. and Jerome P. Lavelle. "Engineering Economic Analysis." Austin, TX: Engineering Press, 1998.
 21. National Renewable Energy Laboratories. S809 Aerofoil data downloaded from,
<http://wind.nrel.gov/designcodes/simulators/wtperf/> (Accessed June 2006)
 22. Poore, R., and T. Lettenmaier. "Alternative Design Study Report: WindPACT Advanced Wind Turbine Drive Train Designs Study" National Renewable Energy Laboratory. <http://www.nrel.gov/docs/fy03osti/33196.pdf> (Accessed March 2007)